Towards Mitigating Environmental Risks for Sustainable Development: The Roles of Migration, Wireless Emergency Alerts, and Federal Disaster Aid

by

WENTIAN JIANG

(Under the Direction of Mateusz Filipski)

ABSTRACT

This dissertation examines how migration, public communication, and disaster assistance affect environmental outcomes and recovery. It comprises three empirical studies using causal inference and high-resolution data to evaluate policy responses to environmental risks in both developing and developed contexts. Chapter 1 investigates how rural out-migration in Mon State, Myanmar, influences local deforestation. Combining household migration surveys with satellite data from 2000 to 2015, the study finds that each additional migrant is associated with reduced forest loss, with remittance income likely enabling a shift away from biomass fuels. Chapter 2 evaluates the U.S. Wireless Emergency Alerts (WEA) system. Using a Regression Discontinuity in Time design around the 2012 rollout, the study finds that WEA reduced storm-related deaths by 4.3 per event day, implying over 3,600 lives saved. Chapter 3 analyzes the effect of FEMA Public Assistance on post-hurricane recovery. Using county-level nighttime light data and an event-study difference-in-differences approach, the study finds that treated counties show stronger recovery trajectories, with effects growing over time. Together, these studies highlight how migration behavior, public information, and federal aid contribute to environmental resilience and disaster response effectiveness.

INDEX WORDS: [Out-migration, Deforestation, Wireless Emergency

Alerts, FEMA Public Assistance, Disaster recovery, Remote sensing data, Nighttime lights, Infrastructure

resilience, Causal inference]

TOWARDS MITIGATING ENVIRONMENTAL RISKS FOR SUSTAINABLE DEVELOPMENT: THE ROLES OF MIGRATION, WIRELESS EMERGENCY ALERTS, AND FEDERAL DISASTER AID

by

Wentian Jiang

M.S., Georgetown University, 2019

A Dissertation Submitted to the Graduate Faculty of the University of Georgia in Partial Fulfillment of the Requirements for the Degree.

DOCTOR OF PHILOSOPHY

ATHENS, GEORGIA

2025

©2025 Wentian Jiang All Rights Reserved

TOWARDS MITIGATING ENVIRONMENTAL RISKS FOR SUSTAINABLE DEVELOPMENT: THE ROLES OF MIGRATION, WIRELESS EMERGENCY ALERTS, AND FEDERAL DISASTER AID

by

Wentian Jiang

Major Professor: Mateusz J. Filipski

Committee: Susana Ferreira

Michael K. Adjemian Jeffrey H. Dorfman

Electronic Version Approved:

Ron Walcott Dean of the Graduate School The University of Georgia August 2025

DEDICATION

To those who believe that progress and sustainability can coexist.

We live in a world facing immense challenges, with climate change standing as one of the greatest threats to human well-being. As a future economist, I dedicate this work to the fight for a more resilient and sustainable future. While some seek to address environmental problems by urging others to consume less or slow development, I believe that dignity, prosperity, and environmental responsibility need not be mutually exclusive.

True solutions will come not from deprivation, but from innovation — from technological breakthroughs like controlled nuclear fusion to better policy and economic design. Though economists alone cannot solve the climate crisis, we can help buy time for science by guiding more efficient resource use, supporting cleaner energy transitions, and shaping more adaptive, inclusive systems. This work is a small step toward that goal.

ACKNOWLEDGMENTS

Six years have passed swiftly — a journey marked by both challenges and moments of quiet joy. Along the way, I have been deeply grateful to my professors and mentors, whose guidance has shaped not only this dissertation but also my growth as a researcher.

I am especially indebted to Dr. Mateusz Filipski, my major professor, for his unwavering support, thoughtful instruction, and unfailing patience. From him, I not only learned how to conduct research, but also what it means to approach academic work with integrity, curiosity, and commitment. His example taught me the attitude and dedication that a true researcher should embody. He was always encouraging and patient with even my most unrealistic or unpolished ideas. Rather than dismissing them outright, he gave me space to explore, make mistakes, and learn through the process — gently guiding me to see my own missteps and improve through experience. I am also grateful for the way he modeled respectful and effective collaboration — always patient, generous, and composed.

I am sincerely thankful to Dr. Susana Ferreira for her invaluable feedback and constructive suggestions that pushed my work forward. I owe special thanks to Dr. Michael Adjemian for helping me through my most difficult time, not only by providing funding, but also with his kindness and understanding. Last in mention, but rich in meaning, I sincerely thank Dr. Jeffrey Dorfman for offering insightful feedback that strengthened my research.

I also wish to thank the faculty and staff of the Department of Agricultural and Applied Economics at the University of Georgia for creating a supportive and intellectually stimulating environment throughout my graduate studies.

To my parents, thank you for your constant support and encouragement throughout this journey. Your belief in me has always been a steady source of strength.

Over the years, I have been surrounded by love, encouragement, and generosity — from family, professors, friends, and even strangers whose names I may never know. I imagined writing each one into this acknowledgment, yet now that I'm here, I still struggle to find the words to fully express what I feel for those who believed in me, understood me, and offered a hand when I needed it most. Perhaps some gratitude is best carried quietly in the heart, where it remains unchanged.

If I haven't named you here, please know it is not out of neglect. I will not forget your kindness. I will repay it — not only to you, but by helping others when I can. I will let the spirit of your generosity live on.

I make this commitment with all sincerity: I may be awkward, distracted, or slow at times — but I will never give up. I will work hard to ensure that your support has not been in vain.

To a better world — cheers!

Contents

A	knov	vledgments	v	
Li	st of]	Figures	viii	
Li	st of	Гables	ix	
In	trodu	ection	I	
I	Cau	sal Effects of Out-Migration on Local Deforestation: Evi-		
	den	ce from Rural Myanmar ¹	3	
	I.I I.2	Introduction	4 6	^I Jiang, W., Filipski, M., and Ferreira, S. Submitted to World Development,
	I.3 I.4	Main Results	13	06/16/25.
	1.5 1.6	Falsification Tests	16 19	
	I.7 I.8	Reverse Causality Checks	2I 24	
	1.9	Conclusion	31	
2	Do l	Mobile-Based Emergency Alerts Save Lives? Evidence from a		
	Reg	ression Discontinuity in Time ²	33	2. 7
	2. I	Introduction	34	² Jiang, W. and Filipski, M Submitted to Journal of
	2.2	Empirical Approach	37	Environmental Economics
	2.3	Empirical Results	42	and Management, 05/18/25
	2.4	Caveats	51	under review as of 06/04/2
	2.5	Conclusion and Discussion	53	
3	The	Effect of Disaster Aid on Recovery: Evidence from FEMA		
	Pub	lic Assistance Program ³	56	³ Jiang, W. and Filipski,
	3. I	Introduction	57	M. To be submitted to a peer-reviewed journal.

3.2	Data	59
3.3	Empirical Strategy	65
3.4	Main Results	69
3.5	Robustness Checks	72
3.6	Heterogeneity Analysis	76
3.7	Caveats	80
3.8	Conclusion	80
Conclus	sion	82
Append	lices	84
A Add	litional Tables	84
Bibliog	raphy	98

LIST OF FIGURES

I.I	Household locations (Picture generated using Google Earth	
	Engine Code Editor)	7
1.2	An example of buffers (Picture generated using Google Earth	
	Engine Code Editor)	7
1.3	Satellite visualization of forest loss (red) in 2015 within a 1-	
	km buffer (blue) around a household in Mon State, based on	
	Hansen et al. (2013)	9
I.4		14
1.5		16
1.6		19
1.7		22
1.8	Two mechanisms linking out-migration to reduced deforesta-	
	tion: (1) a remittance-facilitated energy transition (left), and	
	(2) reduced household wood use due to shrinking household	
	size (right).	29
2.I	Storm fatalities 2000-2024	38
2.2	Storm Fatalities 2000-2024 (Excluding Hurricane Katrina)	49
3. I	VIIRS Black Marble nighttime light imagery of Calcasieu Parish	
	ē 0 ē.	60

LIST OF TABLES

I.I	Summary statistics	IC
1.2	System GMM Estimates of Migration on Deforestation (Buffer	
	Radius = 1000m)	15
1.3	Robustness Checks: OLS Estimates of Migration on Defor-	
	estation	17
I.4	System GMM Falsification Test: Randomly Reassigned Mi-	
	gration (Buffer Radius = 1000m)	20
1.5	System GMM Reverse Causality Checks: Lead Migration and	
	Deforestation	23
1.6	Effect of Land-based Income on Out-migration (OLS, 2015) .	24
1.7	Effect of Migration on Total Income and Expenditure (OLS,	
	2015)	25
1.8	Percent of Each Type of Cooking Fuel	26
1.9	Effect of Migration on Energy Transition Outcomes (OLS, 2015)	30
2.I	Descriptive Statistics: U.S. Storms 2000-2024	37
2.2	Categorical breakdown of storm subtypes	38
2.3	RD estimates of the effect of WEA on deaths/day during storms	43
2.4	RD estimates of the placebo tests using different thresholds	46
2.5	RD estimates of falsification tests using Non-flash flood	47
2.6	RDiT estimates of the effect of WEA on deaths/day during	
	storms (Without Hurricane Katrina)	48
2.7	RD estimates of the effect of WEA on deaths/day during storms	
	(with internet adaptation rate)	50
3. I	Descriptive Statistics: Treated vs. Control Counties	64
3.2	Main Results: Impact of FEMA Public Assistance Program	
	Across Recovery Periods	69
3.3	Robustness Checks: Using Program Eligibility as Treatment .	73
3.4	Robustness Checks: Excluding first 30 days after hurricanes .	74

3.5	Heterogeneous Treatment Effects of FEMA Public Assistance	
	(Main Specification)	77
Aı	System GMM Estimates of Migration on Deforestation (Buffer	
	Radius = 500m)	85
A ₂	System GMM Estimates of Migration on Deforestation (Buffer	
	Radius = 2000m)	86
A3	OLS Estimates of Migration on Deforestation (Clustered Stan-	
	dard Errors, Buffer Radius = 1000m)	87
A4	OLS Estimates of Migration on Deforestation (Lower Than	
	10% Overlap Sample, Buffer Radius = 1000m)	88
A ₅	OLS Estimates of the Effect of WEA Threshold on Storm-	
	Related Deaths per Storm	89
A6	Covariate Balance Before and After IPW	90
A ₇	Robustness Check: Controlling for County-Level Hurricane	
	Preparedness	91
A8	High-Income Counties — Impact of FEMA Public Assistance	
	Across Recovery Periods	92
A9	Low-Income Counties — Impact of FEMA Public Assistance	
	Across Recovery Periods	93
Аю	High-Unemployment Counties — Impact of FEMA Public	
	Assistance Across Recovery Periods	94
AII	Low-Unemployment Counties — Impact of FEMA Public	
	Assistance Across Recovery Periods	95
A12	High Minority Counties — Impact of FEMA Public Assis-	
	tance Across Recovery Periods	96
A13	Low Minority Counties — Impact of FEMA Public Assis-	
	tance Across Recovery Periods	97

INTRODUCTION

Climate change, natural disasters, and environmental degradation are among the most pressing global challenges confronting policymakers and communities. While the impacts of these risks are increasingly visible, the mechanisms through which policies, behavior, and institutions shape environmental and recovery outcomes remain an active area of empirical inquiry. This dissertation contributes to this literature by examining how migration, public risk communication, and federal disaster aid interact with local responses to environmental risk. Across three standalone but thematically related papers, it employs high-resolution remote sensing data, administrative records, and household surveys to provide causal evidence on the effects of behavioral and institutional responses to environmental shocks.

Chapter 1, Causal Effects of Out-Migration on Local Deforestation: Evidence from Rural Myanmar, explores the relationship between rural out-migration and deforestation in Mon State, a region marked by rich tropical forests and sustained deforestation pressures. Using an original panel dataset that merges household migration surveys with annual forest loss and other environmental indices from satellite imagery between 2000 and 2015, the chapter employs dynamic panel system GMM estimation with localized 1000-meter buffers to measure forest impacts. The findings show that each additional migrant is associated with more than 5 square meters less forest loss per year. The analysis suggests that remittance income facilitates a household energy transition away from biomass fuels, offering a novel mechanism through which migration indirectly reduces local deforestation.

Chapter 2, Do Mobile-Based Emergency Alerts Save Lives? Evidence from a Regression Discontinuity in Time, evaluates the effectiveness of the U.S. Wireless Emergency Alerts (WEA) system in reducing storm-related mortality. Exploiting the sharp nationwide implementation of WEA in April 2012, the study applies a Regression Discontinuity in Time design to fatality and damage data

for 361 major storms from 2000 to 2024. It finds that the launch of WEA reduced storm-related deaths by an average of 4.3 fatalities per event day, implying that the system has saved over 3,600 lives since deployment. The analysis quantifies the resulting societal benefit at roughly \$50 billion, with strong support from robustness checks and falsification exercises. These results underscore the role of a centralized wireless risk communication system in delivering life-saving information under extreme weather risk.

Chapter 3, *The Effect of Disaster Aid on Recovery: Evidence from FEMA Public Assistance Program*, examines the post-disaster recovery effects of the FEMA Public Assistance (PA) program. It constructs a county-level panel from 2017 to 2022 that combines FEMA administrative records, socioeconomic indicators, and VIIRS nighttime lights—a proxy for infrastructure functionality and economic activity. Using an event-study difference-in-differences design with inverse probability weighting, the study identifies dynamic treatment effects across five post-hurricane periods. Counties receiving FEMA PA recovered significantly faster than comparable controls, with nightlight intensity increasing 2.3–2.5% more within 6–9 months and 3.3–3.5% more after two years. Results are robust to alternative specifications and alternative treatment definitions. This chapter contributes new evidence on the effectiveness of large-scale public investment programs in fostering community resilience.

Together, these chapters demonstrate how migration, public information systems, and federal aid shape responses to environmental risks. By integrating remote sensing data, administrative microdata, and econometric techniques, this dissertation contributes to the growing body of research on sustainable development, environmental resilience, and public policy effectiveness in the context of climate and disaster risk.

CHAPTER I

CAUSAL EFFECTS OF
OUT-MIGRATION ON LOCAL
DEFORESTATION: EVIDENCE
FROM RURAL MYANMAR⁴

⁴ Jiang, W., Filipski, M., and Ferreira, S. Submitted to World Development, 06/16/25.

1.1 Introduction

Migration is one of the most transformative forces shaping rural livelihoods and landscapes worldwide. Each year, millions of people leave rural areas. They reshape local economies through remittances, labor shifts, and transferring ideas, knowledge, and technologies (Chiodi et al., 2012; Rapoport & Docquier, 2006; J. E. Taylor et al., 2003). Migration also generates profound environmental consequences in the places of origin. These consequences remain underexplored in much of the migration literature. Case studies such as Liu et al., 2007 on Wolong, China, show that out-migration can reduce local environmental pressures, including firewood collection. However, remittance income may stimulate construction activities, agricultural expansion, or increased consumption. These activities can exacerbate resource extraction and environmental pressures (Damon, 2010; Ervin et al., 2020; Gray & Bilsborrow, 2014). The net direction and magnitude of these effects remain theoretically and empirically ambiguous. This ambiguity carries important implications for conservation and sustainable development.

Although the relationship between migration and environmental change has received growing attention recently, much of the literature has primarily examined how environmental stressors—especially climate variability—act as drivers of human mobility. This perspective frames migration as a form of adaptation to climate change, and has motivated a substantial body of research in economics and environmental studies (Cattaneo et al., 2019; Millock, 2015). These studies focus on how temperature shocks, droughts, or other natural hazards influence migration patterns, especially in low-income and agrarian settings.

In contrast, much less is known about how migration, once it occurs, affects environmental outcomes in migrants' places of origin. A small but growing number of studies have begun to explore the environmental consequences of migration, particularly concerning land use and deforestation (Angelsen et al., 2020; Carr, 2009; Ervin et al., 2020). However, findings from this literature remain mixed. Some suggest that out-migration reduces local environmental pressure by lowering household labor supply and firewood demand (Liu et al., 2007; M. J. Taylor et al., 2016). In contrast, others argue that migration-induced remittance flows may fuel environmentally intensive activities, such as land clearing, home construction, or agricultural intensification (Damon, 2010; Gray & Bilsborrow, 2014).

A major limitation in the existing literature is the difficulty of establishing causal effects. Because migration is typically non-random and often co-occurs with environmental shocks or economic changes, distinguishing its independent effect on forest outcomes is difficult. Few studies explicitly address endogeneity concerns or leverage panel data and high-resolution spatial indicators to disentangle competing mechanisms. As a result, there is limited causal evidence on how rural out-migration shapes deforestation in sending areas over time. We contribute to filling this gap by providing credible causal evidence from rural Myanmar. Using dynamic panel estimation, we find that out-migration significantly reduces local deforestation: each additional migrant is associated with approximately a 5.4 m^2 reduction in annual forest loss. This relationship remains robust across multiple model specifications.

Rural Myanmar presents a compelling setting for this inquiry: the country has one of the highest rates of forest dependency in Southeast Asia, with many rural households relying on local forests for fuelwood, food, and construction materials. At the same time, sustained out-migration, especially to neighboring Thailand, has reshaped household labor dynamics and remittance flows in forest-adjacent communities. We construct a novel spatial panel dataset by combining household-level migration histories with high-resolution remote sensing data on forest loss from 2000 to 2015. While most prior studies rely on cross-sectional data and descriptive correlations, our approach addresses key endogeneity concerns, such as unobserved time-invariant household characteristics, reverse causality, and dynamic feedback, using a dynamic panel framework estimated via System GMM (Blundell & Bond, 1998). Specifically, we exploit variation in the timing and intensity of household migration events, control for past deforestation trends through autoregressive terms, and use lagged levels of deforestation as internal instruments. We further incorporate household and year fixed effects to account for unobserved heterogeneity and standard shocks. Instrument validity and model specification are rigorously tested using Hansen J and Arellano–Bond AR(2) diagnostics. In addition, falsification tests with placebo migration variables and reverse causality checks support the causal direction from migration to reduced deforestation. Together, these strategies provide a robust empirical foundation for identifying migration's environmental effects in forest-dependent rural settings.

We further explore a novel mechanism through which migration may reduce deforestation: remittance-induced energy transitions. Specifically, we find that migration facilitates household access to electricity, particularly for cooking, thereby reducing reliance on firewood and charcoal. This mechanism highlights

a previously underappreciated channel linking migration and environmental sustainability.

The remainder of the paper is organized as follows. Section 2 describes the data sources and construction of the panel dataset. Section 3 explains the empirical methodology. Section 4 presents the main estimation results. Section 5 discusses robustness checks. Section 6 conducts falsification tests, and Section 7 examines reverse causality checks. Section 8 explores the mechanisms underlying the main results, including a novel mechanism. Section 9 concludes.

1.2 Background and Data

This study focuses on rural households in Mon State, located in southeastern Myanmar, a region known for its rich tropical forests and environmental diversity. Mon State lies along the Gulf of Martaban and borders Thailand, with communities primarily engaged in subsistence farming, small-scale agriculture, and natural resource extraction. Forests in this region serve as an essential source of livelihood, providing firewood, timber, wild foods, and construction materials, while supporting regional biodiversity. Myanmar is recognized as one of the most forested countries in Southeast Asia, but it has experienced significant tropical deforestation in recent decades. In 2001, Mon State contained approximately 579,200 hectares of tree cover, including primary and secondary forest, covering about 36% of its land area (Global Forest Watch, 2024). From 2001 to 2024, the region lost more than 145,000 hectares of tree cover, equivalent to a 25% decline from its 2001 baseline (Global Forest Watch, 2024). Although Mon State has experienced net forest loss from 2001 to 2024, localized studies report forest growth in certain areas between 2001 and 2010, including annual gains of 60.8 km² and modest carbon sequestration (Kyaw et al., 2020). This suggests forest dynamics in the region are spatially and temporally heterogeneous. Since migration is a common livelihood strategy and a primary income source for many households in Mon State (Filipski et al., 2017), examining its effects on deforestation is essential for understanding local forest dynamics. It underscores the need for household-level analysis of migration's environmental impacts.

To examine the relationship between migration and deforestation, we use household-level data from the 2015 Mon State Rural Household Survey (CESD, 2015), which employed a stratified random sampling design to select a representative sample of villages, as shown in Figure 1.1, and households across Mon State.

Although the survey was conducted cross-sectionally, it includes retrospective information on the year each household member migrated out or returned. We leverage this retrospective detail to reconstruct household-level migration histories and generate a panel structure for out-migration and return migration events. This approach allows us to track annual changes in migration status for each household from 2000 to 2015, enabling panel econometric analysis despite the cross-sectional nature of the baseline survey. From these migration histories, we construct three key cumulative variables at the household-year level: outmigration (Out-migration_{i,t}), return migration (Return-migration_{i,t}), and current migrants (Current Migrants_{i,t}). Out-migration_{i,t} denotes the total number of household members who had left household i between the base year 2000 and year t. Return-migration $_{i,t}$ captures the cumulative number who had returned to the household by year t. We then define Current Migrants $_{i,t}=$ Out-migration_{i,t} – Return-migration_{i,t}, representing the number of household members who remained away as of year t. These cumulative indicators reflect the intensity and persistence of household migration exposure over time and allow us to assess both immediate and lasting effects of household demographic change on local deforestation outcomes.

1.2.1 Construction of the Panel Dataset

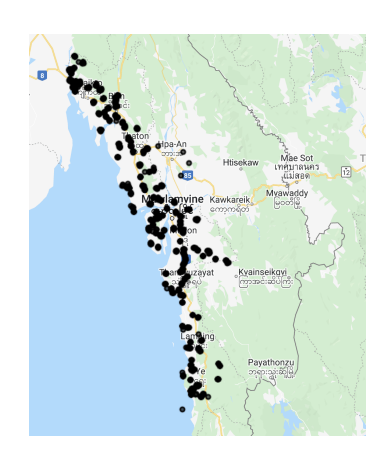


Figure 1.1: Household locations (Picture generated using Google Earth Engine Code Editor)

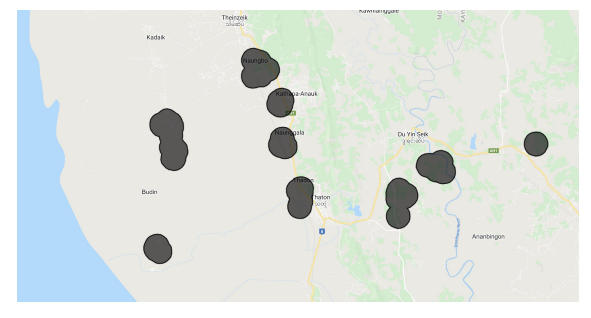


Figure 1.2: An example of buffers (Picture generated using Google Earth Engine Code Editor)

Having constructed a household-level migration panel using retrospective migration histories, we link each household's migration status—captured through Out-migration i, t, Return-migration i, t, and Current Migrants i, t—to spatially

matched environmental variables. Specifically, we geocode each household based on GPS coordinates recorded during the baseline survey and generate a I-kilometer radius buffer around each household location to capture surrounding environmental conditions (see Figure 1.2). Within each buffer, we overlay annual satellite-based raster datasets from 2000 to 2015 and extract environmental indicators, including forest cover loss (Hansen et al., 2013), precipitation (Funk et al., 2015), soil temperature, and surface wind speed (Muñoz Sabater, 2019). This data fusion strategy yields a household-year panel dataset with rich spatiotemporal variation, allowing us to examine how different migration behaviors relate to environmental outcomes over time.

Figure 1.3 presents a satellite-based visualization of forest loss in 2015 surrounding a selected household in rural Myanmar. The map shows a 1-kilometer buffer (blue circle) centered on the household, overlaid with red pixels representing areas where forest loss occurred specifically in the year 2015, as identified by the Global Forest Change (GFC) dataset developed by Hansen et al. (Hansen et al., 2013). Each red pixel corresponds to a 30-meter by 30-meter area (900 m²) where tree canopy cover—originally greater than 30% in the year 2000—was completely removed in that year. This definition of forest loss captures stand-replacing disturbances (i.e., complete canopy removal), regardless of the underlying cause, such as agricultural expansion, infrastructure development, or natural events.

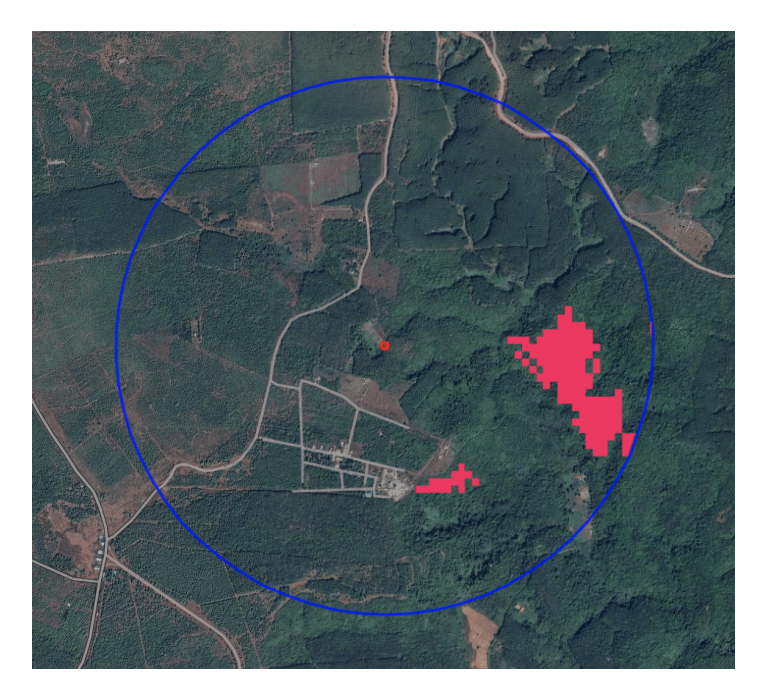


Figure 1.3: Satellite visualization of forest loss (red) in 2015 within a 1-km buffer (blue) around a household in Mon State, based on Hansen et al. (2013).

Importantly, this measure of deforestation differs from forest degradation. The Hansen dataset focuses solely on total canopy loss, thereby providing a conservative estimate of forest change. In contrast, forest degradation refers to partial canopy removal or other disturbances (e.g., selective logging, fire, or fragmentation) that reduce forest quality but may not be detected as a loss in this dataset.

1.2.2 Data Overview

Table 1.1 presents summary statistics for key variables in our merged panel dataset. Forest loss varies widely across households: while some households experience minimal deforestation (as little as o m^2 over the sample period), others experience substantial loss exceeding 471,000 m^2 . Migration also shows considerable heterogeneity, with household-level migration events ranging from 0 to 6 over the 2000-2015 period. These patterns reflect meaningful variation across both environmental exposure and household demographic behavior, strengthening the identification of migration's effect on deforestation. The variation in outcomes and treatment intensity supports the feasibility of household-level panel econometric analysis.

Table 1.1: Summary statistics

Variables	Mean	Min	Max
Deforestation (m ²)	4716 (15266.56)	0	471346
Out migration	0.1276 (0.4346)	О	6
Return migration	0.0172 (0.1696)	О	6
\sum out migration	0.7915 (1.1850)	О	7
\sum return migration	o.o8o6 (o.3577)	О	6
Eastwind (m/s)	0.1578 (0.2210)	-0.348	1.105
Northwind (m/s)	0.6180 (0.1947)	О	1.269
Precipitation (mm)	544.8 (66.0785)	328.8	735
Soil temperature (Kelvin)	300.3 (0.8437)	297.6	302.4
Number of households	703		
Number of observations	11248		

Notes: Standard deviations are shown in parentheses.

1.3 Empirical Methodology

1.3.1 Dynamic Panel Model with Fixed Effects

In this study, we employ a dynamic panel model with fixed effects to estimate the relationship between migration and deforestation, as specified in Equations 1 and 2. Our key explanatory variables include the number of out-migrants (Out-migration $_{i,t}$), return-migrants (Return-migration $_{i,t}$), and current migrants (Current Migrants $_{i,t}$) for household i in year t.

To ensure our estimates reflect population-level dynamics rather than just the sampled households, we apply enumeration area (EA)-level survey weights to the household migration variables. Specifically, each sampled household's migration count is multiplied by its corresponding EA weight, approximating the number of households the sampled unit represents. This weighting adjusts for the sampling design and helps mitigate the risk of overstating per-migrant effects. This is particularly important in settings where spatial buffers used for environmental covariates may encompass other households, including those not captured in the survey sample.

Environmental covariates include total annual precipitation (Precipitation $_{i,t}$, in millimeters), average soil temperature (Temperature $_{i,t}$, in Kelvin), and east and north wind velocities (Eastwind $_{i,t}$ and Northwind $_{i,t}$, in meters per second). These are constructed from remote sensing data and aggregated within a 1-kilometer radius spatial buffer centered at each household's exact geographic coordinates. Since environmental shocks can jointly affect proximate households, using EA weights is a practical way to reduce bias from potential spatial clustering and overlapping exposure zones.

Taken together, this modeling approach helps improve population representativeness and offers a partial correction for potential biases arising from spatial overlap in buffer-based measurements.

$$\begin{split} \text{Deforestation}_{i,t} &= \beta_0 + \beta_1 \text{Deforestation}_{i,t-1} + \beta_2 \textbf{Current Migrants}_{i,t} + \\ &+ \beta_3 \text{Precipitation}_{i,t} + \beta_4 \text{Temperature}_{i,t} + \beta_5 \text{Eastwind}_{i,t} \\ &+ \beta_6 \text{Northwind}_{i,t} + \delta_i + \theta_t + \epsilon_{i,t}, t = 1, 2, \cdots, 16 \end{split}$$

$$\begin{aligned} \text{Deforestation}_{i,t} &= \beta_0 + \beta_1 \text{Deforestation}_{i,t-1} + \beta_2 \sum_{\tau=1}^t \mathbf{Out\text{-migration}}_{i,\tau} \\ &+ \beta_3 \sum_{\tau=1}^t \mathbf{Return\text{-migration}}_{i,\tau} + \beta_4 \text{Precipitation}_{i,t} \\ &+ \beta_5 \text{Temperature}_{i,t} + \beta_6 \text{Eastwind}_{i,t} + \beta_7 \text{Northwind}_{i,t} \\ &+ \delta_i + \theta_t + \epsilon_{i,t}, t = 1, 2, \cdots, 16 \end{aligned} \tag{1.2}$$

Lagged dependent variables are commonly included in dynamic panel models to account for temporal persistence in the outcome variable (Slutzky, 1937; Yule, 1927). In the context of deforestation, this approach captures inertia in landuse practices, gradual forest degradation, and unobserved ecological or socioeconomic drivers that evolve over time. Our inclusion of Deforestationi, t-1 and, in some specifications, Deforestationi, t-2 helps model this temporal dimension of forest loss. This is consistent with recent spatial econometric approaches that explicitly frame deforestation as a spatiotemporal process (Cantillo & Garza, 2022).

To address omitted variable bias and unobserved heterogeneity, we also include two-way fixed effects in Equations (1) and (2)—household fixed effects (δ_i) and year fixed effects (θ_t). These controls, respectively, for time-invariant characteristics (e.g., soil quality, proximity to roads) and for common temporal shocks (e.g., national policies, climate anomalies). Together with AR terms, this modeling strategy allows us to control for both persistent unobserved household-level characteristics and shared temporal dynamics that could confound the migration—deforestation relationship.

1.3.2 Estimation Strategy

We estimate dynamic panel models using the System GMM estimator (Blundell & Bond, 1998). To address potential endogeneity in migration and the lagged dependent variable, we simultaneously use the third, fourth, and fifth lags of deforestation as internal instruments. Including these lagged terms as instruments helps capture the persistence of deforestation over time while ensuring instrument validity. Furthermore, we use the Hansen-Sargan J test to check

for instrumental validity and apply the Arellano-Bond AR(2) test to check for second-order serial correlations, ensuring correct model specification.

Unlike the Difference GMM (Arellano & Bond, 1991), which removes fixed effects by first-differencing and uses lagged levels of the variables as instruments, System GMM combines equations in both levels and differences. This approach improves efficiency and instrument strength, especially when variables are persistent and the time dimension of the panel is short. In our context, where deforestation and migration evolve gradually over time, System GMM is preferred because Difference GMM suffers from weak instruments, which can lead to biased estimates.

1.4 Main Results

Table 1.2 presents estimation results from our specifications utilizing data collected within 1 km buffers, while Figure 1.4 visualizes the key estimates. We observe a robust and statistically significant negative correlation between current migrants or out-migration and deforestation, a finding consistent across autoregressive (AR) models with different covariate sets. Specifically, our main specifications (columns (1) and (2)) indicate that an increase of one current migrant is associated with a reduction in deforestation of approximately 5.439 m^2 . Similarly, each additional instance of out-migration corresponds to a decrease in forest loss of around 5.843 m^2 .

Our estimates reflect the average effect of migration on deforestation, combining both extensive and intensive margins. While our variable Current Migrants $_{i,t}$ captures the intensive margin by measuring the number of household members currently living away, it does not separately identify the extensive margin—whether a household has any migration. Similarly, Out-migration $_{i,t}$ reflects the cumulative number of individuals who have ever migrated out, blending presence and scale.

To further validate our model specifications, we conducted a series of robustness tests, including the Hansen J test, AR(2) tests, and Wald tests for coefficients and time dummies. Specifically, all Hansen J-test results fail to reject the null hypothesis of instrument validity, indicating our models satisfy over-identification restrictions. The p-values of the J statistics are moderate (e.g., around 0.15 for the fully specified model), demonstrating that our models do not suffer from

p-value inflation, a common issue when excessive GMM instruments are used (Roodman, 2009). Thus, our number of instruments, three in number (lags 3, 4, and 5), is appropriately chosen. The Wald tests for coefficients strongly reject the null hypothesis that explanatory variables are jointly zero (P < 0.01), confirming their joint significance, including migration and environmental covariates. The Wald tests for time dummies similarly confirm the joint significance of year-fixed effects, justifying their inclusion.

Additionally, to evaluate the robustness of our results, we compare a fully specified System GMM model, which includes covariates such as precipitation and soil temperature, with models excluding these controls. While the migration effect remains consistent in magnitude and significance, either the Hansen J test or the Arellano-Bond AR(2) test fails in the models without controls, highlighting concerns regarding instrument validity. This occurs because omitting important covariates like precipitation and soil temperature can cause their effects to be absorbed into the error term, violating the key assumption that instruments are uncorrelated with the error term. Such contamination leads to endogeneity in the instrument set, resulting in test failures. The complete model, incorporating all relevant controls, passes both the Hansen test (p = 0.145, p = 0.159) and the Arellano-Bond AR(2) test (p = 0.990, p = 0.994), making it the preferred specification. These findings suggest our main results are robust and not driven by omitted variable bias; rather, the inclusion of additional covariates enhances the reliability and validity of our instrumentation strategy.

Main Results (Effect of Current Migrants or Outmigration on Deforestation)

(4) AR(2) models

Model Specification

(5) W/Out Controls (6) W/Out Controls

Figure 1.4

Table 1.2: System GMM Estimates of Migration on Deforestation (Buffer Radius = 1000m)

	(1) Main	(2) Main models	(3) AR(2)	(4) 4R(2) models	(s) Models W/	(5) (6) Models W/Out controls
Lagged Deforestation $(t-1)$ (m ²)	0.464***	0.464***	0.521*** (0.0638)	0.521*** (0.0636)	0.496*** (0.0739)	0.486***
Lagged Deforestation $(t-2)$ (m ²)			0.251** (0.08II)	0.253**		
Current Migrants	-5.439** (2.618)		-5.663* (2.928)		-8.518*** (2.883)	
∑ Out-migration		-5.843** (2.756)		-6.075* (3.186)		-9.787*** (3.274)
Netum Migration		2.193 (5.084)		2.621 (5.586)		
Precipitation (mm)	265.57*** (72.45)	267.83*** (71.68)	262.67*** (78.42)	265.97*** (77.49)		
Temperaturekelvin)	212.72 (155.54)	212.85 (149.04)	91.82 (161.65)	101.88		
East Wind (m/s)	649.62 (56796)	-758.69 (54841)	-28840 (53424)	-27615 (50338)		
North Wind (m/s)	-67830 (92327)	-67610 (88294)	9966 (\$7979)	3814 (94130)		
Hansen J test p-val	0.145	0.159	0.151	0.163	3.38×10^{-7}	5.42×10^{-7}
AK(2) test p-val Wald test (coefficients)	0.990 1.57×10^{-11}	0.994 1.83×10^{-11}	0.044 8.30×10^{-15}	0.044 1.04×10^{-14}	0.606 3.87×10^{-13}	0.603 5.28×10^{-13}
Wald test (time dummies)	2.89×10^{-12}	1.23×10^{-12}	1.58×10^{-12}	3.66×10^{-13}	3.92×10^{-14}	1.71×10^{-13}
Observations	18681	18681	18681	18681	18681	18681

Note: Robust standard errors in parentheses. " $p<0.1, \mbox{***} p<0.05, \mbox{****} p<0.01.$

1.5 Robustness Checks

To ensure the robustness and credibility of our main findings obtained from the System Generalized Method of Moments (System GMM), we conduct additional analyses employing Ordinary Least Squares (OLS) to estimate the main models, which control household and time-invariant characteristics, thus accounting for unobserved heterogeneity that may bias conventional estimations. Table 1.3 shows the results, and Figure 1.5 visualizes the estimates of current migrants/out-migration. Although OLS estimation results yield smaller magnitude coefficients than the System GMM estimates, they remain statistically significant and consistent in direction. Such differences in magnitude are anticipated due to methodological distinctions; System GMM effectively corrects for potential endogeneity arising from reverse causality and dynamic feedback effects by incorporating lagged dependent variables and internal instruments. In contrast, OLS estimations, while robust to fixed unobserved heterogeneity because of the inclusion of fixed effects in the main models, may underestimate coefficients in the presence of endogeneity or dynamic dependencies—conditions highly likely in our context, as indicated by the significant estimates of the autoregressive (AR) terms. Still, the consistent direction and statistical significance of the OLS estimates corroborate the validity of our primary System GMM models, reinforcing confidence in our main results regarding the impact of out-migration on deforestation.

Robustness Checks (Effect of Current Migrants or Outmigration on Deforestation)

The street of Current Migrants or Outmigration on Deforestation on Deforestati

Figure 1.5

Table 1.3: Robustness Checks: OLS Estimates of Migration on Deforestation

	(1) Main	t) (2) Main models	(3) AR(2)	(4) (4) $AR(2)$ models	(s) Models W,	(5) (6) Models W/out controls
Lagged Deforestation $(t-1)$	0.520***	0.521***	0.486***	0.486***	0.521***	0.521***
Lagged Deforestation $(t-2)$			0.056***	0.056***		
Current Migrants	—I.551** (0.767)		-1.662^{**} (0.814)		-1.527^{**} (0.766)	
∑ Out-migration		-1.608** (0.782)		-1.748** (0.833)		—I.55I** (0.775)
Neturn Migration		0.694 (2.409)		0.477		
Precipitation	-6.277 (6.137)	-6.318 (6.138)	-6.617 (6.427)	-6.686 (6.428)		
Temperature	229.82 (1442.0)	226.81 (1442.1)	256.80 (1502.5)	251.61 (1502.6)		
East Wind	⁻¹⁰¹⁴ (3254)	—100I (3254)	—II79 (3371)	—II59 (3372)		
North Wind	3409 (4244)	3430 (4244)	3293 (4416)	3322 (4417)		
R^2 (within)	0.2136	0.2136	0.2029	0.2029	0.2135	0.2135
F-statistic (overall)	444.7	381.2	331.6	290.2	1333.6	1333.7
Obs	10545	10545	9842	9842	10545	10545

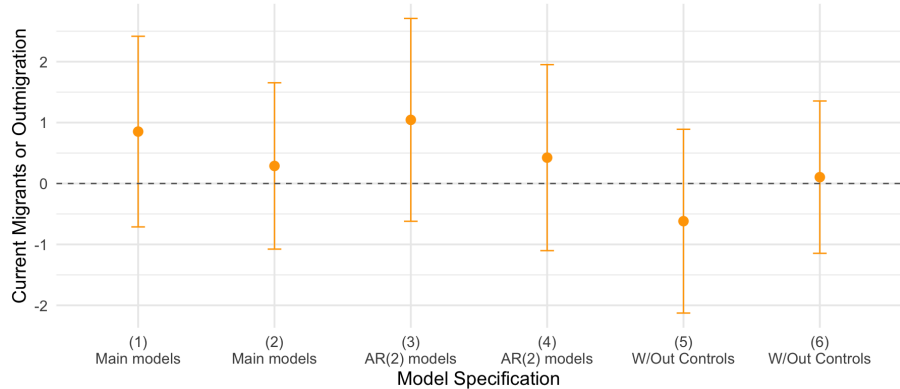
Note: Two-way fixed effects at household and year levels. Robust standard errors in parentheses. ${}^*p < 0.1, {}^{**}p < 0.05, {}^{***}p < 0.01.$

To test the sensitivity of our findings to the spatial scale of environmental measurement, we re-estimate the system GMM models using alternative buffer sizes of 500 meters and 2 kilometers. The 500-meter specification yields no statistically significant results, and the estimated coefficients show no consistent pattern relative to the main model. This is plausibly due to the buffer being too narrow to capture forest use for activities like firewood collection or small-scale land clearing, which likely occur beyond immediate household surroundings. Conversely, the 2-kilometer buffer produces estimates with similar signs to the main 1-kilometer model, but statistical significance is limited to only a subset of specifications. We attribute this attenuation to including a broader, potentially noisier environmental context and more severe buffer overlaps, which may dilute the relationship between migration and local forest outcomes. Taken together, these findings suggest that the 1-kilometer buffer strikes a reasonable balance—broad enough to capture household-related forest use, yet narrow enough to avoid excessive noise from overlapping exposure zones. Full estimation tables for the 500m and 2000m specifications are provided in Appendix Tables A1 and A2.

To address potential concerns arising from spatial buffer overlaps in our dataset, we conduct robustness tests employing two complementary approaches. First, we estimate the dynamic panel models using ordinary least squares (OLS) with clustered standard errors at the village level, which accounts for within-village correlation due to overlapping buffers. These results, presented in Table A₃, remain consistent in magnitude, direction, and statistical significance compared to those obtained using conventional standard errors, indicating that clustering effectively mitigates overlap-induced bias. Second, we re-estimate the models restricting the sample to observations with buffer overlap lower than 10%, as shown in Table A4. While the coefficient estimates maintain similar magnitudes and directions, their statistical significance diminishes, likely reflecting reduced sample size and statistical power. Together, these complementary analyses provide reassuring evidence that spatial buffer overlaps do not materially bias our findings. Nevertheless, future research could further explore advanced spatial econometric techniques or incorporate spatial fixed effects to more directly model spatial dependence.

Figure I.6

Falsification Tests (Effect of Current Migrants or Outmigration on Deforestation)



1.6 Falsification Tests

We randomly reassign the migration variable across villages and years as a falsification check. Specifically, we randomly shuffle the migration variable while preserving the structure of deforestation outcomes and other covariates. This approach breaks any true link between migration and deforestation, while maintaining the underlying panel structure, spatial clustering, and temporal variation in the data.

If the observed association between migration and deforestation in our main results were due to spurious correlation, common trends, or artifacts of the panel structure, we would expect to find similar significant effects even after random reassignment. However, based on the results from Table 1.4 and Figure 1.6, re-estimating our System GMM models with the placebo migration variable yields no statistically significant effects across the different specifications. This outcome confirms that the statistically significant negative impacts we find using the main models are unlikely to be driven by spurious correlation, panel structure artifacts, or model misspecification.

Table 1.4: System GMM Falsification Test: Randomly Reassigned Migration (Buffer Radius = 1000m)

	(I) Main	(2) Main models	(3) AR(2)	(4) (4) models	(5) Models W/	5) (6) Models Wout controls
Lagged Deforestation $(t-1)$	0.469***	0.48I*** (0.0705)	0.528***	0.536***	0.510***	0.506***
Lagged Deforestation $(t-2)$			0.262*** (0.0776)	0.263***		
Current Migrants	0.321 (0.879)		0.673		0.295 (0.747)	
∑ Out-migration		-0.415 (0.663)		-0.369 (0.721)		-1.007 (0.618)
Neturn Migration		-1.046 (2.840)		0.577 (3.169)		
Precipitation	247.05*** (62.18)	195.12*** (58.82)	251.23*** (72.92)	202.00*** (65.59)		
Temperature	273.41* (148.25)	236.28* (131.72)	124.32 (180.29)	110.92 (156.71)		
East Wind	15017 (\$5278)	4719 (49586)	-23650 (57930)	-31378 (55715)		
North Wind	—118910 (92791)	-108830 (82660)	—16564 (113520)	-22078 (100740)		
Hansen J test p-val AR(2) test p-val Wald test (coefficients) Wald test (time dummies)	0.060 0.921 8.30 × 10 ⁻¹³ 1.48 × 10 ⁻¹⁴	$\begin{array}{c} \text{0.022} \\ \text{0.957} \\ 4.01 \times 10^{-12} \\ 4.62 \times 10^{-16} \end{array}$	0.097 0.042 5.32 × 10 ⁻¹⁶ 3.87 × 10 ⁻¹⁴	0.036 0.048 3.11×10^{-16} 2.57×10^{-15}	5.76×10^{-7} 0.627 3.35×10^{-12} $< 2.22 \times 10^{-16}$	6.51×10^{-7} 0.624 3.75×10^{-13} $< 2.22 \times 10^{-16}$
Observations	18981	18681	18681	18981	18681	18981

Note: RA = randomly assigned. Robust standard errors are in parentheses. $^*p < 0.1, ^{**}p < 0.05, ^{***}p < 0.01.$

1.7 Reverse Causality Checks

The potential risk of reverse causality is one of our primary concerns. Therefore, we conduct reverse causality checks from two different perspectives to assess its likelihood. First, we include a lead of the migration variable (i.e., future migration) as a predictor of current deforestation. From results in Table 1.5 and Figure 1.7, in both our main falsification specification and the extended model that includes an additional autoregressive term, the coefficient on future migration is statistically insignificant. Both models also pass the Hansen and AR(2) diagnostic tests, supporting the validity of the specifications. By contrast, the model that includes only lead migration and an AR(1) term yields a statistically significant adverse effect, but fails the Hansen test, indicating that the instruments are invalid. Together, these results support the assumed causal direction from migration to deforestation.

Second, we explore potential mechanisms through which deforestation might lead to out-migration. One possibility is that deforestation reduces land-based income, which in turn induces migration. To examine this, we regress landbased income on out-migration using cross-sectional survey data collected in 2015. As shown in Table 1.6, we find no evidence that lower land-based income is associated with higher out-migration. Another hypothesis is that deforestation degrades the natural environment, prompting households to migrate in search of areas with better environmental conditions. However, based on our survey data and our understanding of migration patterns in rural Myanmar, most migrants move to Thailand primarily for economic reasons rather than environmental concerns. Specifically, over 40% of households in Mon State have at least one member working in Thailand (Filipski et al., 2017). Thus, given this context, ecological degradation seems unlikely to be the primary driver of migration. This finding is consistent with broader evidence from climate migration studies, which suggests that migration decisions are often primarily economically motivated, even in the face of environmental deterioration (Nawrotzki & Bakhtsiyarava, 2017). In summary, neither the dynamic reverse causality checks nor the cross-sectional income analysis provides evidence of reverse causality.

Figure 1.7

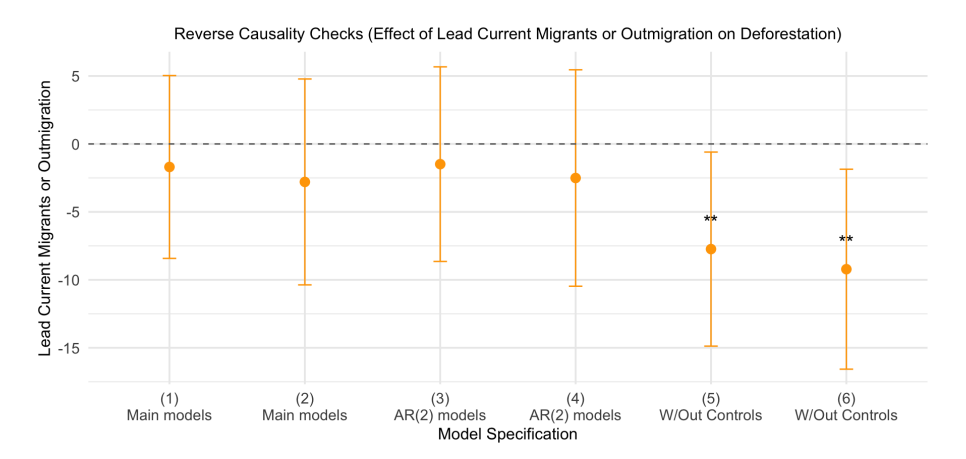


Table 1.5: System GMM Reverse Causality Checks: Lead Migration and Deforestation

	(1) Main	(2) Main models	(3) AR(2)	(4) $AR(z)$ models	(5) Models W/	(5) (6) Models W/out controls
Lagged Deforestation $(t-1)$	o.396*** (o.0798)	0.392*** (0.0799)	0.437***	0.430*** (0.0774)	0.469***	0.454***
Lagged Deforestation $(t-2)$			0.233*	o.222* (o.0925)		
Lead Current Migrants	-1.694 (3.432)		-1.486 (3.653)		7.737*** (3.643)	
Lead ∑ Out-Migration		-2.795 (3.865)		-2.506 (4.063)		-9.216** (3.753)
Lead ∑ Return Migration		-8.792 (6.430)		-7.649 (6.795)		
Precipitation	229.50** (81.70)	217.28** (81.99)	218.54* (88.39)	203.79* (87.48)		
Temperature	247.36 [°] (140.84)	257.56 (149.45)	178.26 (142.53)	192.53 (149.65)		
East Wind	24466 (43377)	31595 (45799)	16354 (43937)	26975 (46728)		
North Wind	97475 (80743)	—107750 (89147)	—54011 (81715)	-67315 (89116)		
Hansen J test p-val AR(2) test p-val Wald test (coefficients)	0.569 0.318 6.29×10^{-9} 1.50 $\times 10^{-13}$	0.716 0.410 5.05×10^{-9}	0.688 0.126 1.06 × 10 ⁻⁶ 2 fo < 10-11	0.807 0.126 1.70 × 10 ⁻⁶ 0.45 × 10 ⁻¹¹	1.34 × 10 ⁻⁶ 0.543 1.94 × 10 ⁻⁶ 1.46 × 10 ⁻¹³	3.53×10^{-6} 0.562 1.29×10^{-6} $6.70 < 10^{-14}$
ward test (unite duminities) Observations	1.30 × 10	1.00 × 100.1 17571	5.30 × 10 17575	2.43 × 10 1757s	17575	0.13 × 10

Note: Lead variables are used to test reverse causality. Robust standard errors in parentheses. $^*p < 0.1, ^{**}p < 0.05, ^{***}p < 0.01$.

Table 1.6: Effect of Land-based Income on Out-migration (OLS, 2015)

	(I)
Dependent variable:	Out-migration (migleft_sum)
Rice income	-2.486×10^{-8}
	(4.201×10^{-8})
Orchard income	-6.968×10^{-9}
	(4.328×10^{-8})
Rubber income	-8.947×10^{-8}
	(1.244×10^{-7})
Rice local wage income	-0.0906
	(0.1625)
Orchard local wage income	0.447*
5.11	(0.2327)
Rubber local wage income	-0.173
D 1 . (1)	(0.2407)
Parcel size (ha)	0.00652
	(0.00633)
Constant	2.171***
	(0.05999)
Observations	703
R-squared	0.0084
Adjusted R-squared	-0.0016
Residual Std. Error	1.302 (df = 695)
F Statistic	o.836 (df = 7; 695)

Note: Robust standard errors in parentheses.

1.8 Discussion and Mechanisms

In the previous sections, we have shown that out-migration reduces deforestation at the local level. One immediate mechanism for this effect is a decrease in daily wood consumption (e.g., firewood, construction wood) due to reductions in household size resulting from out-migration or changes in land-use strategy (M. J. Taylor et al., 2016). However, lifestyle changes, specifically adopting electricity for heating and cooking, facilitated by remittance income, may also contribute to this outcome. This section presents empirical evidence supporting this less-recognized pathway through which out-migration may reduce forest loss via remittance effects.

^{***}p < 0.001, **p < 0.01, *p < 0.05, 'p < 0.1

To assess the existence of remittance effects, we use cross-sectional household survey data from 2015 and regress the number of current migrants and household demographic variables on both total local income and household expenditure, measured in thousands of Kyats. Results in Table 1.7 show that the number of current migrants has no significant effect on households' total local income but has a statistically significant positive impact on their total local expenditure. This finding provides strong evidence of remittance effects, indicating that while local income may remain unchanged, additional remittance income from migrants abroad contributes to higher household spending.

Table 1.7: Effect of Migration on Total Income and Expenditure (OLS, 2015)

	(1)	(2)
Dependent variable:	Total Local Income	Total Local Expenditure
\sum Out-migration (unweighted)	32.32	62.29**
-	(99.82)	(25.42)
Household size	250.87***	169.48***
	(62.06)	(15.80)
Parcel size (ha)	73.84***	9.78^{***}
	(14.83)	(3.78)
Age of head	-18.94*	-7.45^{***}
	(10.10)	(2.57)
Occupation of head	-50.76	33.75***
	(50.63)	(12.89)
Constant	2,652.75***	1,606.81***
	(702.77)	(178.95)
Observations	703	703
R-squared	0.070	0.175
Adjusted R-squared	0.063	0.169
Residual Std. Error	3398 (df = 697)	865.4 (df = 697)
F Statistic	10.48***	29.54***

Note: Robust standard errors in parentheses.

 $^{^5}$ All monetary values are reported in Myanmar Kyat (MMK). The 2015 annual average exchange rate was approximately 1 USD = 1,148 MMK (or 1,000 MMK \approx 0.87 USD), based on data from https://www.exchange-rates.org/exchange-rate-history/mmk-usd-2015.

p < 0.1, p < 0.05, p < 0.01

Table 1.8: Percent of Each Type of Cooking Fuel

Fuel Type	All households	households w/ migrants	households w/o migrants
Electricity	10.65%	12.28%	5.66%
LPG	1.61%	0.81%	3.77%
Kerosene	0.26%	0.48%	1.89%
Firewood	81.81%	79.64%	83.02%
Charcoal	5.68%	6.79%	5.66%

One potential pathway through which out-migration reduces deforestation is via remittance income, which facilitates the adoption of alternative fuels, such as electricity, for cooking and heating. This transition reduces reliance on traditional biomass fuels, including firewood and charcoal. In many developing countries and regions, including rural Myanmar, firewood and charcoal remain the primary sources of household energy (Win et al., 2018). The average annual per capita consumption is estimated at 780 kilograms for firewood and 280 kilograms for charcoal (Kyaw et al., 2020). Meeting these energy needs requires approximately 36 m² and 820 m² of forest area per person per year, respectively (Kyaw et al., 2020). In our sample, 85.6% of households report using firewood, and 13.5% report using charcoal for cooking and heating. As shown in Table 1.8, firewood remains the dominant cooking source, although electricity use is gradually emerging.

Importantly, in rural Myanmar, local communities often have customary rights to collect firewood for household use from nearby forests, a practice recognized under national forest tenure frameworks (Bank, 2020). This institutional context reduces barriers to biomass extraction, which in turn increases household reliance on local forests for energy. Table 1.8 further shows that households with out-migrants have a higher rate of electric cooking adoption and less reliance on firewood than those without migrants. Thus, theoretically, a transition toward electricity use, facilitated by remittance income, could significantly mitigate forest loss by reducing pressure on surrounding forest resources.

To test the hypothesis that migration facilitates energy transitions, we estimate a series of ordinary least squares (OLS) regressions to assess the impact of outmigration on access to electricity and adoption of electric cooking. Our empirical results, presented in Table 1.9, confirm a positive and statistically significant relationship between out-migration and both access to electricity and the adoption of electric cooking. Although our current data limitations prevent a comprehensive exploration of this deforestation-reducing pathway, we pro-

vide strong empirical evidence for its existence and encourage future research to investigate further the role of remittance-facilitated energy transitions in mitigating deforestation.

Specifically, Table 1.9 presents the estimated effects of out-migration on various energy transition outcomes. The dependent variables include: (1) "Electricity Connection," which captures whether a household has an active electricity connection as of 2015; (2) "Electric Cooking," which measures whether electricity is the primary fuel used for cooking in 2015; (3) "Private Electricity," indicating whether the household purchased electricity from private providers in 2015; and (4) "Public Electricity," indicating purchases from public sources in 2015.

The results show that households experiencing out-migration are significantly more likely to adopt electricity for general household use and cooking. Households with out-migrants are approximately 3.7% more likely to have an electricity connection and 2.6% more likely to use electricity as their primary cooking fuel. Additionally, households with out-migrants are marginally more likely to purchase private electricity, although the effect is statistically significant only at the 10% level. In contrast, out-migration has no statistically significant impact on purchasing public electricity. These findings suggest that out-migration facilitates energy transitions primarily through increased access to private electricity sources rather than through public electricity systems.

While these results provide strong cross-sectional evidence, it is essential to acknowledge a limitation: the energy transition data are available only for 2015, whereas our primary deforestation analysis spans from 2000 to 2015. Thus, we cannot directly observe dynamic changes in energy adoption over time. Nevertheless, a back-of-the-envelope calculation suggests that the observed magnitude of energy transitions is plausibly large enough to explain our estimated impacts on deforestation. Specifically, given that firewood consumption typically requires approximately 36 m² of forest area per person annually (Kyaw et al., 2020), and that each migrant is associated with a reduction of approximately 5.4 m² of forest loss per year based on our System GMM estimates, even partial adoption of electricity could substantially reduce biomass extraction pressures. For instance, the 3.7% increase in electricity adoption among migrant households would imply a meaningful shift away from firewood use, consistent with the magnitude of observed forest cover savings. Although this rough calculation does not establish a definitive causal chain, it supports the plausibility of remittance-driven energy transitions as a key mechanism linking migration to localized environmental sustainability.

While our main estimates suggest that current migration significantly reduces deforestation, we find limited environmental impacts for return migration. This may reflect the fact that many households have already undergone energy transitions to cleaner fuels, facilitated by earlier remittance inflows. Preliminary survey evidence suggests that return migrants often contribute to household income diversification and bring back accumulated human capital, enabling access to higher-paying jobs. These improvements may reduce households' reliance on local forests, thereby diminishing the marginal environmental effect of return migration.

Additionally, the duration of migration spells, the length of time individuals remain away from their household, likely plays an important role. Longer-term migration is often associated with more sustained remittance inflows, which can further enhance household capacity to adopt clean energy sources and shift away from biomass dependence. Unfortunately, our dataset does not capture detailed measures of migration duration or remittance timing. Exploring these temporal dynamics represents a promising avenue for future research to better understand the long-run environmental impacts of migration.

More broadly, future work can help clarify the mechanisms through which migration affects land use and forest conservation by differentiating between migration margins (e.g., first-time vs. circular migration) and incorporating richer data on migration profiles and remittance intensity.

Figure 1.8 visually summarizes this proposed causal pathway from migration to environmental outcomes. Overall, the evidence on mechanisms complements our main causal results, suggesting that the environmental impacts of migration extend beyond household size changes to include transformative changes in household energy use.

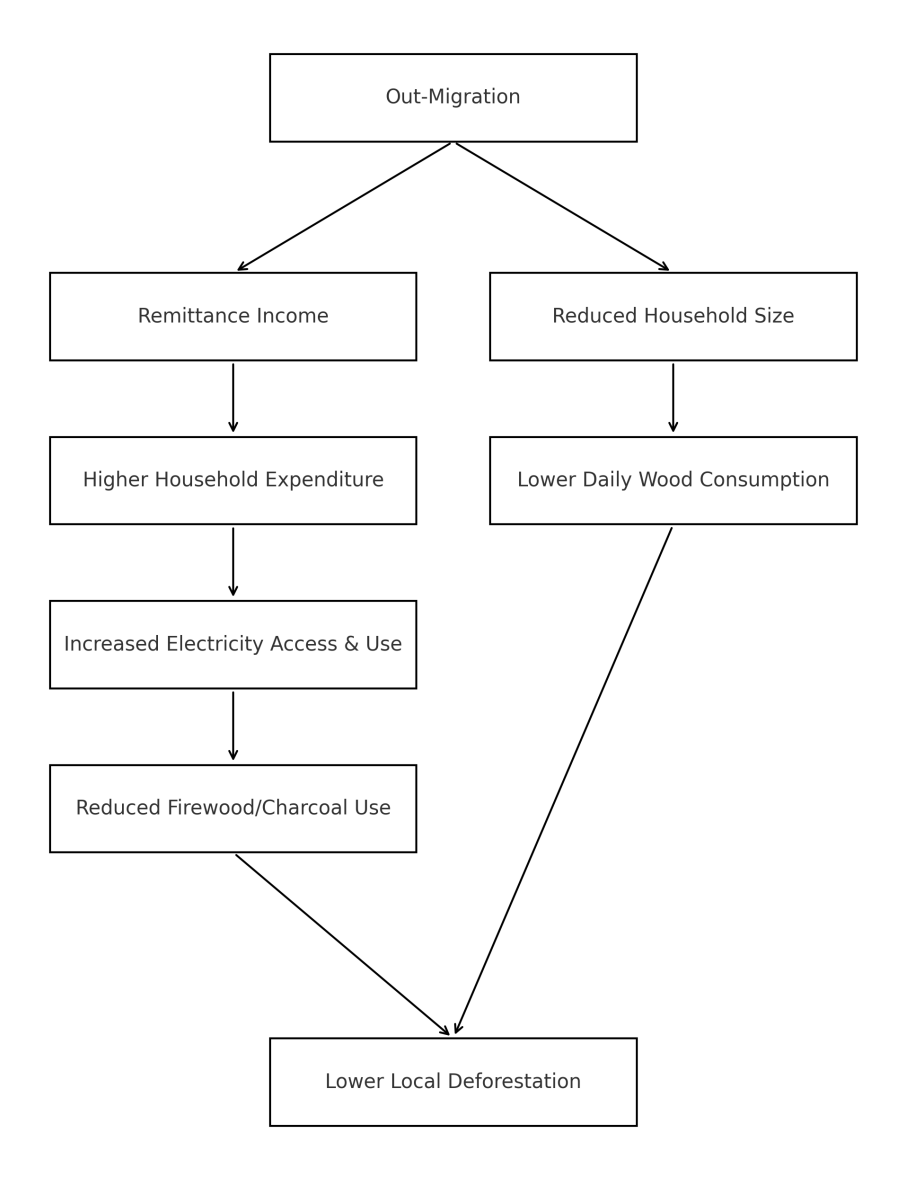


Figure 1.8: Two mechanisms linking out-migration to reduced deforestation: (1) a remittance-facilitated energy transition (left), and (2) reduced household wood use due to shrinking household size (right).

Table 1.9: Effect of Migration on Energy Transition Outcomes (OLS, 2015)

	Electricity Connection	Electric Cooking	Private Electricity Public Electricity	Public Electricity
∑ Out-migration (unweighted)	0.0368**	0.0262**	0.0258*	0.0105
Y Return migration (unweighted)	-0.0176	-0.0267	0.0083	0.0098
	(0.0302)	(0.0198)	(0.0291)	(0.0256)
Total income	1.11×10^{-9}	8.11×10^{-9}	-6.44×10^{-9}	1.44×10^{-8}
	(9.65×10^{-9})	(6.32×10^{-9})	(9.40×10^{-9})	(8.29×10^{-9})
Household size	-0.0081	-0.0013	0.0011	-0.0099
	(0.0090)	(0.0059)	(0.0087)	(0.0077)
Parcel size (ha)	0.0024	0.0022	-0.0025	0.0020
	(0.0022)	(0.0015)	(0.0022)	(0.0019)
Age of head	0.0049^{***}	0.0004	0.0006	0.0034^{***}
,	(0.0015)	(0.0010)	(0.0014)	(0.0013)
Occupation of head	0.0042	0.0101*	-0.0158*	0.0118*
•	(0.0073)	(0.0048)	(0.0071)	(0.0062)
Constant	0.2652^{***}	-0.0106	0.3302***	-0.0131
	(0.1009)	(0.0660)	(0.0978)	(0.0863)
Observations	069	069	703	703
R-squared	0.033	0.023	0.017	0.026
Adjusted R-squared	0.023	0.013	0.007	0.017
Residual Std. Error	0.484 (df = 682)	o.317 (df = 682)	0.472 (df = 695)	o.416 (df = 695)
F Statistic	3.33***	2.29**	1.67	2.68***

Notes: Robust standard errors in parentheses. $^*p < 0.1, ^{**}p < 0.05, ^{***}p < 0.01$

1.9 Conclusion

This study examines the causal relationship between out-migration and local deforestation in rural Myanmar by combining household-level migration survey data with high-resolution remote sensing data over 16 years. Using dynamic panel estimation techniques, we find robust evidence that out-migration mitigates local deforestation at local scales. The credibility of these findings is reinforced through extensive robustness checks across alternative model specifications, falsification tests using randomly reassigned migration variables, and two complementary reverse causality checks: a dynamic lead-migration test and a cross-sectional income mechanism test. Neither of these indicates evidence of reverse causality. In contrast, return migration shows a weak tendency to increase deforestation, although the mechanisms underlying this effect remain empirically inconclusive.

We further explore potential mechanisms through which out-migration reduces forest losses. Our analysis reveals that households experiencing greater out-migration are significantly more likely to access private electricity and adopt electric cooking. This suggests that remittance income helps facilitate an energy transition away from traditional biomass fuels, such as firewood and charcoal, toward cleaner, electricity-based alternatives. This energy transition mechanism provides a novel and underexplored pathway through which out-migration contributes to environmental sustainability, beyond the traditional explanation of reduced household consumption pressure.

Our findings contribute to the growing migration and environmental change literature. While prior studies, such as Ervin et al., 2020, document associations between migration and land cover change in sending communities, our study advances this literature by providing dynamic causal evidence at the household-buffer level and by identifying remittance-induced energy transition as a new and substantive mechanism linking migration to reduced deforestation. By focusing on a rural frontier region like Mon State, Myanmar, our study extends the geographic scope of migration-environment research beyond the more commonly studied settings in Latin America.

This paper offers three primary contributions. First, it reveals the dynamic causal impact of out-migration on local deforestation and explores the distinct effects of return migration. Second, it highlights a novel energy transition mechanism: out-migration facilitates access to electricity, particularly electric cook-

ing, through remittance income, offering an important new channel by which migration can mitigate environmental degradation. Third, it demonstrates how cross-sectional survey data can be transformed into a spatial panel by combining migration histories with historical remote sensing data, providing a replicable approach for studying environmental change in data-scarce settings.

Several caveats should be noted. Although we mitigate omitted variable bias using autoregressive modeling, fixed effects, and System GMM techniques, data limitations—such as the cross-sectional nature of the baseline household survey and the lack of fine-grained ecological variables like soil quality—may still pose risks to causal interpretation. Additionally, although we hypothesize that return migration may foster deforestation through agricultural expansion or construction activities, our empirical analysis does not find statistically significant support for these specific mechanisms. Future research with more detailed land use and infrastructure data could further illuminate the environmental consequences of return migration.

Overall, our findings reveal that migration's environmental impacts are not solely the result of household size changes, but also of profound household-level transformations in energy use.

CHAPTER 2

Do Mobile-Based Emergency Alerts Save Lives? Evidence from a Regression Discontinuity in Time⁶

⁶ Jiang, W. and Filipski, M. Submitted to Journal of Environmental Economics and Management, 05/18/25; under review as of 06/04/25.

2.1 Introduction

Natural disasters pose threats to life, infrastructure, and the economy. Among those, storms (including thunderstorms, hurricanes, tornadoes, or blizzards, depending on geography) have historically been among the most destructive and deadly (Strader et al., 2024; Young & Hsiang, 2024). The United States spends a considerable amount of public funding on disaster prevention and mitigation. In December 2024, the U.S. Congress passed a funding package that included \$110 billion in disaster assistance, allocating \$29 billion for FEMA's Disaster Relief Fund and \$12 billion for the Community Development Block Grant-Disaster Recovery (CDBG-DR) program (NLIHC, 2024). The Federal Emergency Management Agency (FEMA) allocated \$190.6 million to 110 pre-disaster mitigation projects (FEMA, 2024). Publicly funded disaster prevention programs include not only critical infrastructure and environmental buffers, but also effective early warning systems (World Bank & United Nations, 2010). The US has adopted a mobile-based alert system, known as the Wireless Emergency Alert (WEA), to deliver geographically targeted emergency notifications directly to mobile devices (FCC, 2012). In this paper, we evaluate the effectiveness of WEA in reducing storm casualties and provide empirical evidence that sheds light on the potential benefits of public investment in a mobile-based alert system.

From a public economics perspective, early warning systems like Wireless Emergency Alerts (WEA) represent a government response to a classic market failure in risk communication. Hazard warnings are public goods: they are nonexcludable and non-rivalrous. Yet individuals may underutilize or misinterpret such information due to bounded rationality, coordination problems, or limited real-time access. Empirical studies show that improving forecast accuracy can substantially enhance protective behavior and reduce adverse outcomes. For instance, Shrader et al., 2023 finds that increasing the precision of routine weather forecasts by half could prevent roughly 2,200 annual deaths in the U.S. linked to temperature extremes, particularly heat. They estimate this would yield societal benefits of \$2.9 billion annually. Molina and Rudik, 2022 similarly demonstrates that improved hurricane forecasting reduces storm-related damages by nearly 20%, equivalent to about \$5 billion per event. On a global scale, New et al., 2022 identifies early warning systems as a critical low-regrets adaptation strategy that already supports over five billion people. Historical evidence further underscores this value: during the 2004 Indian Ocean tsunami, access to timely disaster warnings significantly lowered mortality in Indian communities even in the absence of formal evacuation protocols (Vincent & Das, 2009).

Classic alert systems have been based on sirens, radio, or television broadcasts. They may help people protect themselves and their properties. However, they may not reach all individuals who could benefit from them. For instance, individuals who fail to tune in to the specific channels at the time of the alert are likely to miss the warning alerts and be unable to take action promptly (Drost et al., 2016). As a potential upgrade to these systems, the United States introduced the Wireless Emergency Alerts (WEA) in April 2012 (FCC, 2012). Developed by the Federal Communications Commission (FCC) jointly with the Federal Emergency Management Agency (FEMA) and other federal agencies, WEA can deliver real-time geographically targeted warnings directly to mobile devices. The widespread adoption of mobile devices in the 21st century has significantly expanded the reach of WEA. Meanwhile, mobile-based alert systems, such as WEA, provide timely and accurate storm warnings directly to individuals with access to mobile devices in affected areas.

While previous studies have examined various aspects of WEA, most focus on implementation and technical functionalities, public perception and response, and content optimization. Regarding functionality, researchers mainly focused on its geographic targeting capabilities (Gao & Wang, 2021), message dissemination efficiency (Lambropoulos et al., 2021), integration with mobile networks (Kumar et al., 2018), reliance on cellular networks (Bitsikas & Pöpper, 2022; Simon et al., 2015), and effectiveness of warning message compositions (Casteel & Downing, 2016; Olson et al., 2024). Meanwhile, research on public perception and response has primarily focused on exploring public awareness, understanding, and trust in warning messages (Bean et al., 2016) and whether targeted recipients take prompt action (Bean & Grevstad, 2022). WEA content optimization, especially the length of warning messages and information composition, is also an essential field of WEA studies (Bean et al., 2023; Best, 2017; NASEM, 2018). As part of ongoing improvements driven by prior research, in 2019, the FCC introduced several enhancements to the WEA system, including longer alert messages (90 to 360 characters), support for Spanish language, public safety messages, and improved display capabilities on mobile devices. Additionally, a new category of alerts ("State/Local WEA Tests") was established to enhance proficiency and public awareness (FCC, 2019).

In contrast, evaluations of WEA's effectiveness in emergency mitigation are scarce. Among those, several studies have analyzed the role of WEA and similar

mobile-based alert systems in mitigating the spread of COVID-19. Yeon et al., 2022 investigated how WEA alerts influenced public compliance with social distancing mandates, finding that regions receiving timely alerts had greater adherence to movement restrictions and reduced mobility patterns. Bean et al., 2022 examined the impact of WEA messages on COVID-19 infection rates and deaths across U.S. states and localities, finding that areas issuing WEA alerts saw estimated reductions in COVID-19 transmission, suggesting that mobile-based emergency alerts can play a role in public health crisis management. Some research focuses on assessing WEA's impact in specific emergency scenarios. For example, Ferris and Newburn, 2017 examined the effectiveness of WEA flood alerts in reducing car accidents, showing that drivers who received timely warnings were more likely to avoid flooding areas, leading to a decline in flood-related traffic accidents. Meanwhile, a thorough evaluation of WEA's performance in storms, the deadliest and most destructive weather-related disasters in the United States (NOAA, 2025), is still lacking. However, such research is essential to public safety and disaster prevention because it provides empirical evidence of the mobile-based warning system's performance in storms to help policymakers assess its effectiveness, justify continued investment, and optimize future improvements in storm response strategies. This study fills this gap by providing the first nationwide empirical assessment and quantification of WEA's impact on storm-related fatalities using a Regression Discontinuity in Time (RDiT) framework over the 2000-2024 period.

To accurately assess the impact of the WEA system on daily average deaths during severe storms, we employ a Regression Discontinuity in Time (RDiT) framework, a method well-suited for evaluating interventions with a single launch date defining clear before and after periods (Hausman & Rapson, 2018). In this case, we set the cutoff as April 2012, when WEA was implemented. We use a bandwidth of 12 years, applying data from 2000 to 2024 to compare storm-caused fatalities before and after introducing WEA. This approach allows for a clear and precise estimation of the WEA system's effect on daily average fatalities during storms, isolating the impact of the intervention from other factors with the assistance of placebo and falsification tests.

Our results indicate that WEA significantly reduces average daily storm-related fatalities by 4.306 per event. We further conducted placebo tests with alternative cutoffs in April 2010, 2011, 2013, and 2014 as part of the robustness checks. The absence of significant effects before 2012 and a less pronounced effect in 2013, likely due to increased smartphone adoption and public familiarity with WEA, further supports the validity of our findings (Levy, 2015; Morss et al.,

2017). Furthermore, We perform a falsification test by examining the impact of WEA on non-flash floods, a category of disasters not covered by WEA. We do not observe a significant effect on non-flash flood fatalities, reinforcing the conclusion that the observed reduction in storm-related fatalities is credited to WEA. Additionally, to address the concern that our findings about WEA's impact might partly result from including an extreme event (Hurricane Katrina), we conduct robustness checks using data without Hurricane Katrina to show the robustness of our results. We further conduct robustness checks on technological advancement by using the percentage of people with an internet connection as a proxy.

The remainder of the paper is organized as follows. Section 2 describes the data, key variables, and the Regression Discontinuity in Time (RDiT) framework, along with robustness checks, placebo tests, and falsification tests. Section 3 presents the main findings and validation results. Section 4 discusses the study's limitations. Finally, Section 5 concludes with key findings and policy implications.

2.2 Empirical Approach

2.2.1 Data

We investigate the treatment effect of Wireless Emergency Alerts (WEA) using data primarily from the Emergency Events Database (EM-DAT) provided by the Centre for Research on the Epidemiology of Disasters (CRED) (D.Guha-Sapir et al., 2015). EM-DAT contains information on over 22,000 disasters worldwide, including 704 storms that occurred in the United States, spanning from 1900 to the present. The database records the destructive consequences of these disasters.

Table 2.1: Descriptive Statistics: U.S. Storms 2000-2024

Variable	Total	Mean	Standard Deviation
Total Deaths	6888	22.510	108.452
Deaths/day		5.127	9.213
Total Damage (Billions USD\$)	1395.138	4.697	16.482

Table 2.2: Categorical breakdown of storm subtypes

Category	Frequency	Proportion
Tornado	103	0.29
Blizzard/Winter storm	69	0.19
Tropical cyclone	61	0.17
Severe weather	43	0.12
Storm (General)	4 I	O.II
Lightning/Thunderstorms	32	0.09
Hail	8	0.02
Derecho	2	0.01
Extra-tropical storm	I	0.00
Sand/Dust storm	I	0.00
Total Storm Counts	361	1.00

We present total counts, means, and standard deviations for total deaths, average daily deaths, and total damages (in billions of US dollars) in Table 2.1, highlighting the fatality and economic impact of storms in the United States. From 2000 to 2024, the events in our dataset account for 6,888 deaths and \$1,395.14 billion in property damage, reinforcing the severe destructiveness of storms. On average, each storm results in 22.51 fatalities, with 5.127 deaths per day during storm events. Table 2.2 presents the frequency distribution of storm subtypes and their proportion to recorded storms in our working data. As expected, tornadoes, blizzards, and tropical cyclones are the most frequent storm types in the United States, aligning with established meteorological patterns.

2.2.2 Graphical Evidence on The Effects of WEA

Figure 2.1: Storm fatalities 2000-2024

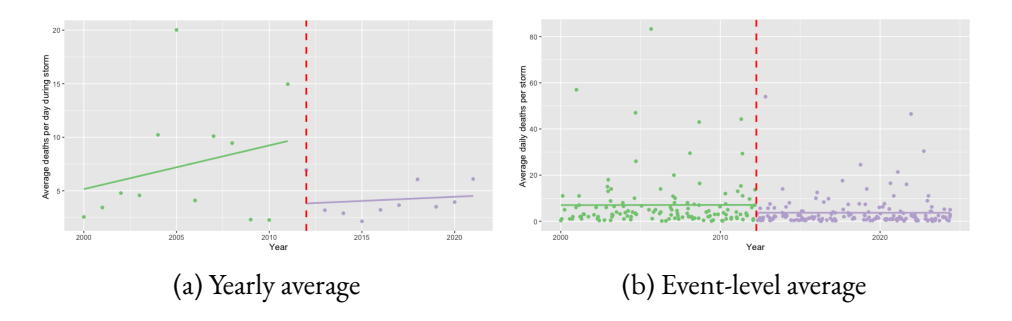


Figure 2.1 illustrates two measures of storm-related fatalities. Figure 2.1a presents the yearly averages of daily deaths, calculated by first determining the average daily deaths for each storm within a year and then averaging these values across all storms in that year. On the other hand, Figure 2.1b shows the event-level average daily fatalities during individual storms.

In both Figures 2.1a and 2.1b, discernible value breakpoints and a substantial reduction in variability are observed immediately following the implementation of the Wireless Emergency Alerts (WEA) system by the National Weather Service in April 2012. This graphical evidence suggests a potential causal impact of WEA on reducing storm-related fatalities. We employ Regression Discontinuity in Time (RDiT) models to quantify this impact. Additionally, we conduct robustness checks, placebo tests, and falsification tests to ensure the validity of our estimates.

2.2.3 Regression Discontinuity in Time (RDiT) Framework

This study adopts a Regression Discontinuity in Time (RDiT) design to identify the causal effect of Wireless Emergency Alerts (WEAs) on storm-related mortality. Our key outcome variable is the average number of deaths per day during each storm event, calculated as the total number of fatalities divided by the storm duration in days. This normalization accounts for heterogeneity in storm duration and yields a consistent, policy-relevant measure of event severity.

Measuring Storm fatalities

Given the nature of Wireless Emergency Alerts (WEAs) as an early warning system, their effectiveness is most salient in preventing imminent storm-related fatalities. Ideally, the most accurate way to evaluate the impact of WEAs would be to examine deaths occurring in the first day—or even the first few hours—of a storm. However, such granular fatality data are unavailable in current disaster databases.

As a second-best approach, we use the average number of deaths per day during each storm, calculated as total fatalities divided by storm duration. This measure helps address several limitations associated with using total deaths alone. First, total deaths ignore the temporal dimension of storm severity—fatalities can occur days after a storm's onset due to secondary hazards such as flooding, infras-

tructure failure, or disruptions to medical services. Second, total death counts are highly sensitive to outliers, with a small number of catastrophic events (e.g., Hurricane Katrina) disproportionately influencing estimates. As shown in Table A5, when using total storm fatalities as the outcome, the estimated treatment effect is heavily distorted by the inclusion of Katrina, illustrating this issue. By normalizing fatalities by storm duration, our outcome mitigates these biases and enables more consistent comparisons across events of differing lengths and intensities.

Moreover, by normalizing deaths by storm duration, we improve comparability across events and better isolate the actual impact of WEA alerts, avoiding the risk that longer-duration storms with slower fatalities distort inference.

Importantly, the storm duration we use is based on EM-DAT's start and end dates, which follow standardized protocols. For U.S. events, EM-DAT primarily relies on disaster onset and closure dates from sources such as FEMA and NOAA. In most cases, these dates represent the official declaration period over which the event had measurable physical or human impact, ensuring consistency across storms.

While this measure may still include fatalities from delayed causes (e.g., patients injured on day I who died later), these deaths are still recorded under the original event in EM-DAT and are appropriately included in the numerator. Our denominator, storm duration, does not account for the injury-to-death time gap, but rather reflects the official time window during which the storm was active. This ensures the resulting outcome variable remains a reasonable proxy for the intensity of storm-related mortality.

Interpretation of Treatment Effects

This outcome reflects both the extensive and intensive margins of storm-related mortality. On the extensive margin, WEAs may reduce the likelihood that any fatalities occur during a storm. On the intensive margin, conditional on fatalities occurring, WEAs may reduce the number of deaths per day. Since our outcome is continuous and often zero, our estimates capture a blend of these two effects. Future work may disentangle them using separate models for death occurrence and intensity.

RDiT Specification

Visual inspection of Figure 2.1 suggests a discontinuity in average daily fatalities after WEAs were introduced in 2012. We use time (centered around April 1, 2012) as the running variable, and define a binary treatment indicator Threshold_i that switches from 0 to 1 at the introduction of WEAs. Following Hausman and Rapson (2018), time can be used as a valid forcing variable when the intervention date is sharp and exogenous.

$$\begin{aligned} \text{Deaths/day}_i &= \beta_0 + \beta_1 \text{Threshold}_i + \beta_2 (\text{Date Centered}_i) + \beta_3 \text{Disaster Subtype}_i \\ &+ \beta_4 \text{Total Damages}_i + \beta_5 \text{threshold}_i \text{Date centered}_i + \epsilon_i \end{aligned} \tag{2.1}$$

The Threshold_i is defined as:

Threshold_i =
$$\begin{cases} 0, & \text{if Date}_i < 04/01/2012\\ 1, & \text{if Date}_i \ge 04/01/2012 \end{cases}$$

The Date centered_i is defined as:

Date centered_i = Date_i
$$-04/01/2012$$

Our model uses several key variables to investigate their impact on average daily deaths during storms. First, our response variable, Deaths/day_i, quantifies the daily death count for each storm i. To facilitate the application of a regression discontinuity design, we introduce the binary variable threshold_i, which takes a value of 1 if the storm occurs in or after 2012 and 0 otherwise. We also incorporate the term (Date centered_i) to capture any linear temporal trend. Additionally, the variable Disaster Subtype_i accounts for the specific subtype of the storm, while Total Damages_i denotes the total damages incurred, adjusted for inflation, and presented in thousands of US dollars. The coefficients β_0 through β_4 are used to estimate the effects of each respective variable on the daily death count during storms. Finally, we introduce the error term ϵ_i to account for unexplained variability in the model.

We have excluded storm magnitudes from our model for two primary reasons. First, we face data limitations regarding storm magnitudes. Second, and more importantly, we view Total Damages as a more accurate measure of the storm's

threat to people. This metric considers both the storm's destructiveness and the value of human property in the disaster area, which is directly correlated with the number of people affected.

2.3 Empirical Results

In section 3.2, we have provided graphical evidence for the existing discontinuity in daily deaths for storms before and after 2012. In this section, we formally exploit the discontinuity in daily deaths during storms using the empirical results generated by estimating the model (2). To ensure robustness, we conduct Placebo and falsification tests using different thresholds and another disaster type, which Wireless Emergency Alerts did not focus on.

2.3.1 Main Results

In Table 2.3, we present Regression Discontinuity in Time (RDiT) estimates using model (1) with data spanning from 2000 to 2024. We set the bandwidth to 12 years. These estimates reveal the impact of key variables of interest, capturing the discontinuity in 2012 that signifies the eligibility threshold for receiving wireless emergency alerts (WEA), on daily storm-related deaths (as shown in Figures 1 and 2).

In Table 2.3, column (1) presents estimates without including the interaction term, providing a baseline assessment of the effect of WEA on daily fatalities during storms. This specification does not account for potential variation in the impact of WEA over time. Column (2), on the other hand, includes the interaction term "Threshold \times Date centered;", allowing us to assess whether the effect of WEA on daily fatalities during storms varies across different temporal trends. Both columns reveal a statistically significant negative impact of WEA on daily fatalities during storms, with Column (2) providing insights into how this effect may change over time.

In summary, the empirical findings in Table 2.3 offer robust evidence supporting the efficacy of wireless emergency alerts in reducing storm-related fatalities while also considering potential variations in the effect over time through the inclusion of the interaction term.

Table 2.3: RD estimates of the effect of WEA on deaths/day during storms

	Dependen	t variable:
	Deaths	per day
	(1)	(2)
Threshold	-4.306**	-4.653**
	(1.829)	(1.840)
Date (centered)	0.0003	0.001*
	(0.0004)	(0.001)
Storm type: Derecho	-5.130	-4.304
	(5.103)	(5.122)
Storm type: Extra-tropical storm	-4.907	-4.92 I
	(7.130)	(7.113)
Storm type: Hail	-1.530	—1.176
71	(3.311)	(3.312)
Storm type: Lightning/Thunderstorms	-2.559	-2.537
71 0 0	(2.077)	(2.072)
Storm type: Sand/Dust storm	— 1.049	-0.619
71	(7.096)	(7.085)
Storm type: Severe weather	-2.354	-2.019
71	(1.635)	(1.647)
Storm type: Storm (General)	-2.759	-2.084
	(1.731)	(1.787)
Storm type: Tornado	-о.118	0.268
	(1.345)	(1.367)
Storm type: Tropical cyclone	-1.774	-1.36o
, , ,	(1.509)	(1.531)
Total damage (Billions USD)	0.347***	0.346***
	(0.027)	(0.027)
Threshold: Date(centered)		-0.001
		(0.001)
Constant	6.954***	7.97I***
	(1.549)	(1.694)
Observations	253	253
\mathbb{R}^2	0.466	0.470
Adjusted R ²	0.439	0.442
Residual Std. Error	7.013 (df = 240)	6.996 (df = 239)
F Statistic	17.424*** (df = 12; 240)	16.326*** (df = 13; 239

Note: *p<0.1; **p<0.05; ***p<0.01

2.3.2 Placebo and Falsification Tests

In our placebo tests, we aimed to strengthen the credibility of our Regression Discontinuity in Time (RDiT) analysis by using 2010, 2011, 2013, and 2014 as placebo thresholds. Table 2.4 presents the empirical estimates from these placebo tests. The headers Threshold=2010, Threshold=2011, Threshold=2013, and Threshold=2014 correspond to the estimated results using 2010, 2011, 2013, and 2014 as placebo thresholds, respectively.

In the case of April 2010 and 2011, used as a placebo threshold, our analysis reveals the non-significant effects of WEA on daily fatalities during storms. This outcome suggests that no similar negative treatment effect likely existed before the implementation of WEA in 2012, reinforcing the validity of our RDD design.

Conversely, we observe statistically significant results when employing 2013 as a placebo threshold. This finding aligns with our hypothesis that adopting new technology is associated with a learning curve. In the early stages following WEA's introduction in 2012, it is conceivable that public awareness and understanding of the system were still in development, potentially resulting in a less pronounced immediate effect. However, as time progressed, our results suggest that the impact of WEA on daily storm-related deaths became increasingly evident, reflecting the gradual growth in public trust and reliance on this lifesaving alert system. Although the results from the 2013 placebo tests offer valuable insights into the dynamics of Wireless Emergency Alert (WEA) adoption and their impact on daily storm-related deaths, it is essential to acknowledge a limitation of our current study. We do not possess direct empirical evidence regarding the public's learning curve associated with WEA adoption and its gradual increase in awareness and understanding. While we posit that such a learning curve may have contributed to the delayed impact observed in 2013, we recognize the need for future studies to provide more concrete evidence. By setting April 2014 as the threshold, we find that the significance observed in 2013 wore off, reinforcing our hypotheses about the effects seen in the 2013 placebo.

To enhance the robustness and credibility of our primary findings, we employ falsification tests utilizing daily fatality data associated with non-flash floods. These falsification tests are particularly pertinent as Wireless Emergency Alerts (WEA) exclusively address flash floods, leaving non-flash floods, predominantly riverine, as a suitable counterfactual for assessing the impact of WEA availability.

The results of our falsification tests are presented in Table 2.5, where we apply Regression Discontinuity analysis.

Our analysis reveals no statistically significant treatment effect of the WEA availability threshold on non-flash floods. This finding effectively negates any assertion that WEA has an impact on daily fatalities during non-flash flood events. Conversely, our results from the falsification tests substantiate the claim that reducing daily fatalities during storms can be attributed to implementing WEA. As a result, these falsification tests support the assertion that the observed reductions in daily fatalities are due to the effectiveness of the WEA system.

In summary, our placebo and falsification tests enhance the validity of our main finding, which is that WEA effectively reduces daily deaths during storms while further exploring the evolving positive influence that WEA has had over time. Acknowledging the limitation related to the absence of direct empirical evidence on the public learning curve serves as an avenue for future research in this critical study area.

Table 2.4: RD estimates of the placebo tests using different thresholds

					7			
				Deaths	Deaths per day			
	Threshold=2010	ld=2010	Thresh	Threshold=2011	Thresho	Threshold=2013	Thresh	Threshold=2014
	(1)	(2)	(3)	(4)	(8)	(9)	(2)	(8)
Threshold	0.292 (2.106)	0.045 (2.096)	-0.265 (1.964)	-1.135 (2.033)	-3.419* (1.866)	-3.408* (1.878)	-2.268 (1.919)	-2.252 (1.919)
Date (centered)	-0.0004 (0.0005)	00.00	-0.0003 (0.0004)	0.001	0.0001	0.00004 (0.001)	-0.0002 (0.0005)	100.00)
Storm type: Derecho	-4.867 (7.329)	-3.287 (7.328)	-4.382 (5.323)	-3.496 (5.335)	-4.044 (5.246)	-4.080 (5.291)	-3.266 (5.325)	-3.954 (5.370)
Stom type: Extra-tropical storm	-2.952 (7.328)	-3.669 (7.289)	-3:349 (7:427)	-3.842 (7.409)	-4.284 (7.305)	-4.306 (7.330)	-3.89I (7.417)	-4.515 (7.444)
Storn type: Hail	-0.831 (3.417)	-0.507 (3.399)	-1.088 (3.451)	-0.842 (3.443)	-1.054 (3.403)	-1.083 (3.443)	-0.884 (3.496)	-1.485 (3.548)
Storm type: Lightning/Thunderstorms	-2.543 (2.149)	-2.422 (2.135)	-2.750 (2.159)	-2.739 (2.151)	-2.541 (2.137)	-2.545 (2.143)	-2.413 (2.198)	-2.552 (2.203)
Storm type: Sand/Dust storm	-0.548 (7.295)	0.572 (7.271)	-0.882 (7.385)	-0.380 (7.367)	-0.224 (7.289)	-0.241 (7.3u)	o.275 (7.411)	-0.0II (7.417)
Storm type: Severe weather	-1.828 (1.983)	-1.745 (1.971)	-2.063 (1.767)	-1.851 (1.766)	-1.856 (1.698)	-1.871 (1.718)	-1.394 (1.724)	-1.734 (1.758)
Storm type: Storm (General)	-1.356 (2.082)	-0.959 (2.079)	-1.666 (1.923)	-1.174 (1.942)	-2.083 (1.859)	-2.117 (1.938)	-1.192 (1.941)	-1.819 (2.041)
Storn type: Tornado	0.463 (1.483)	0.675	0.534 (1.405)	0.835 (1.414)	1.064 (1.423)	1.049 (1.446)	1.603	1.248 (1.499)
Storm type: Tropical cyclone	-0.676 (1.633)	-0.166 (1.645)	-1.185 (1.580)	-0.84I (1.590)	-1.024 (1.576)	-1.047 (1.621)	-0.440 (1.625)	-0.906 (1.691)
Fotal damage (Billions USD)	0.363*** (0.030)	0.360***	0.348***	0.347*** (0.028)	0.343*** (0.028)	0.343*** (0.028)	0.343***	0.341***
[hreshold: Date(centered)		-0.002* (0.001)		100.0)		0.0001		0.001
Constant	4.088** (1.644)	5.686*** (1.839)	4.490*** (1.612)	6.084*** (1.8 <i>9</i> 7)	5.942*** (1.519)	5.901*** (1.659)	4.867*** (1.446)	4.331*** (1.543)
Observations R ²	205	205	238	238	234	234	226	226
Adjusted R ² Residual Std. Error	0.436 7.180 (df = 192)	0.444 7.132 (df = 191)	0.423 7.295 (df = 225)	7.27	0.446 7.201 (df = 221)	0.444 7.217 (df = 220)	0.447 7.314 (df = 213)	0.447 7.314 (df = 212)

Table 2.5: RD estimates of falsification tests using Non-flash flood

	Dependen	t variable:
	Deaths	per day
	(1)	(2)
Threshold	-o.62o	-o. ₇₂₄
	(0.908)	(0.948)
Date (centered)	0.0001	0.0002
	(0.0002)	(0.0003)
Flood type: Riverine flood	-I.256**	-1.4II*
71	(0.601)	(0.704)
Total damage (Billions USD)	-o.oii	-o.oi7
,	(0.070)	(0.072)
Threshold: Date (centered)		-0.0002
,		(0.0004)
Constant	2.425***	2.805**
	(o.688)	(1.117)
Observations	49	49
\mathbb{R}^2	0.121	0.124
Adjusted R ²	0.041	0.023
Residual Std. Error	1.488 (df = 44)	1.502 (df = 43)
F Statistic	1.509 (df = 4; 44)	1.222 $(df = 5; 43)$

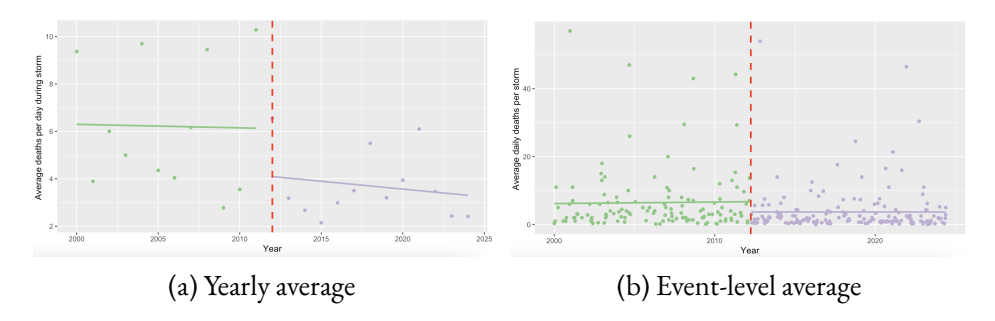
Note: *p<0.1; **p<0.05; ***p<0.01

Table 2.6: RDiT estimates of the effect of WEA on deaths/day during storms (Without Hurricane Katrina)

	Dependen	et variable:
	Deaths	per day
	(I)	(2)
Threshold	-4.218**	-4.575**
	(1.814)	(1.824)
Date (centered)	0.0004	0.001*
	(0.0004)	(100.00)
Storm type: Derecho	-5.039	-4.184
	(5.059)	(5.076)
Storm type: Extra-tropical storm	-4 . 766	-4.779
	(7.069)	(7.050)
Storm type: Hail	-I.428	-1.061
	(3.283)	(3.282)
Storm type: Lightning/Thunderstorms	-2.554	-2.532
	(2.059)	(2.053)
Storm type: Sand/Dust storm	-1.22I	-o.779
	(7.035)	(7.021)
Storm type: Severe weather	-2.416	-2.07I
	(1.622)	(1.633)
Storm type: Storm (General)	-2.705	-2.008
	(1.716)	(1.771)
Storm type: Tornado	-0.028	0.372
	(1.334)	(1.356)
Storm type: Tropical cyclone	-1.197	-o.762
	(1.517)	(1.539)
Total damage (Billions USD)	0.289***	0.288***
	(0.037)	(0.036)
Threshold: Date (centered)		-0.001
		(100.00)
Constant	6.951***	8.002***
	(1.535)	(1.679)
Observations	252	252
\mathbb{R}^2	0.275	0.282
Adjusted R ²	0.239	0.243
Residual Std. Error	6.952 (df = 239)	6.933 (df = 238)
F Statistic	7.567*** (df = 12; 239)	7.203*** (df = 13; 23

Note: *p<0.1; **p<0.05; ***p<0.01

Figure 2.2: Storm Fatalities 2000-2024 (Excluding Hurricane Katrina)



2.3.3 Robustness Checks

Robustness to Hurricane Katrina Inclusion

Figures 2.1a and 2.1b show extreme values in 2005, primarily due to Hurricane Katrina, which claimed over 1,800 lives. While we do not initially filter it out as an outlier in the primary analysis to maintain data authenticity and ensure statistical power, concerns may arise that the significant variation caused by Katrina could skew the results. To address this, we first visualize the yearly average daily deaths and event-level average daily deaths for storms after filtering out Hurricane Katrina in figure 2.2 to double-check for apparent cutoffs and then re-estimate our specification using data that excludes Hurricane Katrina, ensuring that this outlier event does not drive our findings. The plots in figure 2.2a and 2.2b show sharp cutoffs in 2012. Meanwhile, results from table 2.6 are consistent with our main results in table 2.3, confirming the robustness of our results regarding the inclusion of Katrina.

Robustness to Technology Advancement

In the first quarter of 21st century, the world experienced rapid technological advancements. We recognize that new information channels for storm alerts, such as social media platforms, may have emerged as additional ways for people to receive warnings about approaching storms. Although WEA messages should be more timely and accurate than new information channels, this still raises concerns about whether these developments could bias our main results. Specifically, our estimates may overstate the impact of WEA by inadvertently

Table 2.7: RD estimates of the effect of WEA on deaths/day during storms (with internet adaptation rate)

	Dependen	t variable:
	Deaths	per day
	(I)	(2)
Threshold	-4.008**	-4.519**
	(1.983)	(2.011)
Date (centered)	0.0001	0.001
	(0.001)	(100.00)
Storm type: Derecho	-5.030	-4.276
	(5.118)	(5.135)
Storm type: Extra-tropical storm	-5. 110	-5.008
	(7.161)	(7.147)
Storm type: Hail	-1.708	-1.258
••	(3.347)	(3.355)
Storm type: Lightning/Thunderstorms	-2.575	-2.545
,, ,	(2.081)	(2.076)
Storm type: Sand/Dust storm	-1.137	-0.664
••	(7.112)	(7.105)
Storm type: Severe weather	-2.326	-2.013
••	(1.640)	(1.651)
Storm type: Storm (General)	-2.775	-2.103
	(1.734)	(1.794)
Storm type: Tornado	-0.059	0.286
	(1.355)	(1.374)
Storm type: Tropical cyclone	−1 . 761	-1.363
	(1.512)	(1.534)
Total damage (billions USD)	0.346***	0.346***
•	(0.027)	(0.027)
Internet percentage	4.578	1.956
	(11.611)	(11.734)
Threshold: Date (centered)		-0.001
		(100.0)
Constant	3-377	6.425
	(9.202)	(9.431)
Observations	253	253
\mathbb{R}^2	0.466	0.470
Adjusted R ²	0.437	0.439
Residual Std. Error	7.025 (df = 239)	7.010 (df = 238)
F Statistic	16.039*** (df = 13; 239)	15.100*** (df = 14; 23

Note: *p<0.1; **p<0.05; ***p<0.01

capturing the effects of other information channels, such as social media. Given the difficulty of fully accounting for all new information channels, we use the percentage of people with internet connections in the U.S. as a proxy. This data is sourced from Statista, 2024, which reports annual internet penetration rates from 2000 to 2024. The rationale behind this approach is that regardless of the apps or devices used, these new channels depend on internet connectivity. Thus, we use the percentage of people with internet access to approximate the potential life-saving effects of these new information channels during storms.

From Table 2.7, the results align with our main findings, further reinforcing the robustness of our estimates regarding WEA's life-saving impact. Moreover, we find no evidence that the percentage of people with internet connections has a significant effect on storm-related fatalities. This finding raises questions about the effectiveness of new information channels in reducing storm-related deaths substantially. This result aligns with our expectations, as storm alerts are time-sensitive. WEA is designed to be faster and more reliable than unofficial alerts due to its carefully optimized mechanisms. These findings strengthen our confidence in the robustness of our main results, even in the context of technological advancements.

2.4 Caveats

This research provides valuable insights into the life-saving impacts of the Wireless Emergency Alerts system on storms. Meanwhile, several caveats are worth considering. Our primary limitation lies in data availability. Unlike recurring events such as traffic jams or flight delays, storms occur infrequently—an inherently positive fact, but one that limits the number of observations we can collect within a relatively short time frame. Additionally, storms' sudden and unpredictable nature prevents us from using statistical tools to simulate data. As a result, we cannot use narrow bandwidths typical in other Regression Discontinuity Designs (RDD). To ensure sufficient observations, we extend the study period from 2000 to 2024, resulting in a 12-year bandwidth for our analysis. However, a wider bandwidth introduces concerns about potential changes over time that we may not fully control.

While some studies suggest an increasing trend in the frequency and magnitude of storms (Emanuel, 2013; Field et al., 2012), there is no evidence of a significant structural shift in storm patterns over the past two decades that would bias our

estimates. Even if a gradual increase in fatalities is observed, it would not explain the sharp reduction in fatalities observed precisely at the policy cutoff. If storm trends were the primary driver, we would expect a smooth increase in fatalities over time rather than a discrete drop at a specific date. To further address this concern, we incorporate an interaction term between the threshold and date in our model, allowing for the possibility that storm-related fatalities follow an upward trend that changes post-policy implementation. The insignificance of this interaction term suggests that the observed reduction in fatalities is not driven by an underlying increase in storm frequency but rather by implementing the Wireless Emergency Alerts (WEA) system. Additionally, our robustness checks—such as placebo tests using alternative thresholds—further reinforce that the observed decline in storm-related deaths is not an artifact of broader storm trends.

While we are less concerned about changes in storm characteristics, other time-varying factors could introduce bias into our estimates. These include demographic shifts, variations in infrastructure, and housing quality, which are difficult to account for comprehensively. Among these, technological advancements in the early 21st century present the most significant potential source of bias, as they could improve early warning systems and influence storm preparedness independent of WEA. To mitigate this concern, we adopt the percentage of people with internet connection in the U.S. as a proxy for broader technological improvements in information access. However, given that this data is available only at the national level and yearly increments, it may not fully capture local-level technological changes during each storm event.

The invention of the Wireless Emergency Alerts (WEA) system represents a remarkable milestone in technological advancement, but it is not the only innovation in this domain. The emergence of social media, mobile apps, online platforms, and other new information sources also holds the potential for serving as storm alert channels. While the design of WEA ensures its superiority in delivering messages quickly and accurately compared to other information channels, we still aim to account for the impacts that might arise from these alternative sources. Given the impracticality of collecting data on every possible information channel, we use the percentage of people connected to the internet as a proxy. This choice reflects our understanding that internet access is a prerequisite for obtaining information regardless of the specific apps or platforms used on various types of devices.

However, the data we use for the percentage of people with internet connection is annual and aggregated at the national level, rather than event-level data that captures the proportion of people with internet access in the affected storm area at the time of the storm. While we believe this proxy can capture the overall trend of technological advancements' impact on storm fatalities (aside from WEA), its inability to reflect precise, localized, and event-specific conditions limits its accuracy in addressing these impacts.

2.5 Conclusion and Discussion

This study provides empirical evidence that the Wireless Emergency Alerts (WEA) system significantly reduces storm-related fatalities in the United States, demonstrating its value as a public investment in disaster preparedness. By delivering timely and geographically targeted warnings, WEA helps prevent loss of life, making it an effective tool for mitigating storm-related risks in an era of increasing climate threats.

In our dataset of 361 major storm events from 2000 to 2024, we identify 205 events that occurred after implementing the Wireless Emergency Alerts (WEA) system in April 2012. Based on our estimated treatment effect, which suggests that WEA reduces daily average fatalities by 4.3 deaths per storm, and the average length of the included storms is 4.16 days (excluding outlier events with disaster length over 50 days), this implies that WEA may have prevented approximately 3,667 storm-related deaths since its launch. Over the 13 years of WEA operation, this corresponds to roughly 282 lives saved per year. Applying the U.S. Department of Transportation's 2024 Value of a Statistical Life (VSL) of \$13.7 million (USDOT, 2021), we estimate the total societal benefit from reduced fatalities at approximately \$50.23 billion, or about \$3.86 billion per year. These gains reflect the value of mobile-based, publicly provided risk information as a public good, mitigating the fatal consequences of coordination failures and information asymmetries during disasters.

The financial investment required to implement WEA appears modest by comparison. The initial \$106 million in federal funding for WEA was authorized under Section 3010 of the Deficit Reduction Act of 2005 (Public Law 109-171), which established the Digital Transition and Public Safety Fund to support the development of a national alert system (U.S. Congress, 2006). In a 2021 cost assessment, the Federal Communications Commission estimated that wireless

providers would incur a one-time compliance cost of approximately \$14.5 million for technical upgrades and software implementation (FCC, 2021). While ongoing maintenance costs are not publicly detailed, the available figures indicate that WEA's public health and economic benefits substantially outweigh its implementation costs, which suggests a high benefit-cost ratio. These findings reinforce WEA's role as a cost-effective public safety investment with scalable potential as climate-related weather risks continue to rise.

Our results offer valuable insights for both policymakers and the general public. For policymakers, WEA's demonstrated effectiveness suggests that regions without similar alert systems should consider adopting them. Those regions with existing systems should enhance functionality to improve accuracy, timeliness, and public trust. For the general public, our findings reinforce the life-saving importance of acting promptly upon receiving WEA alerts. Public trust and responsiveness to emergency warnings are essential in maximizing the benefits of these systems.

Despite its effectiveness, several challenges remain. Alert fatigue—where repeated exposure reduces responsiveness—could diminish WEA's effectiveness over time (Mileti & Sorensen, 1990; Wogalter, 2018). Similarly, false alarms may erode public trust and discourage timely action (DeYoung et al., 2019). Moreover, the effectiveness of WEA depends not only on timely delivery but also on message clarity, ensuring recipients can easily understand and act on the information (Wood et al., 2012). Increasing public education on WEA's importance and integrating disaster preparedness initiatives can further enhance its impact (Bean & Grevstad, 2022; Wood et al., 2012). Hence, further investments in message clarity, geo-targeting precision, and public awareness campaigns can potentially increase WEA's effectiveness and generate high returns in public safety at a relatively low cost.

Our study provides novel evidence at the national level on the life-saving effects of the mobile-based alert system, specifically the Wireless Emergency Alerts (WEA) system, during severe storms. Even though researchers have long suspected that such systems matter, there has been surprisingly little causal work at a national scale. We show that WEA reduces fatalities likely in a highly cost-effective manner. These results make a strong case for keeping, expanding, and refining mobile-based public warning systems. Our findings have increased relevance in light of the current climatic shifts. As extreme weather risks rise along with climate change, timely and accurate information may become as important as stable physical infrastructure. Mobile-based alerts like WEA help people

take faster and more effective self-protection actions during extreme weather events, and that's a public investment worth making.

CHAPTER 3

THE EFFECT OF DISASTER
AID ON RECOVERY:
EVIDENCE FROM FEMA
PUBLIC ASSISTANCE
PROGRAM⁷

⁷ Jiang, W. and Filipski, M. To be submitted to a peer-reviewed journal.

3.1 Introduction

Natural disasters impose severe and uneven infrastructure shocks across communities, often disrupting electricity access, transportation networks, and other essential public services. In response, governments deploy large-scale post-disaster assistance programs aimed at facilitating recovery. In the United States, the Federal Emergency Management Agency (FEMA) administers the Public Assistance (PA) program, which allocates funds to eligible jurisdictions to repair and restore damaged public infrastructure. Despite the program's scale and fiscal significance, empirical evidence on its effectiveness remains limited. Moreover, recent studies highlight that the distributional effects of FEMA's Individuals and Households Program (IHP) vary with social vulnerability, raising concerns about equity and efficiency in federal disaster response. (Emrich et al., 2022). Similar heterogeneous effects may also be present in the allocation of FEMA Public Assistance funds.

This study evaluates the causal impact of FEMA Public Assistance on posthurricane infrastructure recovery by leveraging satellite-based nighttime light intensity as a proxy for local infrastructure functionality and economic activity. Nighttime lights provide consistent, high-resolution coverage of human settlements and have emerged as powerful tools for quantifying disasters' economic and infrastructural impacts. The Defense Meteorological Satellite Program (DMSP) and the Visible Infrared Imaging Radiometer Suite (VIIRS) are the two main sources of global nightlight data; while DMSP has been used since the early 1990s, VIIRS—launched in 2011—offers significantly higher spatial resolution, radiometric sensitivity, and calibration stability. Recent research demonstrates their validity for this purpose: Gibson et al., 2024 shows that widely used DMSP data can overstate disaster-related losses by more than 50%, highlighting the superior accuracy of VIIRS data in post-disaster contexts. Similarly, Schippers and Botzen, 2023 finds that changes in VIIRS nightlight intensity after Hurricane Katrina closely track population displacement and employment shifts. These findings support using VIIRS-based nightlights to measure FEMA's impact on recovery objectively. By combining this remote sensing data with county-level records of hurricane exposure and federal assistance, we assess how disaster aid shapes recovery trajectories across affected U.S. counties.

Our empirical strategy integrates an event-study difference-in-differences (DiD) design with inverse probability weighting (IPW), enabling us to compare treated and untreated counties across multiple pre- and post-hurricane periods while ad-

justing for observable imbalances. The identification strategy exploits variation in FEMA Public Assistance (PA) receipt among counties exposed to similar hurricane events between 2017 and 2022. Although treatment is not randomly assigned, FEMA allocates aid based on eligibility criteria and demonstrated need; we take several steps to mitigate concerns about selection bias. First, we include controls for hurricane severity (e.g., maximum wind speed and disaster duration) and key socioeconomic characteristics. Second, IPW rebalances the sample based on observable characteristics, improving comparability between treated and untreated counties. Third, we test the assumption of parallel trends using multiple pre-treatment periods. Under the assumption that selection into treatment is based only on observable characteristics, our approach allows for a causal interpretation of medium- and long-run treatment effects.

Residual bias may persist if unobserved damage or vulnerability factors correlate with FEMA aid and recovery outcomes. Importantly, our findings show that treated counties, likely more severely affected, exhibit slower short-term recovery but ultimately outperform control counties in longer-run recovery trajectories. This pattern reinforces the interpretation that FEMA PA meaningfully contributes to post-disaster recovery, and may even underestimate its genuine effect due to conservative bias from non-random assignment.

We find that FEMA assistance leads to statistically and economically significant improvements in nightlight intensity in the medium and long term. While treated counties experience more initial light declines following hurricane on-set—likely reflecting temporary disruptions—light levels begin to rebound by six months and exceed those of comparable untreated counties within one to two years. These results hold across multiple specifications, including models that adjust for social vulnerability, economic conditions, storm severity, and county fixed effects. Robustness checks using FEMA eligibility as an alternative treatment definition yield similar patterns, underscoring the credibility of the findings.

Beyond average effects, we examine whether FEMA PA's efficacy varies by county characteristics. Counties are stratified into high and low groups based on the median of (i) personal income per capita, (ii) unemployment rate, and (iii) minority population share. Recovery is tracked across short-run (0–90 days), mediumrun (180–270 and 365–455 days), and long-run (730–820 days) periods. The results reveal that long-run gains are largest and most stable in high-income (5.13%), low-unemployment (4.25%), and low-minority (4.37%) counties, each exceeding the 3.45% average effect in the full sample. By contrast, low-income,

high-unemployment, and high-minority counties show smaller, more volatile effects, with evidence of pre-trend violations in some cases. These findings suggest that FEMA PA yields its greatest benefits in counties with stronger fiscal capacity, administrative readiness, and infrastructural resilience, while weaker recovery in more vulnerable counties underscores the need to improve equitable access to and absorption of federal disaster assistance.

This paper makes a substantive contribution to disaster recovery and public finance by delivering novel satellite-based evidence on the effectiveness of federal disaster aid. By integrating administrative FEMA data with high-frequency nighttime light indicators in a dynamic panel framework, we illuminate how post-disaster assistance fosters infrastructure resilience and shapes local recovery trajectories. Our findings have important implications for designing recovery policies in an increasingly frequent and severe natural hazards era. They also underscore earlier evidence that strong institutional capacity significantly mitigates disaster impacts, a theme well-documented in the natural disaster economics literature (Kahn, 2005; Tol, 2022).

3.2 Data

We construct a county-level panel dataset that combines information on federal disaster assistance, hurricane severity, nighttime lights, and socioeconomic characteristics. The outcome variable is average nighttime light intensity, measured using VIIRS Black Marble daily imagery (VNP46A2), which captures local infrastructure and economic activity at high spatial and temporal resolution. Our analysis spans counties across the contiguous United States affected by major hurricanes between 2017 and 2022.

Treatment is defined as receipt of FEMA Public Assistance (PA) funding, drawn from the Public Assistance Applicants Program Deliveries dataset (FEMA, 2025). This dataset also provides each hurricane's incident start and end dates, which we use to construct a series of post-hurricane recovery windows. These include two pre-hurricane periods (180–270 days prior and 365–455 days prior), one baseline period (90 days prior), and five post-hurricane periods spanning from 0 days to two years after the event.

We include maximum wind speed (from ERA5-Land hourly reanalysis data (C3S, 2019)), hurricane duration, and socioeconomic and demographic covari-

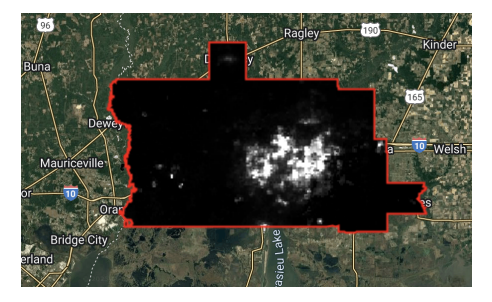
ates to account for key confounders. Real GDP per capita and personal income data are sourced from the U.S. Bureau of Economic Analysis (BEA) (BEA, 2025); population is from the U.S. Census Bureau (U.S. Census Bureau, 2025); and social vulnerability indicators (e.g., poverty, unemployment, minority share, disability) are from the CDC/ATSDR Social Vulnerability Index (SVI) (CDC/ATSDR, 2025).

3.2.1 Nighttime Light Intensity and Recovery Measurement

To measure post-disaster recovery, we use satellite-derived nighttime light intensity from NASA's VIIRS Black Marble dataset (VNP46A2: Lunar Gap-Filled BRDF Nighttime Lights Daily L3 Global 500m) (Román et al., 2018), which provides cloud-free, gap-filled daily imagery at 500-meter spatial resolution. We aggregate these data to the county level using spatial overlays and compute mean intensity values within defined recovery windows centered around each hurricane event.



(a) Nighttime lights in Calcasieu Parish, Louisiana, on August 1, 2020, approximately one month before Hurricane Laura's landfall. (Image generated using Google Earth Engine)



(b) Nighttime lights in Calcasieu Parish, Louisiana, on September 4, 2020, about one week after Hurricane Laura's landfall. (Image generated using Google Earth Engine)

Figure 3.1: VIIRS Black Marble nighttime light imagery of Calcasieu Parish before and after Hurricane Laura.

As an illustrative example, Figure 3.1a and Figure 3.1b present VIIRS Black Marble images of Calcasieu Parish, Louisiana, before and after the landfall of Hurricane Laura on August 27, 2020. The pre-hurricane image, dated August 1, 2020, captures typical nighttime light conditions, while the post-hurricane image, dated September 4, 2020, reflects conditions roughly one week after landfall. These single-date images were selected from one-month windows before and after the hurricane based on visual clarity and mean radiance across the county.

Specifically, we computed the average nightlight intensity for each image over all pixels within the county boundary, and selected the image with the highest mean radiance as the clearest available for that time window. This approach helps avoid cloud-obscured or low-quality images and ensures consistent visual comparison. Visual inspection suggests a modest decline in radiance, particularly around the urban center of Lake Charles, consistent with short-term disruptions to electrical infrastructure.

We define three pre-disaster periods: 365-455 days prior (k=-2), 180-270 days prior (k=-1), and 0–90 days before the disaster (k=0), which serves as the baseline. Post-disaster recovery is measured over five windows: 0–90 days after (k=1), 90–180 days (k=2), 180-270 days (k=3), 365-455 days (k=4), and 730-820 days after the hurricane (k=5). This temporal structure enables us to evaluate both short-term disruptions and long-run recovery trajectories.

3.2.2 Treatment and Hurricane Exposure Variables

Treatment is assigned at the county level and equals one if the county received FEMA Public Assistance following a hurricane disaster declaration. We restrict the sample to counties affected by major hurricanes between 2017 and 2022 with complete records in all data sources. The same FEMA dataset also provides the incident start and end dates, which we use to calculate hurricane duration (incident length).

To better capture storm severity, in addition to hurricane duration, we extract the maximum wind speed for each county during the disaster period from the ERA5-Land hourly reanalysis dataset (C3S, 2019), using both u and v wind components to compute total wind speed via the Euclidean norm.

3.2.3 Socioeconomic and Demographic Covariates

County-level economic indicators, including real GDP per capita and personal income per capita, are obtained from the U.S. Bureau of Economic Analysis (BEA, 2025). County population estimates are drawn from the U.S. Census Bureau (U.S. Census Bureau, 2025).

We incorporate six social vulnerability indicators from the CDC/ATSDR Social Vulnerability Index (SVI) (CDC/ATSDR, 2025): poverty rate, unemployment

rate, elderly share (age 65+), disability rate, minority share, and the proportion of households without vehicles. These measures capture community-level capacity constraints and exposure to systemic risks, which may confound the relationship between FEMA assistance and recovery outcomes.

3.2.4 Measurement of Nighttime Light Recovery

To assess post-hurricane infrastructure recovery, we construct county-level average nighttime light intensity over discrete time windows centered around each hurricane event. Specifically, we define three pre-hurricane periods: 365 to 455 days before the hurricane (denoted as k=-2), 180 to 270 days before (k=-1), and the 90 days immediately preceding the hurricane, which serves as the pre-hurricane baseline (k=0).

Post-hurricane recovery is measured over five windows: 0 to 90 days after the hurricane (k=1), 90 to 180 days (k=2), 180 to 270 days (k=3, representing a half-year window), 365 to 455 days (k=4, one-year window), and 730 to 820 days after the hurricane (k=5, two-year window). This panel structure enables us to analyze short-term and longer-term recovery trajectories in a dynamic event-study framework.

3.2.5 Sample Summary and Covariate Balance

Our sample includes all U.S. counties affected by a major hurricane between 2017 and 2022 with available data across all sources. Counties receiving FEMA Public Assistance following a hurricane are coded as treated. Counties that experienced hurricane events but did not receive aid serve as controls. We apply inverse probability weighting (IPW) to improve covariate balance between treated and untreated groups.

Table 3.1 presents summary statistics comparing treated and control counties across key characteristics. Statistically significant differences are observed for most covariates, highlighting important baseline imbalances between the two groups. For example, treated counties tend to have significantly lower real GDP per capita (mean = \$45.3k) than control counties (\$49.1k), and smaller populations on average. Treated counties also exhibit higher poverty rates, disability shares, and a greater proportion of households without vehicles, all of which

are statistically significant at conventional levels. Conversely, they have lower minority population shares and shorter incident durations than controls.

These differences underscore the need to account for covariate imbalance in the estimation strategy. To address this, we implement inverse probability weighting (IPW) based on a propensity score model that includes socioeconomic and demographic variables, hurricane characteristics, and county-level geographic features. By reweighting observations, IPW improves covariate balance and enhances the credibility of causal estimates derived from our difference-in-differences framework. Post-weighting balance diagnostics are presented in Appendix Table A6, and show substantial reductions in standardized mean differences across all covariates.

Table 3.1: Descriptive Statistics: Treated vs. Control Counties

Variable	Mean (Treated)	Mean (Control)	Difference	Mean (Treated) Mean (Control) Difference Std. Dev (Treated / Control) t-value	t-value
Nighttime Lights (nW cm $^{-2}$ sr $^{-1}$)	6.34	9.28	-2.94	9.85 / 13.30	-18.90
Real GDP per Capita ((thousands, 2017 chained USD)	45.30	49.10	-3.89	20.90 / 30.60	-11.20
Personal Income per Capita (thousands of USD)	47.50	46.80	99.0	п.20 / п.70	4.43
Population	583,986	I,(-422,638	1,212,477 / 1,662,962	-21.90
Poverty Rate	22.10	18.90	3.19	7.28 / 6.45	35.00
Unemployment Rate	6.93	6.95	10.0	2.03 / 2.01	0.53
Elder Rate $(Age > 65)$	01.71	17.10	-0.03	5.57 / 7.25	-0.35
Disability Rate	15.30	14.60	99.0	3.71 / 4.09	12.60
Minority Rate	38.90	44.10	-5.13	16.70 / 18.90	-21.70
No Vehicle Household Rate	6.54	6.12	0.42	2.21 / 1.98	15.00
Incident Length (days)	17.30	23.80	-6.42	13.50 / 12.40	-37.30
Max Wind Speed (m/s)	13.90	14.40	-0.42	6.10 / 5.24	-5.58

3.3 Empirical Strategy

To estimate the causal impact of FEMA Public Assistance on post-hurricane infrastructure recovery, we employ an event-study difference-in-differences (DiD) framework, leveraging variation in treatment status and precise temporal distance to hurricane landfall. Our outcome variable—nighttime light intensity—is derived from satellite-based VIIRS data and serves as a high-frequency, spatially granular proxy for local infrastructure activity and economic functionality at the county level.

Compared to traditional administrative indicators such as GDP or employment, nighttime lights offer several critical advantages for disaster impact assessment. First, they provide daily observations, allowing us to measure recovery trajectories relative to the exact timing of the hurricane, rather than being constrained by coarse calendar-based reporting periods (e.g., quarterly GDP). This temporal precision is particularly valuable when recovery efforts begin immediately following a storm.

Second, nightlight imagery can capture dimensions of recovery that administrative data may overlook. Employment and GDP figures may reflect broader labor markets that extend beyond county boundaries, obscuring localized effects. For example, workers might commute from nearby counties, or reported income may originate from non-residential activities. In contrast, nighttime lights respond directly to changes in the built environment and electricity usage, capturing infrastructure restoration and residential reconstruction that might not be immediately reflected in employment data.

Finally, nightlights offer consistent geographic coverage and minimal reporting delay, making them especially suited for rapid-response and retrospective analyses. Prior research validates their reliability in detecting disaster-related disruptions and recovery patterns across U.S. contexts (Gibson et al., 2024; Schippers & Botzen, 2023).

Our identification strategy relies on comparing treated and untreated counties' changes in nightlight intensity across multiple recovery windows relative to the hurricane event, controlling for county fixed effects and observable covariates. The baseline model is specified as follows:

$$\log(\text{Nightlight}_{it}) = \sum_{k=-3}^{5} \beta_k \cdot \mathbf{1} \{\text{Period}_k\}_{it} \times \text{Treated}_i + X'_{it} \gamma + \mu_i + \epsilon_{it} \quad (3.1)$$

 $\log({\rm Nightlight}_{it})$ denotes the natural logarithm of average nighttime light intensity for county i during the recovery period t. We define six discrete recovery periods indexed by $k \in \{0,1,\ldots,5\}$: (o) the 90 days before the hurricane (pre-hurricane baseline), (i) 0–90 days after the hurricane, (2) 90–180 days after, (3) 180–270 days after (half-year window), (4) 365–455 days after (one-year window), and (5) 730–820 days after (two-year window). The indicator variable $\mathbf{1}({\rm Period}_k)$ equals one if the observation falls within recovery window k, and zero otherwise. Treated $_i$ is a binary variable equal to one if county i received FEMA Public Assistance, and zero otherwise. The interaction term $\mathbf{1}({\rm Period}_k) \times {\rm Treated}_i$ captures the treatment effect of FEMA aid in each post-hurricane period, relative to the pre-hurricane baseline (Period 0), which is omitted from the model as the reference category.

 X_{it} denotes a vector of time-varying county-level covariates, including economic and demographic controls: real GDP per capita, personal income per capita, population, and a set of social vulnerability indicators (e.g., poverty rate, unemployment rate, share of elderly, disabled, minority, and households without vehicles). We also include storm severity controls such as incident duration and maximum wind speed during the hurricane. μ_i denotes county fixed effects, which control for time-invariant unobservable characteristics. Standard errors are clustered at the county level.

This specification allows us to examine the dynamic evolution of nightlight intensity following a hurricane and test whether treated counties recover faster than comparable untreated counties, conditional on baseline observables. The event-study formulation is particularly suited to evaluating the persistence and timing of FEMA's impact across multiple post-hurricane recovery windows.

3.3.1 Testing for Parallel Trends

A key identifying assumption of the DiD framework is that treated and untreated counties would have followed similar pre-hurricane trends in nightlight intensity in the absence of treatment. To assess this assumption of parallel

trends, we extend the event-study model to include three pre-hurricane lead periods and the baseline. Specifically, we collect nightlight data from 365–455 days before the hurricane (coded as k=-2) and 180–270 days before (k=-1), preceding the 90-day baseline period (k=0). Accordingly, we re-code the period indicator Period_k to $\operatorname{span} k \in -2, -1, 0, 1, \ldots, 5$.

We then estimate an augmented event-study specification that includes leads and lags of treatment, with period o (90 days before the hurricane) omitted as the reference. The coefficients on the pre-hurricane interaction terms (k = -2, -1) allow us to directly test for anticipatory or pre-treatment differences in trends between treated and control counties.

3.3.2 Inverse Probability Weighting for Covariate Balance

Although our model includes a rich set of covariates and county fixed effects, we further address pre-treatment imbalances by implementing inverse probability weighting (IPW). This approach re-weights observations to create a pseudo-population in which treatment assignment is independent of observed covariates.

We first estimate a propensity score model predicting the likelihood of receiving FEMA Public Assistance based on pre-hurricane characteristics, including average nightlight before the hurricane, economic indicators, demographic vulnerabilities, county size, forest cover, and storm severity. Stabilized weights are constructed as:

$$w_i = \begin{cases} \frac{\bar{p}}{\hat{p}_i} & \text{if Treated}_i = 1, \\ \frac{1 - \bar{p}}{1 - \hat{p}_i} & \text{if Treated}_i = 0, \end{cases}$$

where \hat{p}_i is the estimated propensity score for county i and \bar{p} is the sample mean of the treatment indicator.

These inverse probability weights are incorporated into the DiD estimation to yield IPW-weighted treatment effects. We examine standardized mean differences (SMDs) before and after weighting to assess whether the weighting procedure improves covariate balance. As shown in Appendix Table A6, all SMDs fall below the conventional 0.1 threshold (Austin, 2009; Stuart, 2010)

post-weighting, including the SMD for pre-hurricane log nightlight, which declines from 0.1888 to 0.0780. Most covariates—particularly socioeconomic and demographic measures—exhibit SMDs below 0.025, indicating excellent balance. These results suggest that the IPW procedure substantially enhances the comparability of treated and control groups.

3.3.3 Summary of Empirical Approach

By combining an event-study difference-in-differences (DiD) design with inverse probability weighting (IPW) and an extended set of pre-treatment periods, our empirical strategy strengthens causal identification along two key dimensions: (1) it supports the parallel trends assumption by explicitly testing for pre-treatment equivalence in trends, and (2) it improves covariate balance between treated and control groups through re-weighting. To further assess the robustness of our findings, we conduct several robustness checks, including redefining treatment based on program eligibility rather than actual fund receipt and excluding the first 30 days of post-hurricane nighttime light data to reduce noise from short-term power outages.

3.4 Main Results

Table 3.2: Main Results: Impact of FEMA Public Assistance Program Across Recovery Periods

	(1)	(2)	(3)	(4)	(5)
Treatment Effects	(1)	(2)	\31	(4)	\)/
Period -2 × Treated	-o.oo86	-0.0085	-0.0082	-o.oo88	-0.0098
Teriou 2 × Treated	(0.0121)	(0.0121)	(0.0121)	(0.0121)	(0.0122)
Period -1 × Treated	-0.0003	-0.0002	0.0001	-0.0005	-0.0015
Terroa T. Treatea	(0.0057)	(0.0057)	(0.0058)	(0.0057)	(0.0056)
Period 1 × Treated	-o.o317***	-0.0316***	-o.o313***	-0.0319***	-0.0329***
	(0.0094)	(0.0094)	(0.0094)	(0.0094)	(0.0094)
Period 2 × Treated	0.0159*	0.0160*	0.0163*	0.0157*	0.0147
	(0.0092)	(0.0092)	(0.0092)	(0.0092)	(0.0093)
Period 3 × Treated	0.0243***	0.0244***	0.0247***	0.0241***	0.0231***
•	(0.0026)	(0.0026)	(0.0026)	(0.0026)	(0.0027)
Period 4 × Treated	0.0006	0.0007	0.0010	0.0004	-0.0006
	(0.0034)	(0.0034)	(0.0035)	(0.0034)	(0.0035)
Period 5 × Treated	0.0345***	0.0346***	0.0349***	0.0344***	0.0333***
	(0.0044)	(0.0044)	(0.0044)	(0.0044)	(0.0047)
Control Variables					
Real GDP per capita	-0.0008	-0.002I	-0.0009	-	_
	(0.0016)	(0.0016)	(0.0018)		
Personal Income per capita	0.0069***	0.0085***	0.0072***	_	_
	(0.001 7)	(0.0014)	(0.0013)		
Population	7.43e-07**	1.19e-06***	1.25e-06***	1.75e-06***	_
	(3.07e-07)	(2.08e-0 7)	(2.10e-07)	(3.17e-07)	
Poverty Rate	-0.0024**	-0.0029***	-0.0013	0.0028**	-
	(0.0011)	(0.0010)	(0.0011)	(0.0012)	
Unemployment Rate	0.0058	-0.0002	0.0062*	-0.0009	_
	(0.0040)	(0.0038)	(0.0033)	(0.0031)	
Elder Rate (Age>65)	0.0025				
D. 1.1. D	(0.0075)				
Disability Rate	-0.0099**				
	(0.0046)				
Minority Rate	0.0093*				
NI WILL THEN	(0.0048)				
No Vehicle HH Rate	-o.oo66				
To dilina Toronto	(0.0046)	***			
Incident Length	0.0009***	0.0014***			
M W: J C J	(0.0003)	(0.0003)			
Max Wind Speed	-0.0010	-0.0017*			
Observations	(0.0009)	(0.0010)	22.744	22.544	22.74
Fixed Effects	22,744 County	22,744 County	22,744 County	22,744 County	22,744 County
RMSE	County	County	County	County	County
Within R^2	0.0477	0.0478	0.0480	0.0487	0.0536 0.061
within 1/	0.258	0.253	0.247	0.224	0.061

Note: Robust standard errors clustered at the county level in parentheses. $^*p < 0.1, ^{**}p < 0.05, ^{***}p < 0.01.$ "-" indicates a variable excluded due to model specification.

Table 3.2 presents the estimated effects of FEMA Public Assistance on posthurricane recovery, measured by changes in average nighttime light intensity at the county level. The analysis is based on an inverse probability weighted (IPW) event-study difference-in-differences (DiD) framework with county fixed effects, which accounts for observable imbalances and time-invariant heterogeneity. Nighttime lights are a widely accepted proxy for local infrastructure functionality and economic activity.

The coefficients on the pre-treatment periods (Periods -2 and -1) are small in magnitude and statistically insignificant across all specifications. Specifically, estimates for Period -2 range from -0.0082 to -0.0098, and for Period -1 from 0.0001 to -0.0015, with none reaching statistical significance thresholds. This lack of differential pre-trends supports the validity of the parallel trends assumption, strengthening the credibility of our identification strategy.

In the immediate aftermath of hurricanes (Period 1: o-9o days), treated counties exhibit significantly slower recovery in nightlight intensity compared to control counties, with estimated changes indicating 3.13% to 3.29% less growth (or greater reduction) relative to pre-hurricane levels than the control group (p < 0.01). This pattern is consistent with delays in FEMA fund disbursement and greater initial damage in treated areas, reflecting the program's needs-based allocation criteria. Although we control for observable disaster severity (e.g., wind speed, incident duration), unmeasured damage or vulnerability may still bias short-run comparisons. Furthermore, nightlight data during this early window may capture transient disruptions and noisy power outages rather than sustained infrastructure loss. Supporting this interpretation, a robustness check that excludes the first 30 days post-disaster yields smaller and statistically weaker negative effects in Period 1.

By Period 2 (90–180 days), the direction of the treatment effect reverses, with treated counties exhibiting relatively greater growth in nighttime light intensity—1.47% to 1.63% higher than control counties relative to pre-hurricane levels—statistically significant at the 10% level (p < 0.1). These positive recovery effects become stronger and more consistent by Period 3 (180–270 days), where treated counties experience significantly higher nightlight growth of 2.31% to 2.47% compared to controls (p < 0.01). The largest treatment effects are observed in Period 5 (730–820 days), with treated counties showing sustained growth of 3.33% to 3.49% more in light intensity relative to the control group (p < 0.01). These results indicate that FEMA Public Assistance supports medium-term recovery and contributes to long-run improvements

in infrastructure-related activity and local economic recovery and growth, as proxied by nightlight intensity.

Estimates for Period 4 (365–455 days) remain statistically insignificant across all models, which may reflect an intermediate stage in the recovery process where resources are still being mobilized or construction projects are underway but not yet complete. Nonetheless, the pattern of steadily increasing effects across Periods 2 through 5 suggests a cumulative and persistent recovery impact from FEMA Public Assistance.

These results are robust across five model specifications that sequentially adjust for economic conditions (e.g., personal income, GDP), social vulnerability factors (e.g., poverty, minority share, disability rate), and hurricane severity (e.g., wind speed, incident duration). Inclusion of these covariates improves precision and confirms the robustness of the treatment effect.

Estimated coefficients for control variables are generally consistent with expectations. Personal income per capita is positively and significantly associated with light intensity, while higher poverty and disability rates are negatively associated, reflecting known disparities in economic resilience and infrastructure investment.

The temporal pattern of treatment effects observed in our analysis aligns closely with FEMA's implementation guidelines for Public Assistance (PA). According to the *Public Assistance Applicant Handbook* (FEMA, 2010), debris removal and emergency work must be completed within six months to remain eligible for reimbursement, while permanent work must be completed within 18 months of the disaster declaration. Moreover, FEMA may reimburse up to 100% of permanent work costs if completed within six months, but only 75% thereafter. These deadlines likely create incentives for local governments to expedite recovery efforts around key thresholds. This helps explain the significant recovery effects observed in Period 3 (180–270 days), which corresponds to the six-month mark, and again in Period 5 (730–820 days), which captures the 18-month deadline. In contrast, the lack of significance in Period 4 (365–455 days) may reflect a lull between the completion of emergency work and the finalization of permanent repairs, as jurisdictions await further funding or manage construction timelines. These institutional constraints and reimbursement incentives provide a plausible explanation for the observed dynamics of nightlight recovery.

The results provide strong evidence that FEMA Public Assistance has a significant and sustained effect on post-hurricane recovery. Treated counties demon-

strate measurable improvements in infrastructure and local economic activity, with recovery effects persisting and amplifying over the two years following major hurricanes.

3.5 Robustness Checks

3.5.1 Using FEMA Public Assistance Eligibility as Treatment

To test the robustness of our main findings, we re-estimate the event-study model using eligibility for FEMA Public Assistance as the treatment variable, rather than actual fund receipt. This specification captures the intent-to-treat (ITT) effect—i.e., the impact of being targeted for aid, regardless of whether funds are ultimately disbursed.

Table 3.3 reports the results. The estimated treatment effects remain consistent with the main specification across all recovery periods. In particular, we observe significant and positive treatment effects in the medium and long run. The estimated coefficients for Period 3 and Period 5 are slightly larger than those based on actual fund receipt (Table 3.2), suggesting that eligibility alone may activate recovery mechanisms even before aid is disbursed. These mechanisms could include strategic planning, accelerated local recovery efforts, or the expectation of forthcoming federal support.

Notably, the parallel trends assumption appears to hold in this specification, as we observe no statistically significant differences in nightlight trends between eligible and non-eligible counties during the two pre-hurricane periods (k=-2 and k=-1). This strengthens the credibility of our identification strategy by supporting the assumption that, in the absence of treatment, both groups would have followed similar trajectories.

Overall, the results using eligibility as treatment reaffirm the credibility of the main findings. The fact that both actual fund receipt and program eligibility yield similar recovery patterns reinforces the conclusion that FEMA Public Assistance substantially accelerates post-hurricane infrastructure recovery.

Table 3.3: Robustness Checks: Using Program Eligibility as Treatment

	(1)	(2)	(3)	(4)	(5)
Treatment Effects	(-)	(2)	()/	(17)	
Period -2 × Treated	-0.0058	-0.0050	-0.0049	-0.0054	-0.0097
	(0.0108)	(0.0106)	(0.0106)	(0.0106)	(0.0108)
Period -1 × Treated	0.0024	0.0042	0.0043	0.0038	-0.0006
	(0.0062)	(0.0062)	(0.0062)	(0.0061)	(0.0055)
Period 1 × Treated	-0.0250***	-0.0260***	-o.o26o***	-0.0264***	-0.0308***
	(0.0096)	(0.0095)	(0.0095)	(0.0094)	(0.0094)
Period 2 × Treated	0.0194**	0.0189**	0.0189**	0.0185**	0.0141
	(0.0094)	(0.0090)	(0.0090)	(0.0090)	(0.0091)
Period $3 \times$ Treated	0.0288***	0.0290***	0.0290***	0.0286***	0.0242***
	(0.0029)	(0.0030)	(0.0029)	(0.0030)	(0.0032)
Period 4 \times Treated	0.0041	0.0038	0.0039	0.0034	-0.0009
	(0.0038)	(0.0040)	(0.0040)	(0.0040)	(0.0039)
Period 5 \times Treated	0.0383***	0.0372***	0.0373***	0.0368***	0.0325***
	(0.0045)	(0.0049)	(0.0049)	(0.0049)	(0.0052)
Control Variables					
Real GDP per capita	-0.0006	-0.0020	-0.0009	-	-
	(0.0015)	(0.0015)	(0.0018)		
Personal Income per capita	0.0068***	0.0085***	0.0073***	_	_
7	(0.0017)	(0.0014)	(0.0013)	- Zakakak	
Population	7.90e-07**	1.22e-06***	1.28e-06***	1.81e-06***	-
D D	(3.05e-07)	(2.06e-07)	(2.10e-07)	(3.22e-07)	
Poverty Rate	-0.0028***	-0.0030***	-0.0015	0.0024**	_
TT 1 D	(0.0010)	(0.0010)	(0.0011)	(0.0011)	
Unemployment Rate	0.0052	-0.0001	0.0062**	-0.0007	_
T11 . D . (A > C)	(0.0038)	(0.0036)	(0.0031)	(0.0030)	
Elder Rate (Age>65)	0.0043				
Disability Data	(0.0072) -0.0106**				
Disability Rate	,				
Minority Rate	(0.0045) 0.0095**				
Willionty Rate	(0.0046)				
No Vehicle HH Rate	-0.0045				
110 Temele 1111 Kate	(0.0039)				
Incident Length	0.0010***	0.0014***			
	(0.0003)	(0.0003)			
Max Wind Speed	-0.0010	-0.0017*			
- I	(0.0009)	(0.0010)			
Observations	22,744	22,744	22,744	22,744	22,744
Fixed Effects	County	County	County	County	County
RMSE	0.0471	0.0473	0.0475	0.0483	0.0531
Within \mathbb{R}^2	0.279	0.277	0.270	0.247	0.088
				17	

Note: Robust standard errors clustered at the county level in parentheses. $^*p < 0.1, ^{**}p < 0.05, ^{***}p < 0.01.$ "-" indicates a variable excluded due to model specification.

3.5.2 Excluding the First 30 Days After Hurricanes

Table 3.4: Robustness Checks: Excluding first 30 days after hurricanes

	(1)	(2)	(2)	(4)	(5)
Treatment Effects	(1)	(2)	(3)	(4)	(5)
Period $-2 \times$ Treated	-0.0102	-0.0101	-0.0098	-0.0104	-o.oii4
Teriod 2× freated	(0.0102	(0.0119)	(0.0119)	(0.0120)	(0.0121)
Period $-1 \times$ Treated	-0.0019	-0.0018	-0.0015	-0.002I	-0.0032
Teriod 17 Treated	(0.0056)	(0.0056)	(0.0056)	(0.0056)	(0.0054)
Period 1 × Treated	-0.0184**	-o.oi83**	-0.0180**	-o.oi86**	-0.0196**
	(0.0083)	(0.0083)	(0.0083)	(0.0083)	(0.0083)
Period 2 × Treated	0.0143	0.0144	0.0147	0.0141	0.0131
	(0.0094)	(0.0094)	(0.0094)	(0.0094)	(0.0095)
Period 3 × Treated	0.0227***	0.0228***	0.0231***	0.0225***	0.0215***
•	(0.0027)	(0.0027)	(0.0027)	(0.0027)	(0.0028)
Period $4 \times$ Treated	-0.0010	-0.0009	-0.0006	-0.0011	-0.0022
	(0.0033)	(0.0033)	(0.0034)	(0.0033)	(0.0034)
Period 5 × Treated	0.0329***	0.0331***	0.0334***	0.0328***	0.0317***
	(0.0043)	(0.0044)	(0.0043)	(0.0044)	(0.0046)
Control Variables					
Real GDP per capita	-0.0009	-0.0022	-0.0010	-0.0010	_
	(0.0016)	(0.0016)	(0.0018)	(0.0018)	
Personal Income per capita	0.0069***	0.0085***	0.0072***	0.0072***	-
	(0.0017)	(0.0014)	(0.0013)	(0.0013)	
Population	7.44e-07**	1.21e-06***	1.26e-06***	1.75e-06***	_
	(3.05e-07)	(2.08e-07)	(2.11e-07)	(3.19e-07)	
Poverty Rate	-0.0024**	-0.0029***	-0.0013	0.0028**	_
	(0.0011)	(0.0010)	(0.0011)	(0.0011)	
Unemployment Rate	0.0058	-0.0003	0.0062*	-0.0009	_
F14D (A	(0.0040)	(0.0038)	(0.0033)	(0.0031)	
Elder Rate (Age>65)	0.0026				
Disability P ato	(0.0075) -0.0098**				
Disability Rate	-0.0098 (0.0046)				
Minority Rate	0.0046)				
Willionty Rate	(0.0048)				
No Vehicle HH Rate	-0.0065				
Two venicle 1111 reace	(0.0045)				
Incident Length	0.0009***	0.0014***			
merdene Zengui	(0.0003)	(0.0003)			
Max Wind Speed	-0.0009	-0.0017*			
r	(0.0009)	(0.001)			
Observations	22,744	22,744	22,744	22,744	22,744
Fixed Effects	County	County	County	County	County
RMSE	0.0470	0.0472	0.0474	0.0481	0.0531
Within \mathbb{R}^2	0.251	0.246	0.239	0.216	0.045

Note: Robust standard errors clustered at the county level in parentheses. *p < 0.1, **p < 0.05, ***p < 0.01. "-" indicates a variable excluded due to model specification.

One potential concern in using nighttime lights as a proxy for infrastructure recovery is that immediate post-hurricane reductions in light intensity may pri-

marily reflect temporary power outages rather than actual damage to infrastructure or sustained economic disruption. In the aftermath of hurricanes, widespread power loss is common and may not accurately represent long-term recovery conditions. To address this concern, we re-estimate our main model after redefining the first post-hurricane recovery window (Period 1) to exclude the first 30 days. In this alternative specification, Period 1 captures the 30–90 day window following the hurricane, thereby aiming to diminish the influence of transitory outages and better isolate changes associated with substantive recovery processes.

As shown in Table 3.4, the results remain consistent with our main findings. In particular, we continue to observe a statistically significant negative treatment effect in Period 1, with treatment estimates slightly attenuated in magnitude compared to the original specification (e.g., -0.0185 vs. -0.0317 in column 1). This pattern is consistent with the interpretation that power outages temporarily depress observed nightlight levels immediately following hurricanes. By excluding the first 30 days, we obtain a more conservative and arguably cleaner estimate of the short-term disruption in local infrastructure and economic activity. The persistence of significant positive treatment effects in later periods (Periods 3 and 5) further confirms the robustness of the FEMA assistance effect over medium- and long-term horizons.

3.5.3 Hurricane Preparedness Across Counties

To address concerns about heterogeneity in disaster preparedness across counties, we construct an experience-based proxy using the number of FEMA Public Assistance (PA) applications each county submitted before a given hurricane. Specifically, for each disaster, we count the total number of PA applications the county filed in response to earlier events, using FEMA's application-level data. This proxy reflects administrative preparedness, capturing institutional familiarity with the federal aid system, staff capacity, and procedural readiness, rather than physical preparedness such as shelters or levees. We include this variable as a control to assess whether baseline differences in administrative capacity bias our estimates. The results, reported in Appendix Table A7, show no statistically significant effect of this preparedness measure on recovery outcomes, and our main estimates remain robust to its inclusion.

3.6 Heterogeneity Analysis

To assess whether the effects of FEMA Public Assistance program vary across socioeconomic contexts, we conduct a heterogeneity analysis by stratifying counties based on three key baseline characteristics: personal income, unemployment rate, and minority population share. For each dimension, counties are divided into high and low groups using the median value in the pre-disaster period. Table 3.5 presents estimates from the main specification for each subgroup. Specifically, we report the interaction effects between treatment and recovery periods across high- and low-income, high- and low-unemployment, and high- and low-minority counties. The results suggest notable differences in both the magnitude and statistical significance of estimated treatment effects across groups. Full regression tables, including all model specifications and control variables, are reported in the Appendix.

Table 3.5: Heterogeneous Treatment Effects of FEMA Public Assistance (Main Specification)

	High Income	Low Income	High Unemployment	Low Unemployment	High Minority	Low Minority
Treatment Effects						
Period $-2\times$ Treated	-0.0090	-0.0084***	-0.0154**	-0.0039	-0.0222***	0.0045
Period $-1 \times$ Treated	-0.0135	0.0128***	0.0001	-0.0016	-0.0075	0.0059
Period $1 \times$ Treated	-0.0446^{***}	-0.0179^{***}	-0.0207***	-0.0401***	-0.0166^{***}	-0.0461^{***}
Period $2\times$ Treated	0.0183	0.0132***	0.0249**	0.0074	0.0280***	0.0043
Period $3\times$ Treated	0.0295***	o.0191***	0.0237***	0.0247***	0.0263***	0.0228***
Period 4× Treated	0.0091	-0.0079^{***}	-0.0034	0.0050	-0.0070^{**}	0.0082**
Period $5 \times$ Treated	0.0513***	0.0170***	0.0260***	0.0425***	0.0258***	0.0437***
Control Variables						
Real GDP per capita	0.0037	0.0029**	0.0007	-0.0049	0.0024	0.0026^*
Personal Income per capita	0.0030	0.0128***	0.0022	0.0055^*	0.0025	0.0045***
Population	2.57e-06***	-1.26e-07	3.69e-06*	4.50e-07	6.79e-07***	1.52e-06***
Poverty Rate	-0.0118***	-0.0024***	-0.0049***	-0.0076***	-0.0010	-0.0022*
Unemployment Rate	0.0162	0.0061	0.0019	-0.0114	0.0019	0.0050
Elder Rate (Age>65)	0.0634^{***}	-0.0112^{**}	0.0213	0.0255	0.0023	0.0036
Disability Rate	0.000	-0.0147***	0.0150*	-0.0247^{*}	-0.0081	-0.0183***
Minority Rate	-0.0055	0.0114***	0.0191***	0.0112	0.0103	0.0122^{***}
No Vehicle HH Rate	0.0244^{***}	0.0026	-0.0147***	-0.0418^*	-0.0077	-0.0001
Incident Length	0.0020^{***}	0.0013***	0.0031***	0.0018*	0.0002	0.0011^{***}
Max Wind Speed	-0.0020	-0.0013***	-0.0003	-0.0003	0.0024	-0.0009

Note: Robust standard errors clustered at the county level in parentheses. *p < 0.1, **p < 0.05, ***p < 0.01. Groups are defined by median splits on pre-disaster county income, unemployment, and minority population share.

3.6.1 Heterogeneous Effects by County Personal Income

We stratify counties into high- and low-income groups based on the median of personal income per capita. The results indicate that FEMA Public Assistance generates more robust and sustained recovery in high-income counties. In the short run (within 90 days), treated high-income counties experience a significant decline in nighttime light intensity, consistent with the average postdisaster impact. However, by the medium run (half to one year), light levels begin to rebound, and by the long run (two years), treated counties exhibit a 5.13% increase in nighttime lights relative to controls—surpassing the 3.45% effect observed in the full sample (Table 3.2). In contrast, while low-income counties also show a positive recovery trend, the effects are smaller, more volatile across periods, and accompanied by evidence of pre-trend violations. These patterns suggest that FEMA assistance may be more effective in areas with greater fiscal and institutional capacity to absorb and implement aid. Higher-income counties typically have stronger local tax bases, more experienced administrative personnel, and better pre-existing infrastructure—all of which could potentially facilitate a faster and more efficient recovery process. In addition, wealthier areas may benefit from broader insurance coverage and private-sector investment, which can complement and amplify the impact of federal disaster support.

3.6.2 Heterogeneous Effects by County Unemployment Rate

To examine heterogeneous treatment effects of FEMA Public Assistance, we stratify counties based on pre-disaster unemployment rates. Specifically, counties are divided into two groups—those with unemployment rates below the median (referred to as "low-unemployment counties") and those above the median ("high-unemployment counties"). In low-unemployment counties, treatment effects are not only statistically significant but also larger in magnitude than those estimated using the full sample. Specifically, in low-unemployment counties, nighttime light intensity in treated areas is approximately one percentage point higher two years after the hurricane than the effect estimated using the full sample, suggesting stronger long-term recovery. This may indicate that FEMA assistance is more effective in counties with stronger labor market conditions, potentially due to better administrative capacity, infrastructure, or access to complementary resources that facilitate more efficient recovery. In contrast, treatment effects in high-unemployment counties are notably smaller, and evidence of pre-trend violations raises concerns about the credibility of causal

interpretation. While this divergence hints at meaningful heterogeneity in disaster recovery outcomes, the findings for high-unemployment counties should be viewed cautiously. Still, the larger and more robust effects observed in low-unemployment areas provide suggestive evidence that the benefits of FEMA PA may be concentrated in counties with lower unemployment rates.

3.6.3 Heterogeneous Effects by County Minority Rate

We stratify counties into high- and low-minority groups based on the median share of minority population. The results reveal notable differences in the magnitude and stability of recovery. In low-minority counties, treatment effects are statistically significant and follow a clear upward trajectory over time. Specifically, nighttime light intensity initially declines in the short run (0–90 days post-disaster), begins to recover in the medium run (180-270 days, 365–455 days), and reaches a long-run (730–820 days) increase of 4.37% relative to control counties. This long-run effect is notably larger than the 3.45% observed in the full sample (Table 3.2), suggesting that low-minority counties may experience more sustained gains from FEMA Public Assistance.

In contrast, high-minority counties also show positive recovery in the medium and long run, with a long-run treatment effect of 2.58%, but estimates are more volatile across periods. Moreover, the presence of a statistically significant decline in nighttime lights during the pre-hurricane period (-2) indicates a violation of the parallel trends assumption. This undermines the credibility of causal interpretation in high-minority counties, and results for this group should therefore be interpreted with caution.

One possible explanation for the stronger recovery in low-minority counties is that these areas may have better access to institutional resources or stronger networks to navigate federal aid programs effectively. They may also face fewer administrative, linguistic, or procedural barriers in applying for and deploying FEMA assistance, enabling faster and more coordinated recovery efforts. Differences in political representation or historical patterns of underinvestment in minority communities could further exacerbate disparities in how disaster assistance is accessed and utilized.

3.7 Caveats

One primary caveat concerns the potential for selection bias in treatment assignment. FEMA Public Assistance is not randomly allocated. Given FEMA's eligibility criteria and needs-based allocation, countries that received aid may have been systematically more damaged by hurricanes than those that did not. While our empirical strategy controls for storm severity (e.g., maximum wind speed, incident duration) and improves balance on observed covariates through inverse probability weighting, unobserved differences in initial damage may persist. Consequently, the lower relative nightlight growth (or greater relative reduction) observed for treated counties in the immediate post-hurricane period (Period 1) could partially signal more extensive initial disruption, rather than an ineffective or delayed policy response. Importantly, the fact that treated counties recover more fully and exceed control levels in subsequent periods, despite likely being hit harder, reinforces the conclusion that FEMA assistance plays a meaningful role in facilitating recovery in the medium to long run.

3.8 Conclusion

This study examines the impact of FEMA Public Assistance on post-hurricane recovery, using satellite-based nighttime light intensity to track recovery trajectories at the county level. By combining an inverse probability weighted difference-in-differences framework with rich panel data on disaster aid, local conditions, and hurricane severity, we provide robust evidence that federal assistance significantly boosts medium- and long-term infrastructure and economic recovery. Treated counties show stronger gains in nightlight intensity, exceeding comparable controls by 3.45% two years after the hurricane, suggesting that FEMA aid plays a meaningful role in enhancing local resilience.

Importantly, our heterogeneity analysis reveals that the benefits of FEMA Public Assistance are not evenly distributed. Recovery outcomes are significantly stronger and more sustained in counties with higher income levels, lower unemployment rates, and smaller minority populations. Long-run gains in nighttime light intensity reach 5.13% in high-income counties, 4.25% in low-unemployment counties, and 4.37% in low-minority counties—each surpassing the average effect in the full sample. In contrast, recovery in low-income, high-unemployment, and high-minority counties is more volatile, with some evidence of pre-trend

divergence that limits causal interpretation. These disparities highlight the importance of fiscal capacity, administrative readiness, and equitable access to aid in shaping recovery trajectories.

Our findings yield several important policy implications. As climate-related disasters grow more frequent and severe, timely and sustained federal assistance is essential for effective recovery. However, the uneven distribution of benefits underscores the need for a more inclusive and adaptive approach. Policymakers should consider tailoring aid delivery strategies to local capacities and investing in the administrative infrastructure of underserved communities. Reducing procedural hurdles and supporting institutional readiness in high-vulnerability areas could help ensure that assistance reaches those most in need.

Alongside these efforts, policymakers should consider integrating advances in artificial intelligence, machine learning, and satellite remote sensing to enhance the speed and precision of disaster impact assessments. These technologies can enable semi-automated systems for early damage detection, cost estimation, and needs-based fund allocation. For instance, automated pre-payments based on real-time satellite assessments could provide immediate relief while more detailed evaluations are underway. Similarly, centralized planning systems powered by real-time data and logistical modeling could support optimized deployment of recovery resources. By shortening the delay between disaster and reconstruction, such innovations can reduce inequities in aid delivery—especially in historically underserved or high-risk regions.

To our knowledge, this is the first study to provide a national-level assessment of FEMA Public Assistance effectiveness using high-frequency, spatially disaggregated indicators. By integrating VIIRS nightlight data with administrative FEMA records and socioeconomic controls in a dynamic panel framework, we contribute novel evidence on the role of federal aid in fostering recovery. Our results emphasize not only the overall effectiveness of public assistance but also the critical need to address structural disparities that shape who benefits most from disaster recovery programs.

Conclusion

This dissertation investigates how migration behavior, wireless public disaster warning, and federal disaster assistance influence environmental outcomes and recovery processes in the face of rising climate-related risks. Across three chapters, it combines rich spatial and administrative datasets with causal inference techniques to evaluate policies and behavioral responses that affect sustainability and resilience in both developing and developed contexts.

Chapter 1 explored the environmental consequences of rural out-migration in Mon State, Myanmar, using a dynamic panel model with household-level survey data and satellite-based forest cover observations between 2000 and 2015. The results reveal that out-migration significantly reduces local forest loss within 1000-meter buffers surrounding villages. Each additional migrant is associated with over a 5-square-meter decrease in deforestation annually. The study finds suggestive evidence that remittance income enables households to shift from firewood and charcoal to electricity for cooking, highlighting a remittance-facilitated energy transition channel. This chapter contributes to the migration—environment literature by identifying a novel behavioral mechanism that links demographic mobility with environmental sustainability.

Chapter 2 evaluated the life-saving effects of the U.S. Wireless Emergency Alerts (WEA) system using a Regression Discontinuity in Time (RDiT) design. Exploiting the April 2012 nationwide rollout of WEA as a sharp policy threshold, it analyzes storm-related mortality from 361 major events between 2000 and 2024. The study finds that WEA reduced fatalities by approximately 4.3 deaths per storm, resulting in an estimated 3,667 lives saved. This translates into a societal benefit of approximately \$50 billion, achieved with relatively low implementation cost. Robustness checks, including placebo and falsification tests, support the validity of the identification strategy. These findings position WEA as a cost-effective digital public good with scalable potential for disaster risk reduction.

Chapter 3 examined the effect of FEMA Public Assistance on post-hurricane infrastructure recovery in the United States. Using a county-level panel from 2017 to 2022 and VIIRS nighttime light intensity as a proxy for infrastructure functionality, the study implements an event-study difference-in-differences framework with inverse probability weighting. Counties that received FEMA PA experienced significantly faster and more sustained recovery, with treated areas showing 2.3–2.5% higher light intensity within 6–9 months post-disaster and 3.3–3.5% higher after two years. The results remain robust across multiple model specifications and treatment definitions, including those based on eligibility thresholds. This chapter provides new causal evidence on the effectiveness of public infrastructure aid in supporting disaster resilience.

Taken together, these studies demonstrate how behavioral, technological, and institutional mechanisms shape environmental outcomes and disaster responses. They highlight the importance of integrating migration policy, information systems, and federal assistance programs into a broader sustainable development agenda.

Future research could extend this work in several directions. For the Myanmar study, better data on remittance use and household energy consumption could further validate the proposed mechanisms. In the WEA chapter, micro-level exposure data could refine the estimated treatment effect and address spatial heterogeneity. The FEMA aid study could be extended to examine longer-term effects on economic activity and incorporate more accurate assessments of disaster damage and recovery. More broadly, this dissertation points to the need for interdisciplinary approaches that combine causal inference, spatial data, and panel analysis to evaluate policy responses under environmental uncertainty.

APPENDIX A ADDITIONAL TABLES

Table A1: System GMM Estimates of Migration on Deforestation (Buffer Radius = 500m)

	(1) Main	(2) Main models	(3) AR(2)	(4) (AR(2) models	(5) Models W/	(5) (6) Models W/Out controls
Lagged Deforestation $(t-1)$	0.390*** (0.091)	0.387***	0.373***	0.370***	0.397*** (0.071)	0.394***
Lagged Deforestation $(t-2)$			-0.048 (0.059)	-0.047 (0.061)		
Current Migrants (weighted)	0.529		0.833		-0.537 (0.812)	
∑ Out-migration (weighted)		0.645 (1.372)		0.986		-0.912 (0.945)
Neturn Migration (weighted)		1.923		1.915		
Precipitation	150.55* (77.11)	149.57 (78.71)	146.54* (72.28)	145.96* (72.92)		
Temperature	62.73 (67.56)	61.29 (69.03)	62.17 (65.60)	60.20 (66.02)	62.73 (67.56)	60.20 (66.02)
East Wind	-7715.1 (21015.0)	-8178.5 (20878.0)	-6430.8 (21890.0)	-7190.7 (21512.0)	-7715.1 (21015.0)	-7190.7 (21512.0)
North Wind	-23231.0 (34612.0)	-22494.0 (35192.0)	-23407.0 (34078.0)	-22330.0 (34112.0)	-23231.0 (34612.0)	-22330.0 (34112.0)
Observations Sargan p-value	18981	18981	18981	18981	18981	010.0
Wald p-value (coefficients) Wald p-value (time dummies)	3.75×10^{-10} 9.18×10^{-4}	7.84×10^{-10} 1.22×10^{-3}	3.73×10^{-9} 3.17×10^{-4}	5.88×10^{-9} 4.18×10^{-4}	1.44×10^{-7} 3.28×10^{-4}	4.59×10^{-8} 1.02×10^{-4}

Note: Robust standard errors in parentheses. * $p<0.1,\ ^{**}p<0.05,\ ^{***}p<0.01.$

Table A2: System GMM Estimates of Migration on Deforestation (Buffer Radius = 2000m)

	(I) Main	(2) Main models	(3) AR(2)	(4) AR(2) models	(5) Models W/	(5) (6) Models W/Out controls
Lagged Deforestation $(t-1)$	0.662*** (0.045)	0.664*** (0.045)	0.709*** (0.052)	0.713*** (0.051)	0.665***	0.667***
Lagged Deforestation $(t-2)$			0.521*** (0.109)	0.518*** (0.III)		
Current Migrants (weighted)	-4.264 (6.696)		-4.959 (6.793)		-23.076** (7.608)	
\sum Out-migration (weighted)		-4.777 (7.074)		-4.466 (7.133)		-21.993^{**} (7.448)
Neturn Migration (weighted)		1.192 (12.270)		-0.706 (12.412)		
Precipitation	-24.72 (29.03)	-28.26 (28.57)	37.86 (28.07)	33.43 (28.66)		
Temperature	257.82 (230.52)	220.85 (217.04)	353.55 (323.56)	289.20 (302.37)	257.82 (230.52)	289.20 (302.37)
East Wind	139900.0	129160.0 (77731.0)	164390.0 (124640.0)	143090.0 (117970.0)	139900.0 (80681.0)	143090.0 (117970.0)
North Wind	-121480.0 (122490.0)	—101280.0 (114820.0)	-172600.0 (194800.0)	-136510.0 (181670.0)	-121480.0 (122490.0)	-136510.0 (181670.0)
Observations Sargan p-value AR(2) p-value Wald p-val (coefficients) Wald p-val (time dummies)	18981 3.77×10^{-15} 8.50×10^{-6} $< 2.22 \times 10^{-16}$ $< 2.22 \times 10^{-16}$	$ \begin{array}{c} 18981 \\ 7.45 \times 10^{-16} \\ 5.11 \times 10^{-6} \\ < 2.22 \times 10^{-16} \\ < 2.22 \times 10^{-16} \end{array} $	$ \begin{array}{l} 18981 \\ < 2.22 \times 10^{-16} \\ \text{o.101} \\ < 2.22 \times 10^{-16} \\ < 2.22 \times 10^{-16} \end{array} $	$ \begin{array}{c} 18981 \\ < 2.22 \times 10^{-16} \\ \text{o.108} \\ < 2.22 \times 10^{-16} \\ < 2.22 \times 10^{-16} \end{array} $	$ \begin{array}{c} 18981 \\ < 2.22 \times 10^{-16} \\ 8.78 \times 10^{-5} \\ < 2.22 \times 10^{-16} \\ < 2.22 \times 10^{-16} \end{array} $	$18981 \\ < 2.22 \times 10^{-16} \\ 1.01 \times 10^{-4} \\ < 2.22 \times 10^{-16} \\ < 2.22 \times 10^{-16} \\ < 2.22 \times 10^{-16}$

Note: Robust standard errors in parentheses. $^*p < 0.1, \,^{**}p < 0.05, \,^{***}p < 0.01.$

Table A3: OLS Estimates of Migration on Deforestation (Clustered Standard Errors, Buffer Radius = 1000m)

	(1) Main models	(2) models	(3) AR(2)	3) (4) $AR(2)$ models	(5) Models W,	(5) (6) Models W/Out controls
Lagged Deforestation $(t-1)$	0.520***	0.521***	0.486***	0.486***	0.520***	0.521*** (0.046)
Lagged Deforestation $(t-2)$			0.056	0.056		
Current Migrants	-1.551* (0.910)		-1.662^{*} (0.934)		—1.527* (0.911)	
∑ Out-migration		-1.608* (0.870)		-1.748* (0.923)		—1.551* (0.832)
∑ Return Migration		0.694 (3.301)		0.477		
Precipitation	-6.277 (5.998)	-6.318 (5.997)	-6.617 (5.604)	-6.686 (5.602)		
Temperature	22.9.82 (1556.2)	226.81 (1556.7)	256.80 (1431.9)	251.61 (1430.1)		
East Wind	-1014.26 (3843.2)	-1001.25 (3843.7)	—п78.73 (3860.2)	-1159.74 (3863.4)		
North Wind	3409.0 (4301.8)	3430.3 (4310.5)	3292.8 (4454.3)	3322.0 (4455.7)		
R-squared	0.214	0.214	0.203	0.203	0.214	0.214
Adj. K-squared Observations	0.156 10545	0.156 10545	0.140 9842	0.140 9842	0.156	0.156

Note: Robust standard errors in parentheses. *p < 0.1, **p < 0.05, ***p < 0.01.

Table A4: OLS Estimates of Migration on Deforestation (Lower Than 10% Overlap Sample, Buffer Radius = 1000m)

	(1) Main	(1) (2) Main models	(3) AR(2)	(3) (4) AR(2) models	(5) Models W,	(5) (6) Models W/Out controls
Lagged Deforestation $(t-1)$	0.437***	0.437*** (0.023)	0.383*** (0.025)	0.382*** (0.025)	0.438***	0.438***
Lagged Deforestation $(t-2)$			o.115*** (0.028)	o.116*** (0.028)		
Current Migrants	-1.182 (1.348)		-1.187 (1.417)		-1.121 (1.346)	
∑ Out-migration		-1.398 (1.352)		-1.462 (1.423)		-1.625 (1.340)
Neturn Migration		-9.647 (6.099)		-11.120* (6.552)		
Precipitation	5.353 (12.678)	5.885 (12.674)	1.677 (13.247)	1.961 (13.239)		
Temperature	\$126.0 (2752.0)	\$120.\$ (2750.4)	5226.1 (2849.2)	5198.1 (2847.1)		
East Wind	9232.0 (6714.0)	-9176.8 (6710.2)	-9811.3 (6923.4)	-9753.5 (6918.5)		
North Wind	-1175.7 (8738.5)	-666.7 (8738.0)	-232.7 (9041.7)	363.6 (9040.5)		
R-squared	0.159	091.0	0.153	0.154	0.157	0.157
Adj. R-squared	060.0	160.0	0.078	0.079	0.090	0.090
Observations	2175	2175	2030	2030	2175	2175

Table A5: OLS Estimates of the Effect of WEA Threshold on Storm-Related Deaths per Storm

		variable:
	Total D	Deaths
	(1) Full Sample	(2) No Katrina
Threshold	-29.167	-21.470**
	(20.192)	(7.509)
Date (centered)	0.001	0.0035*
	(0.0040)	(0.0015)
Disaster Subtype: Derecho	-34.817	-28.234
	(56.339)	(20.961)
Disaster Subtype: Extra-tropical storm	-28.349	-17.782
	(78.724)	(29.282)
Disaster Subtype: Hail	-20.674	—ı3.295
	(36.554)	(13.598)
Disaster Subtype: Lightning/Thunderstorms	-16.450	-16 . 165*
	(22.927)	(8.529)
Disaster Subtype: Sand/Dust storm	1.388	-10.683
	(78.341)	(29.143)
Disaster Subtype: Severe weather	—11 . 675	-16.637**
	(18.056)	(6.747)
Disaster Subtype: Storm (General)	-18.549	-14.447**
	(19.108)	(7.108)
Disaster Subtype: Tornado	-12.576	-6.299
	(14.847)	(5.548)
Disaster Subtype: Tropical cyclone	-60.62I***	-20.348***
	(16.655)	(6.317)
Total damage (billions USD)	5.44I***	1.428***
	(0.297)	(0.152)
Constant	34·371*	33.535***
	(17.098)	(6.431)
Observations	253	253
\mathbb{R}^2	0.597	0.315
Adjusted R ²	0.577	0.280
Residual Std. Error	77.43 (df = 240)	28.80 (df = 239)
F Statistic	29.66*** (df = 12; 240)	9.14*** (df = 12; 239

Note: *p<0.1; **p<0.05; ***p<0.01

Table A6: Covariate Balance Before and After IPW

Variable	SMD (Unweighted)	SMD (Weighted)
Outcome and Covariates		
log(Nightlight)	-0.1846	0.0801
Real GDP per capita	-o.1486	-0.0075
Personal Income per capita	0.0588	0.0049
Population	-0.2904	0.0010
Poverty Rate	0.4640	-0.0234
Unemployment Rate	0.0071	-0.0165
Elderly Rate (Age > 65)	-0.0046	-0.0030
Disability Rate	0.1676	-0.0055
Minority Rate	-0.2876	-0.0126
No Vehicle HH Rate	0.1989	-0.0077
Incident Length	-0.4946	0.0090
County Area (km²)	-0.1205	0.0069
Forest Cover (%)	0.1228	0.0024
Max Wind Speed (During Incident)	-0.0740	0.0060
Effective Sample Sizes	Control	Treated
Unadjusted	11,296	11,448
Adjusted	9,372.07	10,235.51

Note: Standardized mean differences (SMD) are shown before and after applying inverse probability weighting (IPW).

Table A7: Robustness Check: Controlling for County-Level Hurricane Preparedness

	(1)	(2)
Treatment Effects		
Period $-2 \times$ Treated	-0.0087	-0.0086
	(0.0119)	(0.0119)
Period $-1 \times$ Treated	-0.0002	-0.0001
	(0.0057)	(0.0057)
Period 1× Treated	-o.o316***	-o.o315***
	(0.0093)	(0.0093)
Period 2× Treated	0.0160*	0.0161*
	(0.0091)	(0.0092)
Period 3× Treated	0.0243***	0.0244***
	(0.0026)	(0.0026)
Period 4× Treated	0.0006	0.0007
	(0.0034)	(0.0034)
Period 5× Treated	0.0345***	0.0346***
	(0.0044)	(0.0044)
	` ','	· · · · · ·
Control Variables		
Real GDP per capita	-0.0008	-0.002I
1 1	(0.0016)	(0.0016)
Personal Income per capita	0.0069***	0.0085***
1 1	(0.0017)	(0.0014)
Population	7.45e-07**	1.20e-06***
1	(3.07e-07)	(2.08e-07)
Poverty Rate	-0.0024**	-0.0029***
,	(0.0011)	(0.0010)
Unemployment Rate	0.0058	-0.0002
1 7	(0.0040)	(0.0038)
Elder Rate (Age > 65)	0.0025	, ,
()	(0.0075)	
Disability Rate	-0.0099**	
•	(0.0046)	
Minority Rate	0.0093*	
,	(0.0048)	
No Vehicle HH Rate	-0.0066	
	(0.0046)	
Incident Length	0.0009***	0.0014***
8	(0.0003)	(0.0003)
Max Wind Speed	-0.0010	-o.ooi7*
1	(0.0009)	(0.0010)
Past PA Applications	-9.62e-07	-1.41e-06
1 1	(2.14e-06)	(2.56e-06)
Observations	22,744	22,744
Fixed Effects	County	County
RMSE	0.0477	0.0478
Within R^2	0.257	0.253
	٧٠-١/	~· -);

Note: Robust standard errors clustered at the county level in parentheses. ***p < 0.01, **p < 0.05, *p < 0.1. Past PA Applications is the preparedness proxy based on previous FEMA applications.

Table A8: High-Income Counties — Impact of FEMA Public Assistance Across Recovery Periods

	(1)	(2)	(3)	(4)	(5)
Treatment Effects		. ,		() /	(3)
Period -2 × Treated	-0.0090	-0.0089	-0.0087	-0.0085	-0.0077
	(0.0236)	(0.0236)	(0.0236)	(0.0237)	(0.0236)
Period -1 × Treated	-0.0135	-0.0135	-0.0132	-0.0131	-0.0123
	(0.0084)	(0.0084)	(0.0084)	(0.0084)	(0.0088)
Period 1 \times Treated	-0.0446**	-0.0445**	-0.0443**	-0.0441**	-0.0433**
	(0.0183)	(0.0183)	(0.0182)	(0.0182)	(0.0183)
Period 2 \times Treated	0.0183	0.0184	0.0186	0.0188	0.0196
	(0.0182)	(0.0182)	(0.0182)	(0.0181)	(0.0181)
Period $3 \times$ Treated	0.0295***	0.0296***	0.0299***	0.0300***	0.0308***
	(0.0045)	(0.0045)	(0.0045)	(0.0044)	(0.0045)
Period $4 \times$ Treated	0.0091	0.0092	0.0094	0.0096	0.0104
	(0.0084)	(0.0084)	(0.0084)	(0.0085)	(0.0087)
Period 5 \times Treated	0.0513***	0.0514***	0.0516***	0.0518***	0.0526***
	(0.0077)	(0.0077)	(0.0077)	(0.0077)	(0.0080)
Control Variables					
Real GDP per capita	0.0037	-0.0021	-0.0001	_	_
reem of r per empres	(0.0030)	(0.0027)	(0.0026)		
Personal Income per capita	0.0030	0.0083***	0.0070***	_	_
Torona morno per capita	(0.0031)	(0.0018)	(0.0019)		
Population	2.57e-06***	2.10e-06***	2.40e-06***	2.40e-06**	_
1	(4.07e-07)	(4.60e-07)	(4.78e-07)	(9.28e-07)	
Poverty Rate	-o.o118***	-0.0048*	-0.0021	0.0025	_
•	(0.0037)	(0.0027)	(8100.0)	(0.0021)	
Unemployment Rate	0.0162	0.0091	0.0089	-0.0142	_
1 ,	(0.0139)	(0.0162)	(0.0124)	(0.0119)	
Elder Rate (Age>65)	0.0634***	,	,	, , ,	
(0),	(0.0207)				
Disability Rate	0.0019				
·	(0.0161)				
Minority Rate	-0.0055				
	(0.0091)				
No Vehicle HH Rate	0.0244***				
	(0.0071)				
Incident Length	0.0020***	0.0011***	_	_	_
-	(0.0006)	(0.0005)			
Max Wind Speed	-0.0020	-0.0031	_	_	_
	(0.0023)	(0.0024)			
01		11,368	11,368	11,368	11,368
Observations	11,368	11,500	11,,000	,,,	//
Fixed Effects	11,368 County	County	County	County	County

Note: Robust standard errors clustered at the county level in parentheses. $^*p < 0.1, ^{**}p < 0.05, ^{***}p < 0.01.$ "-" indicates a variable excluded due to model specification.

Table A9: Low-Income Counties — Impact of FEMA Public Assistance Across Recovery Periods

	(1)	(2)	(3)	(4)	(5)
Treatment Effects				() /	
Period -2 × Treated	-0.0084**	-o.oo84**	-o.oo86**	-0.0094***	-0.0096***
	(0.0036)	(0.0036)	(0.0035)	(0.0036)	(0.0036)
Period -1 × Treated	0.0128***	0.0128***	0.0126***	0.0118***	0.0116***
	(0.0030)	(0.0031)	(0.0031)	(0.0031)	(0.0030)
Period 1 × Treated	-0.0179***	-0.0179***	-o.o181***	-0.0189***	-0.0191***
	(0.0033)	(0.0034)	(0.0033)	(0.0033)	(0.0034)
Period 2 × Treated	0.0132***	0.0132***	0.0130***	0.0122***	0.0120***
	(0.0035)	(0.0036)	(0.0036)	(0.0036)	(0.0035)
Period 3 × Treated	0.0191***	0.0191***	0.0190***	0.0181***	0.0179***
•	(0.0029)	(0.0029)	(0.0029)	(0.0030)	(0.0030)
Period $4 \times$ Treated	-0.0079**	-0.0079**	-o.oo81**	-o.oo89**	-0.0091**
	(0.0036)	(0.0037)	(0.0036)	(0.0036)	(0.0036)
Period 5 × Treated	0.0170***	0.0170***	0.0168***	0.0160***	0.0158***
	(0.0051)	(0.0051)	(0.0050)	(0.0050)	(0.0051)
Control Variables					
Real GDP per capita	0.0029*	-0.0003	-0.0006	_	_
	(0.0017)	(0.0013)	(0.0021)		
Personal Income per capita	0.0128***	0.0113***	0.0079***	_	_
	(0.0014)	(0.0013)	(0.0015)		
Population	−1.26e-07	1.02e-06***	1.33e-06***	1.53e-06***	_
	(2.90e-07)	(1.97e-07)	(1.75e-07)	(3.43e-07)	
Poverty Rate	-0.0024***	-o.oo31***	-0.0005	0.0009	_
	(0.0009)	(0.0009)	(0.0015)	(0.0012)	
Unemployment Rate	0.0061	0.0031	0.0113***	0.0013	_
	(0.0038)	(0.0031)	(0.0026)	(0.0033)	
Elder Rate (Age>65)	-0.0112^*				
	(0.0059)				
Disability Rate	-o.0147**				
	(0.0066)				
Minority Rate	0.0114***				
	(0.0029)				
No Vehicle HH Rate	0.0026				
	(0.0093)				
Incident Length	0.0013***	0.0019***	-	_	_
	(0.0002)	(0.0003)			
Max Wind Speed	-0.0013**	-0.0022**	-	_	_
	(0.0006)	(0.0010)			
Observations	11,376	11,376	11,376	11,376	11,376
Fixed Effects	County	County	County	County	County
RMSE	0.0381	0.0382	0.0384	0.0388	0.0406
Within R ²	0.1628	0.1558	0.1472	0.1313	0.0466

Note: Robust standard errors clustered at the county level in parentheses. *p < 0.1, **p < 0.05, ***p < 0.01. "-" indicates a variable excluded due to model specification.

Table A10: High-Unemployment Counties — Impact of FEMA Public Assistance Across Recovery Periods

	(1)	(2)	(3)	(4)	(5)
Treatment Effects					
Period $-2 \times$ Treated	-0.0154**	-0.0156**	-0.0158**	-0.0161**	-0.0160**
	(0.0071)	(0.0071)	(0.0070)	(0.0070)	(0.0070)
Period $-1 \times$ Treated	0.0001	-0.0001	-0.0003	-0.0006	-0.0005
	(0.0107)	(0.0106)	(0.0106)	(0.0105)	(0.0105)
Period 1× Treated	-0.0207***	-0.0209^{***}	-0.0211****	-0.0214^{***}	-0.0213***
	(0.0066)	(0.0067)	(0.0067)	(0.0067)	(0.0067)
Period 2× Treated	0.0249**	0.0247**	0.0245**	0.0243**	0.0243**
	(0.0103)	(0.0103)	(0.0104)	(0.0104)	(0.0104)
Period 3× Treated	0.0237***	0.0235***	0.0234***	0.0231***	0.0231***
	(0.0029)	(0.0029)	(0.0030)	(0.0031)	(0.0031)
Period 4× Treated	-0.0034	-0.0036	-0.0037	-0.0040	-0.0040
	(0.0048)	(0.0047)	(0.0047)	(0.0047)	(0.0047)
Period 5× Treated	0.0260***	0.0258***	0.0257^{***}	0.0254***	0.0254***
	(0.0062)	(0.0062)	(0.0062)	(0.0063)	(0.0063)
Control Variables					
Real GDP per capita	0.0007	0.0008	-0.0004	_	-
	(0.0008)	(0.0018)	(0.0021)		
Personal Income per capita	0.0022	0.0051***	0.0037*	_	-
	(0.0016)	(0.0012)	(0.0018)		
Population	3.69e-06*	5.20e-06***	3.21e-06*	2.11e-06*	-
_	(1.59e-06)	(1.10e-06)	(1.40e-06)	(1.25e–06)	
Poverty Rate	-0.0049***	-0.0018	-0.0012	0.0000	_
	(0.0011)	(0.0011)	(0.0011)	(0.0010)	
Unemployment Rate	0.0019	-0.0027	0.0002	-0.0027	_
71. 7. (4)	(0.0036)	(0.0045)	(0.0028)	(0.0026)	
Elder Rate (Age>65)	0.0213	-	_	_	-
Di Lili D	(0.0145)				
Disability Rate	0.0150*	_	_	_	_
Mr D	(0.0063)				
Minority Rate	0.0191***	_	_	_	_
NI WILLIUID .	(0.0053) -0.0147***				
No Vehicle HH Rate		_	_	_	-
T. 11 T 1	(0.0042)	0.001.4***			
Incident Length	0.0031***	0.0014***	_	_	_
M W: 1 C 1	(0.0009) -0.0003	(0.0003) -0.0014			
Max Wind Speed			_	_	-
Observations	(0.0010)	(0.0012)	77.0(9	** *(9	***************************************
Fixed Effects	11,368	11,368	11,368	11,368	11,368
RMSE	County	County	County	County	County
Within R^2	0.0399	0.0400	0.0401	0.0401	0.0401
within ti	0.091	0.089	0.086	0.083	0.083

Note: Robust standard errors clustered at the county level in parentheses. $^*p < 0.1, ^{**}p < 0.05, ^{***}p < 0.01.$ "-" indicates a variable excluded due to model specification.

Table A11: Low-Unemployment Counties — Impact of FEMA Public Assistance Across Recovery Periods

	(1)	(2)	(3)	(4)	(5)
Treatment Effects	(1)	(2)	(3)	(4)	(3)
Period $-2 \times$ Treated	-0.0039	-0.0038	-0.0035	-0.0036	-0.0043
Teriod 2% Treated	(0.0203)	(0.0203)	(0.0202)	(0.0203)	(0.0204)
Period $-1 \times$ Treated	-0.0016	-0.0015	-0.0011	-0.0013	-0.0020
Teriod 1× Heated	(0.0052)	(0.0052)	(0.0053)	(0.0052)	(0.0020
Period 1× Treated	-0.0401^{***}	-0.0400^{***}	-0.0396**	-0.0398***	-0.0404^{***}
Teriod 1× Treated	(0.0151)	(0.0151)	(0.0152)	(0.0151)	(0.0152)
Period 2× Treated	0.0074	0.0075	0.0079	0.0077	0.0071
renod 2× Treated	(0.0125)	(0.0125)	(0.0126)	(0.0125)	
Period 3× Treated	0.01257	0.0125)	0.01267	0.01257	(0.0125) 0.0244***
Period 5× Treated					
Period 4× Treated	(0.0044)	(0.0045)	(0.0045)	(0.0044)	(0.0045)
Period 4× Treated	0.0050 (0.0046)	0.0052 (0.0046)	0.0055 (0.0047)	0.0053 (0.0046)	0.0047
Period 5× Treated	0.0425***	0.0427***	0.0430***	0.0428***	(0.0051) 0.0422***
Period 5× Treated					
	(0.0067)	(0.0067)	(0.0067)	(0.0066)	(0.0073)
Control Variables					
Real GDP per capita	-0.0049	-0.0059	0.0017	_	_
rear 321 per eupreu	(0.0039)	(0.0040)	(0.0029)		
Personal Income per capita	0.0055*	0.0100***	0.0051*	_	_
resona mesme per supru	(0.0029)	(0.0031)	(0.0021)		
Population	4.50e-07	1.36e-06**	1.30e-06*	2.28e-06***	_
ropulation	(4.41e-o ₇)	(5.08e-07)	(6.43e-o7)	(9.61e-o7)	
Poverty Rate	-0.0076^{***}	-0.0074**	-0.0043	0.0007	_
roverty reace	(0.0021)	(0.0032)	(0.0030)	(0.0037)	
Unemployment Rate	-0.0114	-0.0270	-0.0308	-0.0453^{**}	_
o nemproyment reace	(0.0111	(0.0165)	(0.0227)	(0.0204)	
Elder Rate (Age>65)	0.0255	(0.0103)	(0.022/)	(0.0204)	_
Lider reace (rige > 0))	(0.0138)				
Disability Rate	-0.0247^*	_	_	_	_
Disability Teace	(0.0116)				
Minority Rate	0.0112	_	_	_	_
Transcriby Teace	(0.0074)				
No Vehicle HH Rate	-0.0418^*	_	_	_	_
110 /011010 1111 10110	(0.0245)				
Incident Length	0.0018*	0.0016*	_	_	_
merdent Zength	(0.0007)	(0.0007)			
Max Wind Speed	-0.0003	-0.0019	_	_	_
ma opeca	(0.0000)	(0.0013)			
Observations	11,376	11,376	11,376	11,376	11,376
Fixed Effects	County	County	County	County	County
RMSE	0.0536	0.0538	0.0540	0.0542	0.0595
Within R^2	0.244	0.238	0.234	0.226	0.070
	V-277	0.250	V.27T	0.220	

Note: Robust standard errors clustered at the county level in parentheses. *p < 0.1, **p < 0.05, ***p < 0.01. "-" indicates a variable excluded due to model specification.

Table A12: High Minority Counties — Impact of FEMA Public Assistance Across Recovery Periods

	(1)	(2)	(3)	(4)	(5)
Treatment Effects	(*/	\2)	\31	\†/	()/
Period $-2 \times$ Treated	-0.0222***	-0.0222***	-0.0222***	-0.0223***	-0.0236***
	(0.0059)	(0.0059)	(0.0059)	(0.0059)	(0.0057)
Period $-1 \times$ Treated	-0.0075	-0.0074	-0.0074	-0.0075	-0.0089
	(0.0090)	(0.0091)	(0.0091)	(0.0091)	(0.0087)
Period $1 \times$ Treated	-0.0166***	-0.0165^{***}	-0.0165^{***}	-0.0167^{***}	-0.0180***
	(0.0041)	(0.0041)	(0.0041)	(0.0041)	(0.0044)
Period $2\times$ Treated	0.0280***	0.0280***	0.0280***	0.0279***	0.0266**
	(0.0092)	(0.0092)	(0.0092)	(0.0093)	(0.0096)
Period 3× Treated	0.0263***	0.0263***	0.0263***	0.0262***	0.0249***
D - 14 - T - 1	(0.0031)	(0.0031)	(0.0031)	(0.0031)	(0.0033)
Period 4× Treated	-0.0070* (0.0041)	-0.0070* (0.0041)	-0.0070* (0.0041)	-0.0071* (0.0041)	-0.0084** (0.0038)
Period 5× Treated	0.0041)	0.0259***	0.0259***	0.0257***	0.00387
renou o × meateu	(0.0042)	(0.0042)	(0.0042)	(0.0042)	(0.0043)
	(0.0042)	(0.0042)	(0.0042)	(0.0042)	(0.0043)
Control Variables					
Real GDP per capita	0.0024	0.0010	0.0004	-	-
	(0.0025)	(0.0023)	(0.0020)		
Personal Income per capita	0.0025	0.0051**	0.0053^{***}	_	_
	(0.0023)	(0.0023)	(0.0016)		
Population	6.79e-07***	1.02e-06***	1.03e-06***	1.27e-06***	-
	(2.48e-07)	(1.53e-07)	(1.66e–07)	(1.79e–07)	
Poverty Rate	-0.0010	-0.0016	-0.0004	0.0037**	-
	(0.0020)	(0.0015)	(0.0013)	(0.0018)	
Unemployment Rate	0.0019	-0.0049	0.0036	-0.0007	-
T11 D (A > C)	(0.0044)	(0.0041)	(0.0042)	(0.0050)	
Elder Rate (Age>65)	0.0023	_	_	_	_
Disability Rate	(0.0139) -0.0081				
Disability Kate	-0.0061 (0.0066)	_	_	_	_
Minority Rate	0.0103	_	_	_	_
Willionty Rate	(0.0072)				
No Vehicle HH Rate	-0.0077	_	_	_	_
The vermone Till Peace	(0.0083)				
Incident Length	0.0002	0.0010**	_	_	_
O	(0.0004)	(0.0005)			
Max Wind Speed	0.0024	0.0005	_	_	_
•	(0.0021)	(0.0016)			
Observations	11,368	11,368	11,368	11,368	11,368
Fixed Effects	County	County	County	County	County
RMSE	0.0397	0.0398	0.0399	0.0402	0.0450
Within R^2	0.281	0.277	0.274	0.261	0.073

Note: Robust standard errors clustered at the county level in parentheses. $^*p < 0.1, ^{**}p < 0.05, ^{***}p < 0.01.$ "-" indicates a variable excluded due to model specification.

Table A13: Low Minority Counties — Impact of FEMA Public Assistance Across Recovery Periods

	(1)	(2)	(3)	(4)	(5)
Treatment Effects					
Period $-2 \times$ Treated	0.0045	0.0048	0.0053	0.0051	0.0040
	(0.0202)	(0.0202)	(0.0201)	(0.0203)	(0.0205)
Period $-1 \times$ Treated	0.0059	0.0063	0.0067	0.0066	0.0054
	(0.0051)	(0.0051)	(0.0052)	(0.0051)	(0.0052)
Period 1× Treated	-0.0461***	-0.0458***	-0.0453***	-0.0455****	-0.0466***
	(0.0157)	(0.0158)	(0.0158)	(0.0157)	(0.0156)
Period 2× Treated	0.0043	0.0046	0.0051	0.0049	0.0038
	(0.0128)	(0.0129)	(0.0129)	(0.0128)	(0.0127)
Period 3× Treated	0.0228***	0.0231***	0.0235***	0.0234***	0.0222***
	(0.0041)	(0.0041)	(0.0042)	(0.0041)	(0.0043)
Period 4× Treated	0.0082*	0.0086*	0.0090**	0.0089**	0.0077
	(0.0045)	(0.0045)	(0.0045)	(0.0044)	(0.0050)
Period 5× Treated	0.0437^{***}	0.0441***	0.0445^{***}	0.0444***	0.0432***
	(0.0076)	(0.0076)	(0.0075)	(0.0075)	(0.0082)
Control Variables					
Real GDP per capita	0.0026*	-0.0000	0.0024	_	-
	(0.0013)	(0.0016)	(0.0035)		
Personal Income per capita	0.0045***	0.0059***	0.0048***	_	-
	(0.0015)	(0.0012)	(0.0018)	0.00	
Population	1.52e-06***	2.19e-06***	2.06e-06***	2.88e-06***	-
	(3.52e-07)	(2.36e-07)	(2.93e-07)	(3.89e-07)	
Poverty Rate	-0.0022*	-0.0038***	-0.0015	0.0003	_
** 1 5	(0.0012)	(0.0011)	(0.0019)	(0.0019)	
Unemployment Rate	0.0050	-0.0042	0.0060	0.0002	_
71. 7. (1)	(0.0047)	(0.0043)	(0.0054)	(0.0045)	
Elder Rate (Age>65)	0.0036	_	_	-	_
Di Lili D	(0.0061)				
Disability Rate	-0.0183***	_	_	_	_
Mr D	(0.0048)				
Minority Rate	0.0122***	_	_	_	_
NI WI: LIHID .	(0.0041)				
No Vehicle HH Rate	-0.0001	_	_	_	-
T. 11 T 1	(0.0040)	0.0000***			
Incident Length	0.0011***	0.0020***	_	_	_
M W: 1 C 1	(0.0004) -0.0009	(0.0004) -0.0018**			
Max Wind Speed			_	_	-
Observations	(0.0006)	(0.0008)	** == (*** 6=6	*** == (
Observations Eiged Effects	11,376	11,376	11,376	11,376	11,376
Fixed Effects	County	County	County	County	County
RMSE	0.0533	0.0535	0.0540	0.0544	0.0599
Within R^2	0.274	0.268	0.255	0.244	0.082

Note: Robust standard errors clustered at the county level in parentheses. $^*p < 0.1, ^{**}p < 0.05, ^{***}p < 0.01.$ "-" indicates a variable excluded due to model specification.

BIBLIOGRAPHY

- Angelsen, A., Aguilar-Støen, M., Ainembabazi, J. H., Castellanos, E., & Taylor, M. (2020). Migration, remittances, and forest cover change in rural guatemala and chiapas, mexico. *Land*, 9(3). https://doi.org/10.3390/land9030088
- Arellano, M., & Bond, S. (1991). Some tests of specification for panel data: Monte carlo evidence and an application to employment equations (2). https://www.jstor.org/stable/2297968
- Austin, P. C. (2009). Balance diagnostics for comparing the distribution of base-line covariates between treatment groups in propensity-score matched samples. *Statistics in Medicine*, 28(25), 3083–3107.
- Bank, W. (2020). An assessment of forest tenure in myanmar: Securing forest tenure for sustainable livelihoods [Accessed on 28-Apr-2025].
- BEA. (2025). Real gdp per capita and personal income per capita, county-level [BEA: U.S. Bureau of Economic Analysis Accessed: 01/01/2025.].
- Bean, H., & Grevstad, N. (2022). Wireless emergency alerts: Public understanding, trust, and preferences following the 2021 us nationwide test. *Journal of Contingencies and Crisis Management*, 31, 273–288. https://doi.org/10.1111/1468-5973.12438
- Bean, H., Grevstad, N., Meyer, A., & Koutsoukos, A. (2022). Exploring whether wireless emergency alerts can help impede the spread of covid-19. *Journal of Contingencies and Crisis Management*, 30(2), 185–203. https://doi.org/https://doi.org/10.1111/1468-5973.12376
- Bean, H., Liu, B. F., Madden, S., Sutton, J., Wood, M. M., & Mileti, D. S. (2016). Disaster warnings in your pocket: How audiences interpret mobile alerts for an unfamiliar hazard. *Journal of Contingencies and Crisis Management*, 24(3), 136–147. https://doi.org/https://doi.org/10.1111/1468-5973.12108
- Bean, H., Takenouchi, K., & Cruz, A. M. (2023). Combining probabilistic hazard information forecast graphics with wireless emergency alert messages: An exploratory, qualitative study. *Weather, Climate, and Society*, *15*(4), 843–861. https://doi.org/10.1175/WCAS-D-22-0140.1

- Best, E. (2017). Development of hybrid notification systems for use in storm-based warnings in rural communities. *Natural Hazards Review*, 18(4), 05017001. https://doi.org/10.1061/(ASCE)NH.1527-6996.0000250
- Bitsikas, E., & Pöpper, C. (2022). You have been warned: Abusing 5g's warning and emergency systems. *Proceedings of the 38th Annual Computer Security Applications Conference*, 561–575. https://doi.org/10.1145/3564625.3568000
- Blundell, R., & Bond, S. (1998). Initial conditions and moment restrictions in dynamic panel data models. *Journal of Econometrics*, 87(1), 115–143.
- C₃S. (2019). *Eras-land hourly reanalysis dataset* (tech. rep.) (C₃S: Copernicus Climate Change Service, Available via the Copernicus Climate Data Store.). Copernicus Climate Change Service.
- Cantillo, T., & Garza, N. (2022). Armed conflict, institutions and deforestation: A dynamic spatiotemporal analysis of colombia 2000–2018. *World Development*, 160, 106041. https://doi.org/10.1016/j.worlddev.2022. 106041
- Carr, D. L. (2009). Population and deforestation: Why rural migration matters. *Progress in Human Geography*, 33(3), 355–378. https://doi.org/10.1177/0309132508096031
- Casteel, M. A., & Downing, J. R. (2016). *Journal of Homeland Security and Emergency Management*, 13(1), 95–112. https://doi.org/doi:10.1515/jhsem-2015-0024
- Cattaneo, C., Beine, M., Fröhlich, C. J., Kniveton, D., Martinez-Zarzoso, I., Mastrorillo, M., Millock, K., Piguet, E., & Schraven, B. (2019). Human migration in the era of climate change. *Review of Environmental Economics and Policy*, 13(2), 189–206. https://doi.org/10.1093/reep/rezoo8
- CDC/ATSDR. (2025). Social vulnerability index (svi) data and documentation for u.s. counties [Accessed July 12, 2025.].
- CESD. (2015). Mon state rural household survey (msrhs) [(CESD: Centre for Economic and Social Development)].
- Chiodi, V., Jaimovich, E., & Montes-Rojas, G. (2012). Migration, remittances and capital accumulation: Evidence from rural mexico. *The Journal of Development Studies*, 48(8), 1139–1155. https://doi.org/10.1080/00220388.2012.688817
- Damon, A. L. (2010). Agricultural land use and asset accumulation in migrant households: The case of el salvador. *Journal of Development Studies*, 46, 162–189. https://doi.org/10.1080/00220380903197994
- DeYoung, S. E., Sutton, J. N., Farmer, A. K., Neal, D., & Nichols, K. A. (2019). "death was not in the agenda for the day": Emotions, behavioral re-

- actions, and perceptions in response to the 2018 hawaii wireless emergency alert. *International Journal of Disaster Risk Reduction*, *36*, 101078. https://doi.org/10.1016/j.ijdrr.2019.101078
- D.Guha-Sapir, R.Below, & Ph.Hoyois. (2015). EM-DAT: The CRED/OFDA International Disaster Database www.emdat.be Universitè Catholique de Louvain Brussels Belgium.
- Drost, H., Brooks, H. E., & Elsner, J. B. (2016). Severe weather warning communication: Factors affecting reception, comprehension, and response. *Weather, Climate, and Society*, 8(4), 407–419. https://doi.org/10.1175/WCAS-D-15-0035.1
- Emanuel, K. (2013). Downscaling cmip5 climate models shows increased tropical cyclone activity over the 21st century. *Proceedings of the National Academy of Sciences*, 110, 12219–12224. https://doi.org/10.1073/pnas.1301293110
- Emrich, C. T., Aksha, S. K., & Zhou, Y. (2022). Assessing distributive inequities in fema's disaster recovery assistance fund allocation. *International Journal of Disaster Risk Reduction*, 74, 102855. https://doi.org/https://doi.org/10.1016/j.ijdrr.2022.102855
- Ervin, D., Lopéz-Carr, D., Riosmena, F., & Ryan, S. J. (2020). Examining the relationship between migration and forest cover change in mexico from 2001 to 2010. *Land Use Policy*, *91*, 104334. https://doi.org/https://doi.org/10.1016/j.landusepol.2019.104334
- FCC. (2012, April). Wireless emergency alerts: Second report and order and second order on reconsideration (PS Docket No. 15-91) (Federal Communications Commission, Accessed: January 30, 2025). Federal Communications Commission. https://www.fcc.gov/ecfs
- FCC. (2019, November). New Enhancements to Wireless Emergency Alerts Will Be Available on December 13, 2019 (tech. rep. No. DA 19-1208) (Federal Communications Commission, Public Notice, PS Docket Nos. 15-91, 15-94). Federal Communications Commission. https://www.fcc.gov/document/new-enhancements-wireless-emergency-alerts-available-dec-13-2019
- FCC. (2021). Fcc proposes new rules for emergency alert systems [Federal Communications Commission, Accessed 2025-05-01].
- FEMA. (2010). *Public assistance applicant handbook (fema p-323)* [FEMA: Federal Emergency Management Agency Accessed June 27, 2025]. Federal Emergency Management Agency. Washington, DC. https://www.fema.gov/pdf/government/grant/pa/fema323_app_handbk.pdf

- FEMA. (2024). Fy 2024 pre-disaster mitigation congressionally directed spending [Federal Emergency Management Agency, Accessed: February 27, 2025].
- FEMA. (2025). Public assistance applicants program deliveries, version 1 (fema public assistance program) [FEMA: Federal Emergency Management Agency, Accessed: 01/01/2025].
- Ferris, J. S., & Newburn, D. A. (2017). Wireless alerts for extreme weather and the impact on hazard mitigating behavior. *Journal of Environmental Economics and Management*, 82, 239–255. https://doi.org/https://doi.org/10.1016/j.jeem.2016.11.002
- Field, C. B., Barros, V. R., Stocker, T. F., Dahe, Q., & Dokken, D. J. (2012). Managing the risks of extreme events and disasters to advance climate change adaptation. *Managing the Risks of Extreme Events and Disasters to Advance Climate Change Adaptation: Special Report of the Intergovernmental Panel on Climate Change*. https://doi.org/10.1017/CBO9781139177245
- Filipski, M. J., Van Asselt, J., Nischan, U., Belton, B., Htoo, K., Win, M. T., Hein, A., Kham, L. S., Naing, Z. M., Payongayong, E., & Boughton, D. (2017). *Rural livelihoods in mon state: Evidence from a representative household survey* (tech. rep. No. 1638). International Food Policy Research Institute (IFPRI). https://ideas.repec.org/p/fpr/ifprid/1638. html
- Funk, C., Peterson, P., Landsfeld, M., Pedreros, D., Verdin, J., Shukla, S., Husak, G., Rowland, J., Harrison, L., Hoell, A., & Michaelsen, J. (2015). The climate hazards infrared precipitation with stations—a new environmental record for monitoring extremes. *Scientific Data*, *2*(1), 150066. https://doi.org/10.1038/sdata.2015.66
- Gao, S., & Wang, Y. (2021). Assessing the impact of geo-targeted warning messages on residents'evacuation decisions before a hurricane using agent-based modeling. *Natural Hazards*, 107(1), 123–146. https://doi.org/10.1007/s11069-021-04576-1
- Gibson, J., Jiang, Y., Zhang, X., et al. (2024). Are disaster impact estimates distorted by errors in popular night-time lights data? *Economics of Disasters and Climate Change*, 8, 391–416. https://doi.org/10.1007/s41885-024-00152-6
- Global Forest Watch. (2024). Mon state forest dashboard: Cover, loss, and trends (2001–2024) [Accessed June 15, 2025].

- Gray, C. L., & Bilsborrow, R. E. (2014). Consequences of out-migration for land use in rural ecuador. *Land Use Policy*, *36*, 182–191. https://doi.org/10.1016/j.landusepol.2013.07.006
- Hansen, M. C., Potapov, P. V., Moore, R., Hancher, M., Turubanova, S. A., Tyukavina, A., Thau, D., Stehman, S. V., Goetz, S. J., Loveland, T. R., Kommareddy, A., Egorov, A., Chini, L., Justice, C. O., & Townshend, J. R. (2013). High-resolution global maps of 21st-century forest cover change. *Science*, 342, 850–853. https://doi.org/10.1126/science.1244693
- Hausman, C., & Rapson, D. (2018). Regression discontinuity in time: Considerations for empirical applications. *Annual Review of Resource Economics*, 10(1), 533–552. https://doi.org/10.1146/annurev-resource-121517-033306
- Kahn, M. E. (2005). The death toll from natural disasters: The role of income, geography and institutions. *Review of Economics and Statistics*, 87(2), 271–284. https://doi.org/10.1162/0034653053970334
- Kumar, S., Erdogmus, H., Iannucci, B., Griss, M., & Falcão, J. D. (2018). Rethinking the future of wireless emergency alerts. *Proceedings of the ACM on Interactive, Mobile, Wearable and Ubiquitous Technologies*, 2, 1–33. https://doi.org/10.1145/3214274
- Kyaw, K. T. W., Ota, T., & Mizoue, N. (2020). Forest degradation impacts firewood consumption patterns: A case study in the buffer zone of inlay lake biosphere reserve, myanmar. *Global Ecology and Conservation*, *24*, e01340. https://doi.org/10.1016/j.gecco.2020.e01340
- Lambropoulos, D., Yousefvand, M., & Mandayam, N. (2021). Tale of seven alerts: Enhancing wireless emergency alerts (weas) to reduce cellular network usage during disasters. https://arxiv.org/abs/2102.00589
- Levy, S. R. (2015). The evolving role of social media in crisis response: How public safety organizations are leveraging online tools to improve disaster preparedness and response. *Journal of Homeland Security and Emergency Management*, 12, 615–634. https://doi.org/10.1515/jhsem-2014-0105
- Liu, J., Dietz, T., Carpenter, S. R., Alberti, M., Folke, C., Moran, E., Pell, A. N., Deadman, P., Kratz, T., Lubchenco, J., Ostrom, E., Ouyang, Z., Provencher, W., Redman, C. L., Schneider, S. H., & Taylor, W. W. (2007). Complexity of coupled human and natural systems. *Science*, 317(5844), 1513–1516. https://doi.org/10.1126/science.1144004
- Mileti, D. S., & Sorensen, J. H. (1990). Communication of emergency public warnings: A social science perspective and state-of-the-art assessment. *Communication of Emergency Public Warnings: A Social Science Per-*

- spective and State-of-the-Art Assessment. https://www.osti.gov/biblio/6137387
- Millock, K. (2015). Migration and environment. *Annual Review of Resource Economics*, 7(1), 35–60. https://doi.org/10.1146/annurev-resource-100814-125031
- Molina, R., & Rudik, I. (2022). The social value of predicting hurricanes [http://dx.doi.org/10.2139/ssrn.4266614]. *CESifo Working Paper No. 10049*. https://doi.org/10.2139/ssrn.4266614
- Morss, R. E., Demuth, J. L., & Lazo, J. K. (2017). The growing use of social media in weather, water, and climate communication: Implications for research and operations. *Bulletin of the American Meteorological Society*, *98*, 2225–2234. https://doi.org/10.1175/BAMS-D-15-00281.1
- Muñoz Sabater, J. (2019). Eraș-land monthly averaged data from 1950 to present [DOI: 10.24381/cds.68d2bb30. Accessed on 25-03-2022].
- NASEM. (2018). Emergency alert and warning systems: Current knowledge and future research directions [National Academies of Sciences, Engineering, and Medicine]. The National Academies Press. https://doi.org/10.17226/24935
- Nawrotzki, R. J., & Bakhtsiyarava, M. (2017). International climate migration: Evidence for the climate inhibitor mechanism and the agricultural pathway. *Population, Space and Place*, 23(4), e2033. https://doi.org/10.1002/psp.2033
- New, M., Reckien, D., Viner, D., Adler, C., Cheong, S.-M., et al. (2022). Decision-making options for managing risk. In: Pörtner HO, Roberts DC, Tignor M, et al. (eds.), Climate Change 2022: Impacts, Adaptation and Vulnerability. Contribution of Working Group II to the Sixth Assessment Report of the IPCC, 2539–2654.
- NLIHC. (2024). Congress passes funding deal and disaster aid package to prevent government shutdown [National Low Income Housing Coalition,

 Available at: https://nlihc.org/resource/congress-passes-funding-deal-and-disaster-aid-package-prevent-government-shutdown (Accessed: February 27, 2025)].
- NOAA. (2025). Billion-dollar weather and climate disasters: Summary statistics [National Oceanic and Atmospheric Administration, Accessed: February 4, 2025]. https://www.ncei.noaa.gov/access/billions/summary-stats
- Olson, M. K., Sutton, J., Cain, L. B., & Waugh, N. (2024). A decade of wireless emergency alerts: A longitudinal assessment of message content and

- completeness. *Journal of Contingencies and Crisis Management*, *32*(1), e12518. https://doi.org/https://doi.org/10.1111/1468-5973.12518
- Rapoport, H., & Docquier, F. (2006). Chapter 17 the economics of migrants' remittances. In S.-C. Kolm & J. M. Ythier (Eds.), *Applications* (pp. 1135–1198, Vol. 2). Elsevier. https://doi.org/https://doi.org/10.1016/S1574-0714(06)02017-3
- Román, M., Wang, Z., Sun, Q., Kalb, V., Miller, S., Molthan, A., Schultz, L., Bell, J., Stokes, E., Pandey, B., Seto, K., & et al. (2018). Nasa's black marble nighttime lights product suite. *Remote Sensing of Environment*, 210, 113–143. https://doi.org/10.1016/j.rse.2018.03.017
- Roodman, D. (2009). A note on the theme of too many instruments*. *Oxford Bulletin of Economics and Statistics*, 71(1), 135–158. https://EconPapers.repec.org/RePEc:bla:obuest:v:71:y:2009:i:1:p:135-158
- Schippers, V., & Botzen, W. W. (2023). Uncovering the veil of night light changes in times of catastrophe. *Natural Hazards and Earth System Sciences*, 23, 179–204. https://doi.org/10.5194/nhess-23-179-2023
- Shrader, J., Bakkensen, L., & Lemoine, D. (2023). Fatal errors: The mortality value of accurate weather forecasts [https://www.nber.org/papers/w31361]. NBER Working Paper No. w31361.
- Simon, T., Goldberg, A., & Adini, B. (2015). Socializing in emergencies—a review of the use of social media in emergency situations. *International Journal of Information Management*, 35, 609–619. https://doi.org/10.1016/j.ijinfomgt.2015.05.002
- Slutzky, E. (1937). *The summation of random causes as the source of cyclic processes* (2). https://about.jstor.org/terms
- Statista. (2024). Internet penetration rate in the united states from 2000 to 2024 [Retrieved February 27, 2025, from https://www.statista.com/statistics/209117/us-internet-penetration/].
- Strader, S. M., Gensini, V. A., & Wagner, A. N. (2024). Changes in tornado risk and societal vulnerability leading to greater impacts in the united states. *npj Natural Hazards*, *I*(I), 20. https://doi.org/10.1038/s44304-024-00019-6
- Stuart, E. A. (2010). Matching methods for causal inference: A review and a look forward. *Statistical Science*, 25(1), 1–21.
- Taylor, J. E., Rozelle, S., & de Brauw, A. (2003). Migration and Incomes in Source Communities: A New Economics of Migration Perspective from China. *Economic Development and Cultural Change*, 52(1), 75–101. https://doi.org/10.1086/380135

- Taylor, M. J., Aguilar-Støen, M., Castellanos, E., Moran-Taylor, M. J., & Gerkin, K. (2016). International migration, land use change and the environment in ixcán, guatemala. *Land Use Policy*, 54, 290–301. https://doi.org/https://doi.org/10.1016/j.landusepol.2016.02.024
- Tol, R. S. J. (2022). State capacity and vulnerability to natural disasters [ISBN: 978-1-83910-373-5]. In M. Skidmore (Ed.), *Handbook on the economics of disasters* (pp. 434–457). Edward Elgar.
- U.S. Census Bureau. (2025). County population estimates, 2020s [Accessed: 01/01/2025.].
- U.S. Congress. (2006). Deficit reduction act of 2005, public law 109-171, section 3010 [Accessed: 2025-05-01].
- USDOT. (2021). Revised departmental guidance on valuation of a statistical life in economic analysis [USDOT: U.S. Department of Transportation, Effective Date: April 28, 2025. Accessed: 2025-05-01].
- Vincent, J. R., & Das, J. (2009). Death and property damage from the 2004 indian ocean tsunami: The roles of information and income. *Proceedings of the National Academy of Sciences*, 106(12), 4841–4846. https://doi.org/10.1073/pnas.0810440106
- Win, Z. C., Mizoue, N., Ota, T., Kajisa, T., Yoshida, S., Oo, T. N., & Ma, H.-o. (2018). Differences in consumption rates and patterns between firewood and charcoal: A case study in a rural area of yedashe township, myanmar. *Biomass and Bioenergy*, 109, 39–46. https://doi.org/https://doi.org/10.1016/j.biombioe.2017.12.011
- Wogalter, M. S. (2018). Communication-human information processing (chip) model. *Forensic Human Factors and Ergonomics*. https://api.semanticscholar.org/CorpusID:195508065
- Wood, M. M., Mileti, D. S., Kano, M., Kelley, M. M., Regan, R., & Bourque, L. B. (2012). Communicating actionable risk for terrorism and other hazards. *Risk Analysis*, 32, 601–615. https://doi.org/10.1111/risa.12850
- World Bank & United Nations. (2010). *Natural hazards, unnatural disasters: The economics of effective prevention.* https://openknowledge.worldbank.org/handle/10986/2512
- Yeon, D., Kwak, M., & Chung, J.-B. (2022). Effectiveness of wireless emergency alerts for social distancing against covid-19 in korea. *Scientific Reports*, 12(1), 26–27. https://doi.org/10.1038/s41598-022-06575-Z
- Young, R., & Hsiang, S. (2024). Mortality caused by tropical cyclones in the united states. *Nature*, 615(7950), 123–129. https://doi.org/10.1038/s41586-024-07945-5

Yule, G. U. (1927). On a method of investigating periodicities in disturbed series, with special reference to wolfer's sunspot numbers. https://about.jstor.org/terms